STYRENE-MALEIC ANHYDRIDE AND STYRENE-MALEIMIDE BASED COPOLYMERS AS BUILDING BLOCKS IN MICROENCAPSULATION PROCEDURES

By

ANNA SHULKIN, M.Sc.

A Thesis

Submitted to the School of Graduate Studies

In Partial Fulfillment of the Requirements

For the Degree

Doctor of Philosophy in Chemistry

McMaster University

PREFORMED POLYMERS AS BUILDING BLOCKS IN MICROENCAPSULATIONS

DOCTOR OF PHILOSOPHY (2002)
(Chemistry)

McMaster University
Hamilton, Ontario

TITLE: Styrene-Maleic Anhydride and Styrene-Maleimide Based Copolymers as Building Blocks in Microencapsulation Procedures

AUTHOR: Anna Shulkin, M. Sc. (Bar-Ilan University)

SUPERVISOR: Professor H. D. H. Stöver

NUMBER OF PAGES: (xxv, 198)

Abstract

This thesis addresses the formation and properties of capsule walls formed from new types of wall-former materials such as styrene-maleic anhydride and styrene-maleimide based preformed hydrophobic polymers. During the course of this study two new methods of encapsulation were developed: interfacial encapsulation based on the cross-linking reaction between oil-soluble styrene-maleic anhydride (SMA) copolymer and a water-soluble polyamine, or alternatively the hydrolysis reaction of *tert*-butylstyrene-maleic anhydride copolymers to produce non-cross-linked microcapsules, and photoinduced phase-separation encapsulation.

The internal morphologies of the produced SMA microcapsules were found to depend primarily upon polymer/core-solvent interactions and rate of amine addition. Thus, the transition from matrix structures to hollow particles was observed with increasing volume fraction of hydrophobic non-solvent, dodecyl acetate, or alternatively by slowing the rate of polyamine addition. The effect of polymer loading, type of polymer and polyamine, and molecular weight of the preformed polymer on the observed morphologies was also investigated.

The interfacial reaction between styrene-maleic anhydride type of copolymers and polyamines was shown to be fast in order of minutes. Hydrolysis, as the side reaction, was not found to play a significant role in the interfacial encapsulation reaction between SMA copolymers and amines.

Styrene-maleimide based capsules were prepared by photostimulated precipitation of azobenzene-functionalized copolymers dissolved in an oil phase and dispersed in a continuous phase. This microencapsulation process was found to be irreversible, and the resulting microcapsule walls were permanent even during storage in the dark, or irradiation with visible light.

Acknowledgements

I wish to express my thanks to my research supervisor, Professor Harald Stöver, for his guidance and enthusiasm. His support, encouragement and criticism made me not only a better scientist but also a better and stronger person. He has opened for me a door into beautiful and fascinating world of science and while doing so became a good friend.

I would also like to thank my supervisory committee members, Professor Robert Pelton and Doctor John Brennan for their ideas and advice.

Special thanks go to my three lab partners and dearest friends, Janevieve Jones, Lisa Croll and Mukkaram Ali. You have made the last four years the most remarkable and enjoyable experience of my life. My morning coffee will never be the same without you.

I am also in grateful appreciation to the rest of the Stöver Research Group members, both past and present; Randy, Jeff, Wen Hui, Nick, Daryl, Guodon, Yen, Ester, Christina, Poonam and Geoff.

Finally, I wish to thank my family for their love, support, patience and inspiration. This thesis is dedicated to two amazing men, my husband and dad, and two equally fascinating women, my mom and my sister.

Table of Contents

List of Figure

Chapter 1.

Chapter 2.1.

Chapter 2.2.

Chapter 3.

Chapter 4.

Chapter 5.

List of Tables

List of Schemes

List of Abbreviations

SMA50 copolymer – Styrene- *alt*-maleic anhydride copolymer

SMA32 copolymer – Styrene-*co*-maleic anhydride copolymer with 32 weight % maleic anhydride units

SMA14 copolymer – Styrene-*co*-maleic anhydride copolymer with 14 weight % maleic anhydride units

***t*-BuSMA50 copolymer** – *tert*-Butylstyrene-*alt*-maleic anhydride copolymer

TEPA- Tetraethylenepentamine

HMDA – Hexamethylenediamine

IGEPAL – Nonyl-phenyl-oligo-ethyene glycol

PVA – Poly(vinylalcohol)

AIBN – 2,2′-Azobis-(2-methylpropionitrile)

PAMA – 4-Phenylazomaleinanil

PMI – Pnenylmaleimide

ESEM – Environmental Scanning Electron Microscope

TEM – Transmission Electron Microscope

General Remarks

This thesis has been prepared in a modified "sandwich" format. Each chapters (except of first, introductory chapter) is loosely based on an accepted journal article or manuscript in preparation.

The work presented in this thesis i.e. the research ideas described in here as well as the manuscripts, papers, and chapters writing and formatting, were solely developed by Anna Shulkin with editorial contributions from Dr. Stöver.

CHAPTER 1

Introduction to Interfacial Microencapsulation: Mechanism and Applications

Anna Shulkin

Department of Chemistry, McMaster University

1280 Main St. West Hamilton, Ontario, Canada L8S 4M1

"Microencapsulation is like the work of a clothing designer. He selects the pattern, cuts the cloth, and sews the garment in due consideration of the desires and age of his customer, plus the locale and climate where the garment is to be worn. By analogy, in microencapsulation, capsules are designed and prepared to meet all the requirements in due consideration of the properties of the core material, intended use of the product, and the environment of storage..."
Asajo Kondo in *Microcapsule Processing and Technology*, Marcel Dekker, Inc., New York, 1979.

1.0 General Introduction

Microencapsulation began with the creation of a living cell. Most of the one-celled plants and animals are living examples of the wonders of microencapsulation. Their natural capsular membranes are remarkably successful in fulfilling special functions such as protection of interior material (core), and control of the flow of materials (permeation) across the cell membrane. Because of their outer protection, plant seeds and bacteria spores can remain viable for over 100 years. Other walls such as charged lipid bilayers can act as permeability valves. For example, the permeability of cytoplasmic membranes may be 10^{10} times larger for water than for ions. Even chicken eggs have been engineered with a protective wall, thick enough to provide protection during incubation, and still thin enough to allow the chick to score and break the shell at the point of hatching.[1]

Man's attempt at copying nature's capsule walls began in 1940 when a young chemist from Dayton, Ohio, Barret Green, prepared the first gelatin microcapsules. Already in the early 1950s, Green and Schleicher introduced carbonless copy paper based on microencapsulation of dyes. Today microencapsulation involves many engineering techniques and scientific disciplines, and has applications in many fields including medicine, biotechnology, chemical industry and food and agriculture.

Microcapsules are small containers, spherical or irregular, usually polymeric, in the size range of about 50 nm to 2,000 μm in which active components (core materials) are encapsulated (Figure 1.1).

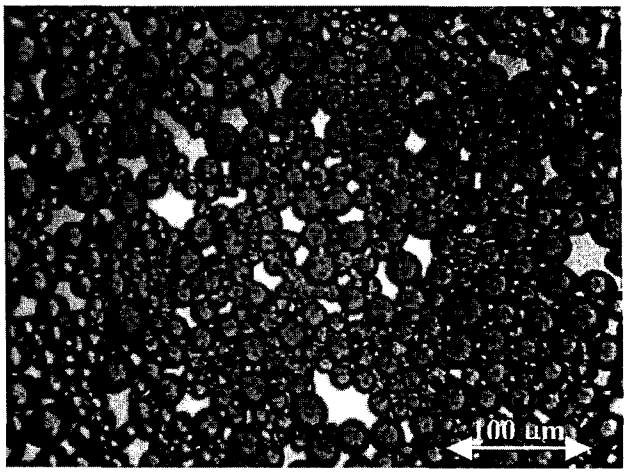

Figure 1.1 – Optical microscopy image of polyurea microcapsules containing a mixture of alkyl acetates.

The core materials can be gaseous, liquid or solid, or may be themselves be an emulsion or a suspension. Microcapsules may have different internal morphologies, including monolithic (matrix), polynuclear, mononuclear (reservoir), multi-walled or multi-core (Figure 1.2).[2]

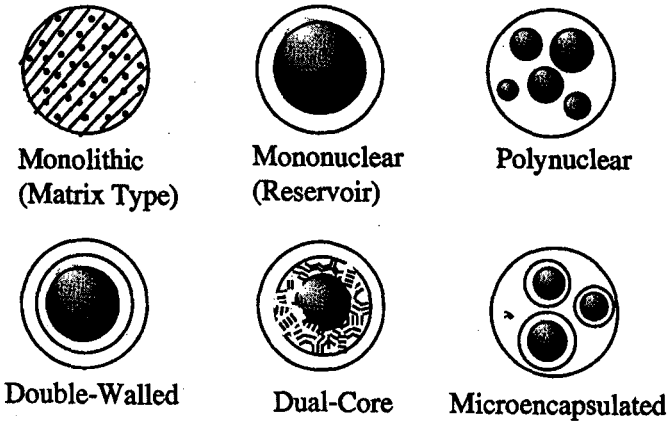

Figure 1.2 – Microcapsule morphologies.

Microencapsulation methods can be costly, but offer significant advantages such as protection of reactive components from light and oxidation, mixing of immiscible or incompatible materials, masking odor and controlled, sustained and triggered release.

The microencapsulation methods are often divided into physicochemical, mechanical, and chemical processes.[2] In the physicochemical methods, microcapsule shells are formed from preformed polymers by processes such as solvent removal, gelation or coacervation. Mechanical processes include a variety of spraying, coating and micronization processes. Chemical processes are essentially polymerization and polycondensation processes in which microcapsules walls are formed by *in-situ* polymerization. The polymers used in polycondensation encapsulations include a range of polyurethanes, polyureas, polyamides and polyesters, with different polymers offering different properties. In general, the core material, desired release pattern, and storage stability of the microcapsules affect the choice of the polymer used for the shell material. The compatibility of the core substance with the monomer mixture used in polycondensation encapsulation is critical and also influences the nature of the formed polymer. The search for less toxic and more biocompatible approaches in polycondensation encapsulations is another driving force for the development of new methods.

1.1 Interfacial Polycondensation Encapsulation

Interfacial polycondensation is one of the most common methods for preparing microcapsules. Chang introduced this method in 1960 for the preparation of artificial

cells.[3,4] Since then this method has been widely employed in biotechnology, industrial encapsulation, agriculture, and pharmaceuticals.

In interfacial encapsulation, two polycondensation reactants meet at the interface of the two immiscible phases and rapidly react to form a polymer film.[5] The encapsulation process can be divided into three major steps:

1. emulsification of the organic phase containing hydrophobic monomer into the continuous aqueous phase (or vise versa) containing suitable stabilizers,
2. addition of amine to the reaction mixture, and
3. rapid polycondensation of monomers at the interface.

Most of the literature concerning interfacial polycondensation encapsulations involves the formation of polyamide and polyurea microcapsules from hydrophobic terephthaloyldichloride (TDC) (in case of polyamide microcapsule formation, Figure 1.3) or di- and tri- functional isocyanates such as hexamethylenediisocyanate (HDI), and toluenediisocyanate (TDI) (in case of polyurea microcapsule formation Figure 1.4), with water-soluble polyamines such as diethylene triamine (DETA).

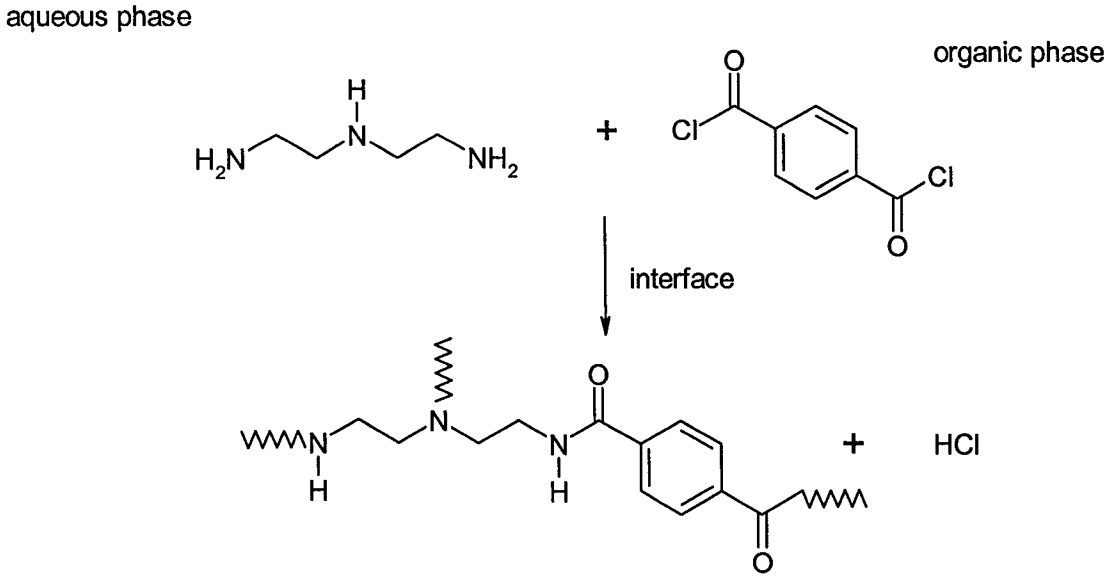

Figure 1.3 – Polyamide formation via interfacial reaction between TDC and DETA.

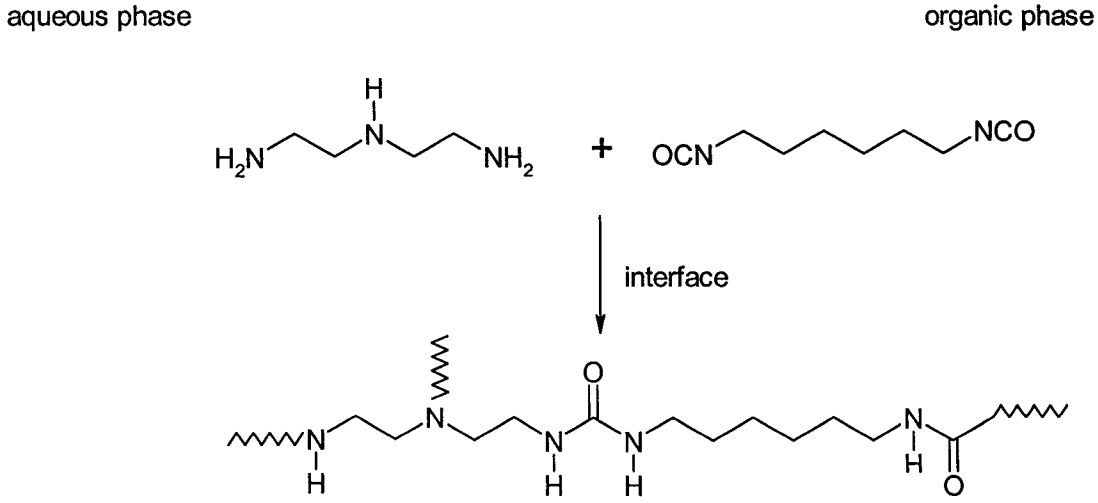

Figure 1.4 – Polyurea formation via interfacial reaction between HDI and DETA.

1.1.1 Interfacial Reaction

In the early 1950s a groups of chemists, lead by Emerson L. Wittbecker, Paul W. Morgan and Stephanie L. Kwolek, in the Textile Fibers Department, Pioneering Research Laboratory of the DuPont Company began to explore interfacial polycondensation as a route to polymers that could not be prepared by melt polymerization techniques.[6] Interfacial polycondensation offers an elegant and easy way for the preparation of high molecular weight polymers, that does not require a stoichiometric balance of the two monomers, high temperatures, nor sophisticated laboratory equipment. A wide variety of polyamides, polyurethanes, polysulfonamides, polyurea and polyphenyl esters may be prepared in this fashion from reactive monomers. Their preparation, as well as principles of interfacial polycondensation and parameters affecting polymer formation at the interface, are well described in a collection of 11 papers published in *the Journal of Polymer Science* **1959,** *XL*, 289-418.

One of the most well-known interfacial reactions involves the condensation between adipoyl chloride dissolved in an organic phase and hexamethylenediamine (HMDA) dissolved in an aqueous phase, to produce the polyamide Nylon 6,6 (Figure 1.5).

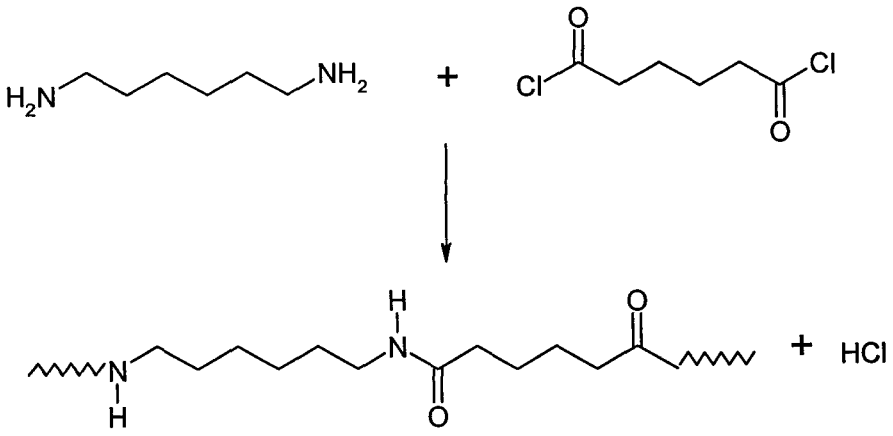

Figure 1.5 - Formation of Nylon 6,6.

Interfacial polycondensations can be performed under unstirred or stirred conditions.[7] In the stirred interfacial procedure the two phases are combined rapidly with vigorous agitation. Detergents such as sodium lauryl sulfate are often used as an aid to better mixing. Although, the order of monomer addition is not important in stirred interfacial polycondensations and sometimes reverse compared with the encapsulation procedure, there is no doubt that this technique is the first prototype of the interfacial polycondensation encapsulation.

1.1.2 Emulsification

The first step in interfacial encapsulation method is the production of a stable emulsion of desired size. The size distribution of the emulsion droplets and final microcapsules is a function of many parameters including the design of the vessel in which they are produced, stirring speed, emulsifying time, and the type and the concentration of the stabilizer used. The emulsification step also affects the wall thickness of the formed microcapsules.

1.1.2.1 Stabilization

Stabilizers decrease the droplet size by lowering the oil-water interfacial tension, and control the particle size by suppressing droplet coalescence and coagulation. There are two methods by which emulsion droplets can be stabilized: electrostatic stabilization and steric stabilization.

Electrostatic stabilization involves the introduction of a charged layer, either anionic or cationic, on the surface of emulsion droplets by use of ionic surfactants. Ionic surfactants are much more effective than non-ionic surfactants in decreasing the interfacial tension. Therefore, smaller particles are usually produced when ionic surfactants are employed. Electrostatic stabilization provides the emulsion droplets and forming microcapsules with a potential energy barrier via Coulombic repulsion, which prevents droplets coalescence. Ionic surfactants on the droplet surface are accompanied

by an equal number of counterions in the surrounding medium to maintain electroneutrality. The charged groups and their counterions create an electrical double layer, that stabilizes the emulsion droplets by electrostatic repulsion (Figure 1.6). The thickness of this double layer is a function of the ionic strength of the dispersion medium.

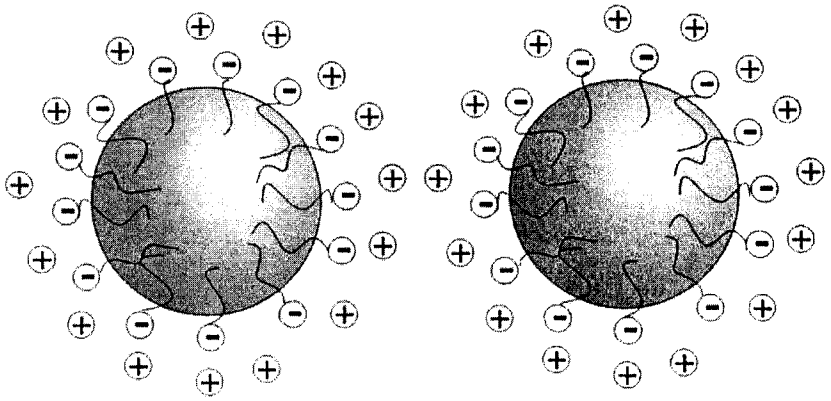

Figure 1.6 – Electrostatic stabilization of emulsion droplets.

Anionic surfactants include fatty acid soaps (sodium or potassium stearate, laurate, palmitate), sulfates and sulfonates (sodium dodecyl sulfate and sodium dodecylbenzene sulfonate). Sodium dodecyl sulfate is probably the most common example of an ionic surfactant family (Figure 1.7).

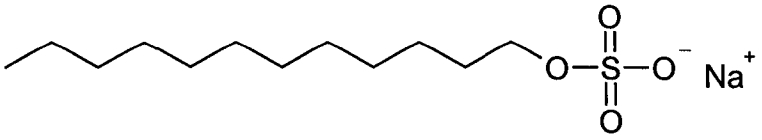

Figure 1.7 – Structure of SDS.

Small ionic surfactants are rarely used in interfacial encapsulation procedures, probably due to the high sensitivity of the formed microcapsules to changes in pH over a wide range. Higher molecular weight surfactants such as lignin sulfonates have been explored more often recently.

Steric stabilization is overall still the most common method of stabilization in interfacial encapsulation procedures. The most effective steric stabilizers are block and graft copolymers, in which part of the copolymer molecule is soluble in the dispersion medium and part is soluble in the dispersed phase. The mechanism of stabilization involves a repulsive force between the particles that results from osmotic pressure. When two droplets approach each other the concentration of polymer chains in the overlap region between them increases. This leads to a corresponding osmotic force that tries to dilute the polymer chains and in the process pushes the droplets apart (Figure 1.8)

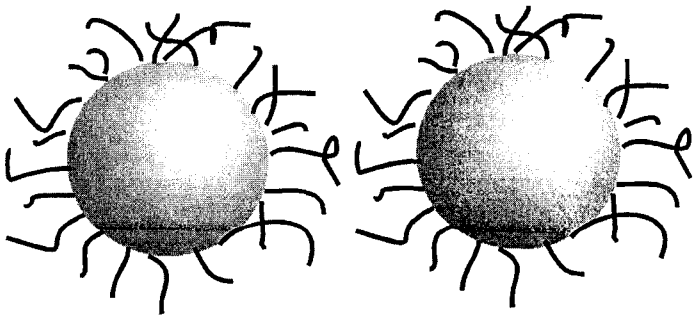

Figure 1.8 – Steric stabilization of emulsion droplets.

Stabilizers such as partially hydrolyzed poly(vinyl acetate) (PVA), polyvinylpyrrolidone (PVP), gelatin, polyoxyethylene derivatives of sorbitan fatty esters (Tweens), polyoxyethylene fatty ethers (Brijs) and polyoxyethylene phenyl ethers (Igepals) are often used in interfacial encapsulations. The interfacial tension between oil and water interface decreases with increasing stabilizer concentration, up to the point where complete coverage of oil droplet is achieved.

1.1.2.2 Effect of Steering Speed

A great number of articles have been published dealing with the experimental investigation of the effect of agitation rate on the droplet size distribution in liquid-liquid dispersion systems.[8,9,10,11,12] In principle, the mean size of the droplets in a liquid-liquid dispersion is determined by the balance between the turbulent forces tending to break up the droplets, and the interfacial tension and viscosity forces holding a droplet together. Therefore, the droplet size distribution shifts to smaller diameter with increasing agitation rate since the turbulence energy required for drop breakage increases. For example, it was found that in terephthaloyldichloride / diethylene triamine systems an increase in emulsification speed brings about the formation smaller capsules with relatively narrow size distribution.[9, 11, 13] However, at a certain agitation speed a limiting diameter value is achieved, and droplet diameter remains constant.

1.1.2.3 Effect of Emulsification Time

A two-phase system in an agitated vessel requires a certain length of time to establish equilibrium between breakup and coalescence of the droplets. This time varies from several minutes to several hours, depending on the dispersion system. For example, Langner et *al.* required 2 hours to reach constant droplet sizes in polymerizing and non-polymerizing styrene/water emulsions.[14] However, such long emulsification times are undesirable in interfacial encapsulations due to the possible hydrolysis of the oil soluble monomer. Therefore, short emulsification times, on the order of a few minutes, are commonly used in interfacial encapsulations, even if the oil droplets have not reached their equilibrium size yet.

1.1.2.4 Effect of Oil Phase

The correlation between droplet mean diameter d to the vessel geometry and the physical properties of the dispersion system is described in equation 1.1.[15]

$$d/D_I = b(1+c\varphi)(N_{We})^{-0.6} \qquad 1.1$$

where $N_{We} = \rho_c(N^*)^2 D_I^3/\sigma$ is the Weber number of the main flow, D_I is the diameter of the impeller, N^* is the impeller speed, ρ_c is the density of the continuous phase, σ is the interfacial tension, b and c are correlation parameters, and φ is the volume fraction of the dispersed phase. Thus an increase in the dispersed phase volume fraction shifts the average droplet size to a larger diameter, due to the higher droplet collision and coalescence frequencies.

The viscosity of the dispersed phase also affects the size of the droplets. In general high-viscosity oil phases show a greater resistance to breakage and deformation than low-viscosity liquids.[15,16,17] Consequently, they form larger and more stable emulsion droplets compared to the low-viscosity ones. Therefore, emulsions with broad droplet size distribution are obtained when the viscosity of the internal phase is increased.

1.1. Encapsulation

The second step of interfacial encapsulation process is the interfacial reaction itself, which starts with an addition of polyamine to the continuous aqueous phase. The oil droplets formed during emulsification now serve as "templates" for the formation of interfacial capsule walls.[18] The particle formation processes typically involve diffusion of the amphiphilic polyamine into the organic phase, to form a growing polymer wall on the organic side of the interface. The final morphologies of wall and capsule are determined largely by the polymer - core solvent interactions. Two extreme situations are described, leading to the formation of matrix systems and microcapsules (hollow particles), respectively (Figure 1.9).

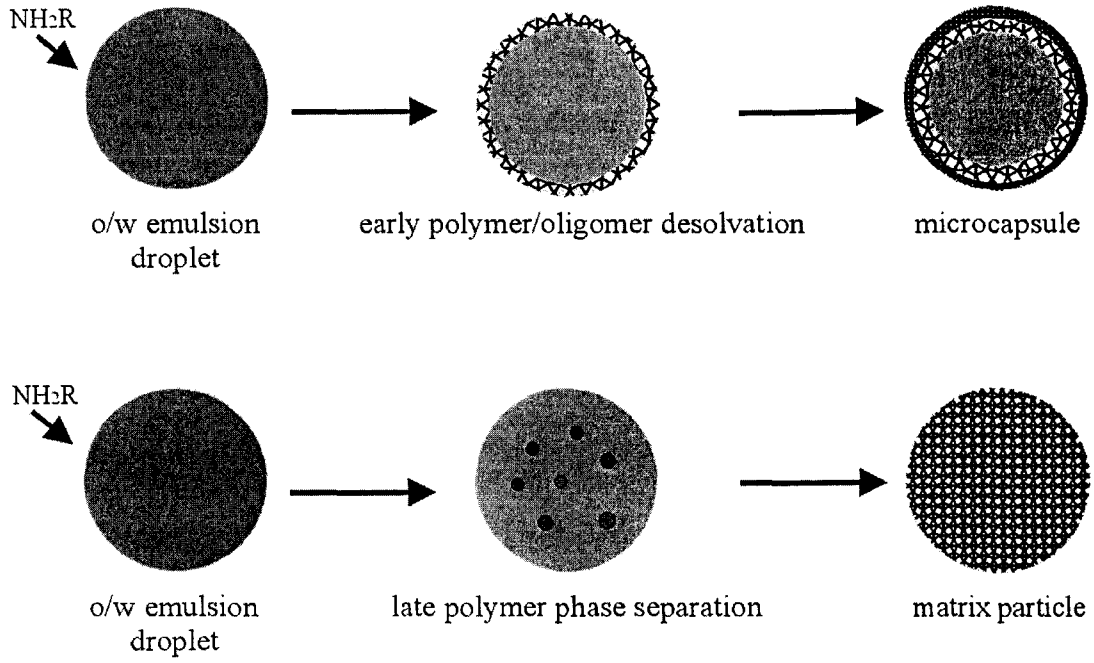

Figure 1.9 –Mechanism of particle formation by interfacial encapsulation.

When the initially formed oligomers are highly soluble in the droplet phase they grow inside the droplet, irrespective of where they are formed. This leads to the formation of solid particles (matrix structures). However, when the initially formed oligomers are insoluble in the droplets, they tend to desolvate and collect at the oil-water interface. Under these conditions, the precipitated oligomer/polymer chains initially form a thin membrane around the droplets. Further polycondensation, usually occurring on the oil side of the membrane, then leads to the formation of a polymer shell around the droplet, and ultimately to hollow particles. Intermediate situations are observed for moderate

polymer / core solvent interactions. Thus, when short polymer chains formed at the initial stages of the encapsulation are soluble in the droplets, but precipitate during the course of the polycondensation, this may cause the formation of more or less porous walls, depending on the degree and rate of polymer precipitation inside the droplets / particles.

The process of microcapsule formation proceeds in three stages: initial period, membrane formation and membrane growth.

1.1.3.1 Initial Period of Microencapsulation

The initial period of polycondensation leads to formation of the first thin film of polymer around the oil droplets. In the polycondensation encapsulation with sebacoyl chloride (SBC) and hexamethylenediamine (HMDA), the solubility of SBC in aqueous phase is negligible, while HMDA can partition into the organic phase. Therefore, the locus of polymerization is in the organic phase. The reaction between isocyanates and polyamines is similarly localized on the organic side of the interface.

1.1.3.2 Membrane Formation and Growth

The process of the membrane formation and growth is largely controlled by the solvency of the medium. Thus, the solvent should favor the precipitation of the formed polymer at the interface, but it also should allow the in-diffusion of the polyamine, required for continued growth of the wall membrane.[7,18,19,20] The diffusion of the

polyamine will be improved by the swelling of the membrane by the organic phase. The strength of the polymer-solvent interactions will influence not only the morphology, the thickness of the formed wall, but also the conversion of the polymerization. The polymerization rate is also influenced by the rate of mass transfer of the polyamine.[21]

1.1.3.3 Polymer-Solvent Interactions

The choice of the organic phase in interfacial encapsulation procedures is extremely important and must be directed by a clear understanding the polymer-solvent interactions. The comparison between the solubility parameters of the polymer and the solvent provides the guideline for the prediction of the polymer-solvent relationship during encapsulation procedures. The definitions of the solubility and interaction parameters and methods for the measuring the former are described below.

The process of dissolving a solute, whether it be a small molecule or an amorphous polymer, is governed by the free energy of mixing, ΔG_m, as shown in Equation 1.2,

$$\Delta G_m = \Delta H_m - T\Delta S_m \qquad (1.2)$$

where ΔH_m and ΔS_m are the enthalpy and entropy of mixing, respectively, and T is the temperature in Kelvin. A negative ΔG_m predicts that dissolution will occur spontaneously, driven by either the enthalpic or the entropic term, or by both. For an ideal

solution, in which the solute and solvent are similar in dimension, the entropy of mixing is always positive, and the solute-solute, solute-solvent and solvent-solvent interactions are equal such that ΔH_m is zero, and mixing is entropy driven. However, polymer solutions typically exhibit non-ideal characteristics because polymer-solvent interactions are rarely equal to solvent-solvent interactions, leading to a non-zero enthalpic terms ΔH_m. In addition, deviations from ideal behavior for the entropy of mixing exist, because the solute, for instance an amorphous polymer, and the solvent molecules have very different dimensions. Nevertheless, the dissolution of a high-molecular-weight molecule such as a polymer almost always leads to a net increase in entropy. Therefor, the sign and magnitude of the enthalpy term usually is the deciding factor in determining the sign of the Gibbs free energy change, and hence whether dissolution will occur or not. Flory and Huggins attempted to describe the non-ideal enthalpic behavior of polymeric solutions in term of contact energy.[22] The Flory expression of the enthalpy of mixing is described in Equation 1.3.

$$\Delta H_m = kT\chi n_1 \phi_2 \qquad (1.3)$$

where k is the Boltzmann constant, n_1 is the amount of solvent, ϕ_2 is volume fraction of polymer, and χ is known as the Flory-Huggins interaction parameter and is a very

important measure in polymer science as it relates the effect of the polymer chains on the energetic state of the solvent molecule. This term predicts that a polymer will be soluble in a given solvent for values of χ smaller than 0.5. This parameter is specific to a particular polymer-solvent combination. However, the Flory-Huggins theory has limitations and is not always easy to use. On the other hand a simple and useful method to estimate the polymer-solvent interactions was needed to solve some commonly encountered problems in industry. For example, the initial choice of an elastomer for the seals in the landing gear of the DC-8 aircraft resulted in serious jamming because the seals became swollen when in contact with the hydraulic fluid. This almost led to grounding of the plane but replacement with an incompatible elastomer made from ethylene-propylene copolymer rectified the fault.[22]

To avoid such problems Hildebrand's semi-empirical approach based on the premise that "like dissolves like" may be used to estimate polymer solubility.[23, 24] Hildebrand modified an equation originally developed to calculate the enthalphy of mixing from the vapor pressure of a binary mixture of liquids. The modified equation is of the form,

$$\Delta H_m = V\left(\left(\frac{\Delta E_1^v}{V_1}\right)^{1/2} - \left(\frac{\Delta E_2^v}{V_2}\right)^{1/2}\right)^2 \phi_1\phi_2 \qquad (1.4)$$

where **V**= volume of the mixture, ΔE_i^v= energy of vaporization of species ***i***, V_i = molar volume of species ***i***, ϕ_i = volume fraction of ***i*** in mixture. The Hildebrand solubility parameter, δ, is defined as $\delta = (c_i w_{ii}/2v_i)^{1/2}$ where c_i is the number of contacts one molecule can make with other molecules, w_{ii} is the interaction energy of the different molecular contacts, and v_i is the molar volume. ΔE_i^v is the energy required to vaporize a volatile liquid since the molecules are taken from their equilibrium distance to an infinite separation in the vapor phase where all the c_i contacts with w_{ii} energy are broken. Therefore the solubility parameter definition can be rewritten using the cohesive energy density (CED), ΔE_i^v per cm^3 as follow,

$$\delta_i = \left(\frac{\Delta E_i^v}{V_i} \right)^{1/2} \qquad (1.5)$$

The incorporation of Equation 1.5 into Equation 1.4 gives the heat of mixing per unit volume for a binary mixture (Equation 1.6).

$$\frac{\Delta H_m}{V} = (\delta_1 - \delta_2)^2 \phi_1 \phi_2 \qquad (1.6)$$

For small molecules the solubility parameter can be measured in a straightforward manner, however, in the case of polymers, which are not vaporizable, the solubility parameter must be estimated. This is typically done by assigning it the solubility

parameter of the small molecule that swells a lightly crosslinked version of the polymer the greatest, or alternatively, that of the molecule which produces the highest intrinsic viscosity of the polymer solution. For an ideal solution the enthalpy of mixing is zero and therefore $\delta_1 = \delta_2$. In practice, polymers usually dissolve when the difference between the solubility parameters of the polymer and the solvent is less that approximately 2 $(cal/cm^3)^{1/2}$. However, while the Hildebrand solubility parameter describes the enthalpy change on mixing of nonpolar systems well, it does not give uniform results when extended to polar and hydrogen-bonded systems. Here it is sometimes observed that polymers dissolve even through their solubility parameters are considerably different. To explain this observation, Hansen divided the single solubility parameter into a three dimensional solubility parameter comprised of a hydrogen-bonding term, a dipolar term, and dispersion term. For many polar solvents where hydrogen-bonding and dipolar interactions are dominant, this method is much more accurate for predicting solubility.[25]

Equation 1.7 relates the Hildebrand solubility parameter and the Flory interaction parameter.[26]

$$\chi = 0.34 + \frac{V_1}{RT}(\delta_1 - \delta_2)^2 \qquad (1.7)$$

The effective solubility parameter of a mixture of solvents δ_m, can be estimated from Equation 1.8,

$$\delta_m = \phi_a \delta_a + \phi_b \delta_b \qquad (1.8)$$

where ϕ_a, ϕ_b and δ_a, δ_b are the volume fractions and the solubility parameters of the solvents a and b, respectively.[27,28] Consequently, dissolution of a polymer may be observed in a mixture of solvents where the individual solvents would not dissolve the polymer.

1.1.3.4 Membrane Morphology

Microcapsules prepared by interfacial encapsulation typically have an asymmetric wall morphology consisting of a dense skin and a more porous sub-layer.[29, 30,31,32,33] Figure 1.10 shows the cross-section transmission electron image of a typical polyurea microcapsule.[34]

Figure 1.10 –Asymmetrical wall morphology of polyurea microcapsules.

This morphology is the result of a two step mechanism of membrane formation and growth. In the early stage of the polymerization the dense top-layer is formed, if the correct solvency conditions are met. The polymerization rate at this stage is limited by the rate of transport of amine molecules into the organic phase. Once a membrane skin has been formed, further growth of the membrane is determined by the relative permeabilities of the skin to the reacting monomers, and by the respective monomer solubilities in the two phases. In the case of polyamide and polyurea membranes, where the membrane growth occurs on the organic side of the interface, the growth rate of the membrane sublayer as well as its morphology are controlled by the diffusion of amine through the membrane skin.

Several authors have tried to explain the porous morphology of the sub-layer. Janssen and te Nijenhuis[34] reported that they were able to detect small droplets on the organic side of the membrane. Based on this observation they proposed that the volume of the organic phase decreases during the wall formation, and as a consequence water diffuses in and causes the formation of the aqueous phase droplets on the organic side of the wall. The continuously formed polymer on the organic side precipitates out around these droplets causing the formation of porous membrane structures. Toubeli and Kiparissides[35] offered a different explanation for the porous structure of the sublayer. They considered the polyamide capsule membrane to be formed by aggregation of unstable colloidal particles linked by amide linkage. Accordingly, polyamide chains formed in the organic phase would precipitate to form unstable colloidal particles, having some unreacted amine and carboxylic groups on their surface. Aggregation of these particles would then lead to the formation of a low density structure, which would continue to react and to became more and more dense. The size and the arrangement of the polyamide micro-particles would determine the scale of heterogeneity and the porosity of the primary membrane skin. The size of the basic colloidal particles would in turn depend on the polymerization rate (e.g. monomer concentration at the reaction front), the polymer solubility in the organic phase and the number of particles formed. The membrane porosity would be controlled by the molecular properties of the colloidal particles (e. g. polymer composition, degree of crosslinking, and number of unreacted surface functional groups), the size of particles as well as the rates of particles formation

and aggregation. They postulated that since the rate of polymerization changes during the membrane growth, the size, number of colloidal particles linked and particle arrangement is also changing, causing the formation of sublayers with a more porous morphology than seen in the original skin.

The porosity and structure of the capsule walls can be controlled by a number of factors such as the chemical character and concentration of the monomers, the type of organic solvent, the crystallinity of the forming polymer, and the temperature of the reaction. For example, Alexandridou et *al.*[36] showed that capsules produced by the interfacial condensation of terephthaloyl dichloride (TDC) and diethylene triamine (DETA) have porous morphology. However, addition of HMDA to the aqueous DETA resulted in microcapsules with smooth and dense membrane walls. Toubeli and Kiparissides[35] reported that the (DETA, TDC) membrane morphology was significantly affected by the initial concentration of DETA. It was found that the skin roughness and porosity of the polyamide membranes increased with the DETA concentration. At the same time, the sublayer porosity decreased as the DETA concentration increased. Vanbesien[37] reported that increasing the temperature of the interfacial polyurea condensation encapsulation has a significant effect on capsule morphology. Microcapsules with a thicker and denser sublayer were produced at high temperatures. Solvency as discussed previously affects the rate of the polycondensation reaction and hence the morphology of the formed microcapsules.[2]

In summary, microcapsule morphology can be controlled through experimental parameters. As a result, the release from these microcapsules can regulated to the some extend as will be discussed in the following sections.

1.2 Controlled-Release Microcapsule Systems

1.2.1 Controlled-Release Technology in Agriculture

In recent years, controlled-release (CR) technology has found major applications in the delivery of a wide range of bioactive molecules such as fertilizers, pesticides, insecticides, and pheromones.[38,39,40] The CR systems have many benefits compared to traditional "straight concentrates" systems and the more innovative emulsion concentrates (EC) and dispersion concentrates (DC) systems. Their major advantages are

1) reduction of phytotoxicity,

2) increased persistence and, hence, lower amounts and frequency of application,

3) reduction of environmental pollution due to volatilization, drift, and leaching,

4) prevention of thermal, chemical, photolytic, or biological degradation of the active ingredient either on the foliage or in the soil,

5) reduction in handling hazards caused by dermal and inhalation toxicity..

In spite of these advantages, CR technology has not entered the agricultural sector in a significant way until recently. Reasons for this delay include the processing cost, the cost of polymer matrices with controlled release properties, carry-over problems, and delay in the active ingredient absorption rate. The present market in agricultural products for CR systems is less than 5 % of the overall agricultural market.[41] However, the recent developments in CR systems for the pharmaceutical market, and increased concerns about the environmental safety of the existing agricultural products pushed the agricultural industry to renew its attention to CR technology. In agriculture, the CR technology covers four major areas: 1) chemical pesticides, herbicides and fungicides, 2) fertilizers and nutrients, 3) peptides, proteins, and viruses and 4) pheromones. Of these, the major CR product developments have taken place in the delivery of chemical pesticides and several commercial products are on the market at present. The use of pheromone-release systems is next in importance, with applications such as trapping and mating disruption.

1.2.2 CR Devices

CR systems for the delivery of chemical pesticides are typically based on microencapsulation methods, in particular those based on interfacial polycondensation, coacervation and in-*situ* polymerization. Among these, interfacial polycondensation is the most useful method for industrial production. The size and wall thickness of the

resulting microcapsules can be controlled relatively easily by controlling the amount of monomers, and the process conditions.

On the other hand, different approaches compete for the worldwide market in controlled release of sex pheromones used both for monitoring, and mating disruption, of insect pests.[42, 43, 44] Besides active devices such as automatic dispensers, these include different passive devices such as polymer membranes, rubber septa, plastic flakes, pheromone-saturated twist-ties, and hollow fibers. Generally, the inherent shortcoming of these passive, matrix type devices is the necessity to fulfill a dual function in providing a pheromone release surface as well as serving as a reservoir for the pheromone. Thus, the rate at which pheromone is released decreases as its concentration in the dispersing device, or the surface area wetted by the pheromone, decreases. This means that the most desirable zero order release can not be obtained and that dispensers need to be replaced at regular, relatively short intervals to maintain both the integrity of the trapping system and optimum pheromone release level for the insect concerned. Therefore, the agricultural industry turned towards the microencapsulation as the most practical, cheap and easy to control method of delivering pheromones. In addition, previous experience with the encapsulation of chemical pesticides can be utilized in the development of methods for the microencapsulation of pheromones. The main advantages of microcapsule formulations are that:

1) the formulations can be diluted with water or liquid fertilizers and sprayed

using conventional equipment, allowing uniform field coverage

2) the formulation is composed of discrete, sprayable particles as opposed of aggregates, and

3) the release rate can be varied to some degree by varying the microcapsules size, wall thickness and the microcapsule wall permeability.

Polyurea as well as polyamide microcapsules have been extensively used for the encapsulation of pesticides and pheromones. [45,46,47,48,49,50]

The main advantage of polyurea microencapsulation, compared with polyamide microencapsulation, is that the polyaddition reaction does not yield hydrogen chloride as the side product, so hence a neutralizing base is not required in the aqueous phase (Figure 1.3 and 1.4). Another advantage of the polyurea microencapsulation is that the microcapsules can be produced in the absence of polyamine via hydrolysis, as described by Scher. This reaction proceeds through carbamic acid and subsequent decarboxylation to the amine, which then reacts with a second isocyanate to form a urea linkage (Figure 1.11). This process is usually carried out at higher temperature. It is facile and avoids the need to separate the encapsulated material from excess amines. Both versions of polyurea microencapsulation share two disadvantages, however:

1) their high reactivity toward active ingredients, such as fill components carrying hydroxyl, amine, or other nucleophilic groups. and,

2) isocyanates, and in particular the more volatile components, are known sensitizers that can induce strong allergic reactions after repeated exposure.

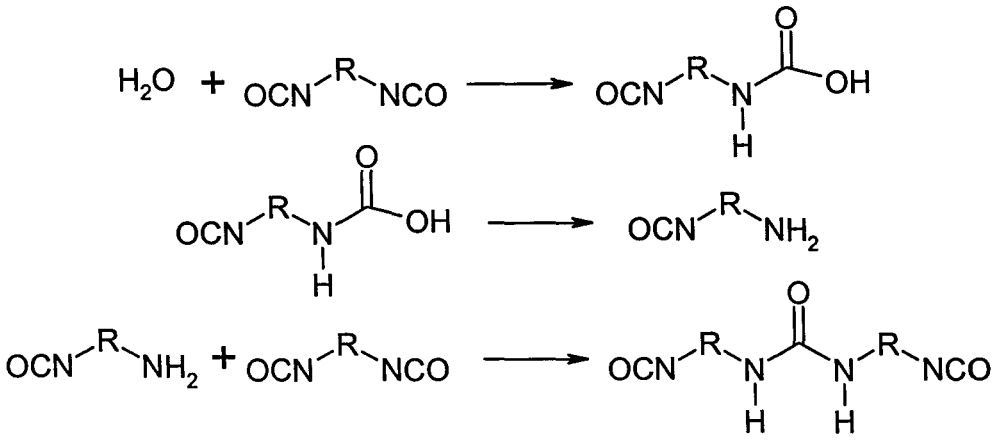

Figure 1.11 – Polyurea formation via hydrolysis.

1.2.3 Microcapsule Release Kinetics

In diffusion-controlled release from non-degradable membrane devices, two distinct types of release devices dominate:

1) reservoir systems in which the active ingredient is encapsulated within rather thin release controlling membrane, and

2) monolithic systems wherein the active ingredient is dissolved in the release-controlling matrix.

The most common description of reservoir release follows Fick's diffusion equation. This equation assumes the rate of transport through a unit cross section to be proportional to the concentration gradient ($\partial c / \partial x$) along the x direction:

$$F = -D\left(\frac{\partial c}{\partial x}\right) \tag{1.9}$$

For a spherical reservoir this equation takes the following form:[5]

$$\text{Release Rate} = \frac{dM}{dt} = 4\pi DK\Delta C \frac{r_0 r_i}{r_0 - r_i} \tag{1.10}$$

where D = diffusion coefficient, K = distribution coefficient, ΔC = the concentration difference across the wall, r_i = the radius of the inner side of the membrane, and r_0 = the outer radius, therefore $r_0 - r_i$ = thickness of the microcapsule wall.

The above relation predicts that if the active ingredient is enclosed within a membrane, and if the concentration is maintained constant within this reservoir, then a steady state will be established during which the release rate would be zero order with regards to the amount of active ingredient. Equation 1.10 also demonstrates the relation between the thickness of the capsule wall (r_o-r_i) and the rate of release. As the wall of the capsule becomes thicker the rate of release from the capsule decreases.

On the other hand, monolithic systems in which the active ingredient is dissolved or dispersed in a polymer matrix, do not have zero-order release kinetics. Active ingredient is released from the surface layers of a matrix device first, and the distance that the encapsulated material must diffuse to reach the surface increases with time. Hence, matrix systems exhibit slowly declining rates of release. For the delivery of an active ingredient that has been dissolved in a spherical polymer bead of radius r_0, the solutions of Equation 1.9 to describe the rate of release are given as[41]

$$\frac{dM_t / M_\infty}{dt} = 6\left(\frac{Dt}{r_0^2 \pi}\right)^{1/2} - \frac{3Dt}{r_0^2} \qquad M_t / M_\infty < 0.5 \qquad (1.11)$$

$$\frac{dM_t / M_\infty}{dt} = 1 - \frac{6}{\pi^2}\exp\left(\frac{-\pi^2 Dt}{r_0^2}\right) \qquad M_t / M_\infty > 0.5 \qquad (1.12)$$

From these equations, it is apparent that the first 50% of encapsulated material is released at a rate, which decreases as the square root of time, while the rate of release of the remaining material drops off exponentially.

Although the theoretical release profile described in Equation 1.10 suggests a linear rate of release over time, the actual release curve for reservoir devices is more complicated. Figure 1.11 depicts a typically reservoir release curve.[5] Initially, a rapid

release of some of the active ingredient is commonly observed (region **I**, Figure 1.12). This so-called "burst effect" is common to many encapsulation systems, and is attributed to the presence of some active ingredient within the polymer wall, on the outer wall surface, and even in the continuous medium. The following region on the release curve is a zone of constant, or zero order, release rate (region **II**), which continues as long as the concentration of active ingredient, though not its total amount, remains constant in the core. The third region (region **III,** Figure 1.12) shows a drop-off in release as the result of the declining concentration of active concentration in the core of the microcapsules (first order release).

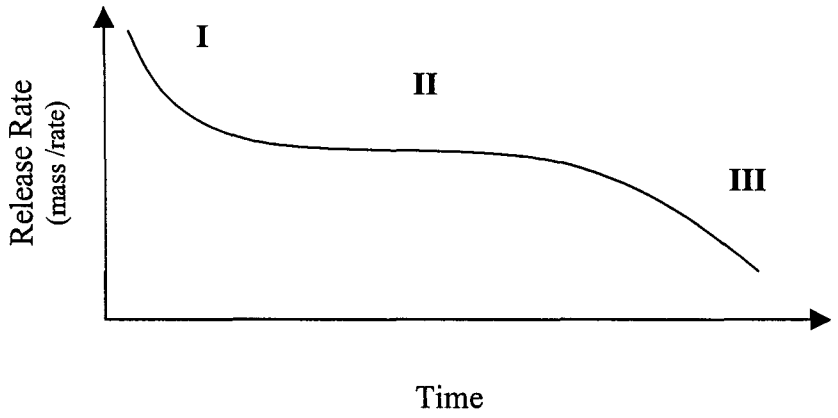

Figure 1.12 - A typical release rate profile of a pesticide from reservoir microcapsules.[5]

The process of diffusion controlled release from a mixed reservoir can be looked at as a membrane separation method. Several mechanisms have been reported to describe the transport in the membranes: transport through bulk material (dense membrane),

Knudsen diffusion in narrow pores, viscous flow through large pores or surface diffusion along pore walls.[51,52] In practice, the transport through the microcapsule membrane is a result of the combination of more than one mechanism due to the asymmetrical structure of most capsule walls. The rate of release through microcapsule walls is affected by the characteristics of the membrane (porosity, crystallinity, thickness, cross-linking density) as well as by the nature of the encapsulated material itself. For example, release may be accelerated if the active component has a higher affinity for the polymer walls, or if a plastizicer has been added to the capsules.[51] In this case release is enhanced due to the increased swelling and local mobility of the polymer chains in the capsule wall. However, the relation between the active component, the capsule walls and the release rate is made more complicated by the fact that the active influences the membrane morphology as well. Yadov *et.al.* gave a very elegant example of how to control both the morphology, and the release of cyclohexane, from non cross-linked polyurea capsules.[53,54] They prepared polyurea microcapsules with different degrees of crystallinity by changing the volume ratio of organic to aqueous phases, which under their experimental conditions was controlling the rate of polymerization. It was shown that permeability and hence the release rate of the encapsulated cyclohexane decreased with increasing crystallinity of the capsule walls.

A number of studies established the relationship between thickness and crosslink density of the microcapsule walls and the release rate.[55,32,5] It was experimentally shown

that increasing the wall thickness and cross-link density decreases the permeability and release from the microcapsules.

So far only the parameters and models, which affect and describe the diffusion-controlled release were discussed. However, the combination of the diffusion and the rupture release has also been observed in literature in case of polyamide microcapsules.[29,30,31,32,33] It was demonstrated that depending on the wall characteristics (permeability) the diffusion, rupture or the combination of the two release mechanisms can occur.

1.2.4 Release Determination

Determination of release kinetics plays a crucial role in the design and development of release devices. The relevance of release rates determined by any particular experimental method depends on the chemical or physical release mechanism and also on the medium for the release. Release from CR devices can be studied directly by measuring diffusion into a surrounding solution, or evaporation into air, or indirectly by measuring the residual active component remaining in the capsules, or even by measuring the effect on the area of impact (e.g. evidence of crop protection by encapsulated pesticide). The rates at which pheromones or any other volatile encapsulated material are emitted from a controlled-release formulation can be measured by three general methods: 1) collection of pheromone after release; [56] 2) extraction of

pheromone remaining in the formulation; [57,5] and 3) measurement of the loss in weight of the CR device after a definite period of exposure.[56] In general, measurement of pheromone release based on weight-loss is done by storing the device in a temperature-controlled room having a constant air-flow, and allowing diffusion to transport evaporated pheromone away from the formulation. In case where analysis of the compound can be done by spectrophotometry, extraction of the formulation at intervals of release can be very efficient.

1.3 Styrene-Maleic Anhydride (SMA) Copolymers

Alternating copolymers (ABABAB polymer chain structure) have significant scientific and industrial importance. Alternating copolymers of styrene and maleic anhydride (SMA) have been used for decades as adhesive and for coating applications.[58] They are easily formed by free radical copolymerization of maleic anhydride and styrene and modified by reacting the functional anhydride groups with different nucleophilies (Figure 1.13)

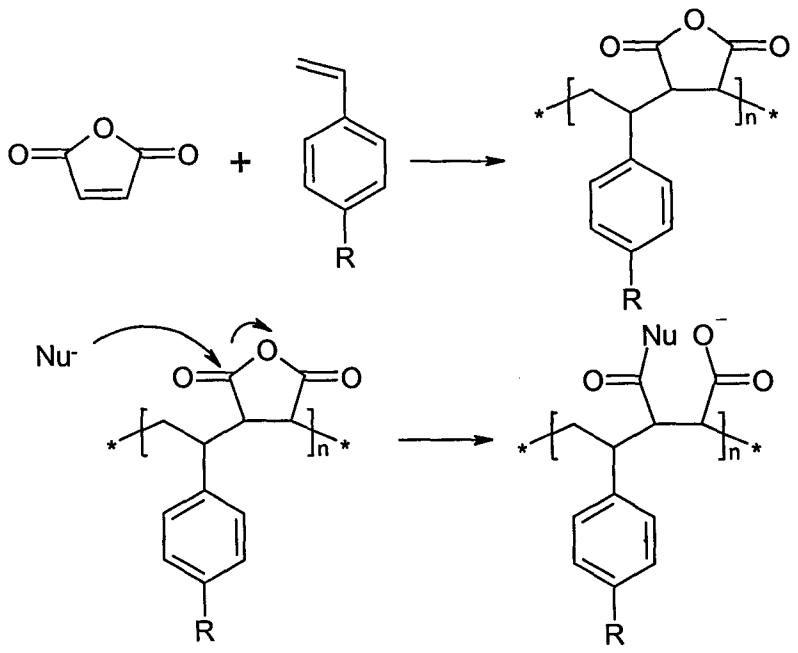

Figure 1.13 – Formation and reactivity of styrene-maleic anhydride type copolymers.

Modified styrene-maleic anhydride copolymers form stable monolayers, and good, heat stable LB films, and can be used in various fields such as electronics, coatings and material separation.[59] Mixed with starch, SMA copolymers are widely used in the paper industry as surface-sizing agents to enhance printability.[60] Recently, polyelectrolyte behaviours of the hydrolyzed SMA copolymers became of the focus of many researches. Such polyelectrolytes undergo various conformations transitions induced by changes in pH, [61,62] two-step dissociation process of dicarboxylate groups,[63,64] and binding of

counterions.[65,66] The ability of the alternating copolymers to assemble and form either intramolecular[67,68] or intermolecular[69] associates has also been investigated. Such interesting properties of SMA copolymers are attributed to the presence of both non-polar and polar groups on the same polymer, that interact through hydrophobic interactions, and hydrogen bonding and ionic interactions, respectively.

1.3.1 Kinetics of Free Radical Copolymerization

The mechanism of free radical copolymerization, similar to any radical polymerization, can be divided into three stages (Scheme 1.1). The first step in the free radical polymerization (initiation step) consists of the formation of radicals, usually by decomposition of a free radical initiator, and the addition of these primary radical to the monomer. 2,2′-azobisisobutyronitrile (AIBN) is a common example of a free radical initiator (Figure 1.14).

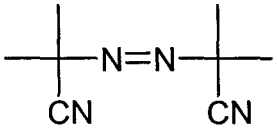

Figure 1.14 - Structure of AIBN.

The second step of the polymerization is the propagation step, which involves addition of monomers to the initial radicals to produce polymer chains.

The third and final step is the termination, involving radical destruction by two main mechanisms: combination, and disproportionation. Termination by combination occurs when two polymer radicals couple to form one inactive chain. Termination by disproportion takes place when a hydrogen radical that is located on a carbon *beta* to one radical center is transferred to another radical center. Radical chain transfer reactions to monomer or solvent are other mechanisms for termination, however these processes are often negligible and can be controlled by choosing appropriate experimental conditions. During the propagation step four reactions can occur (Scheme 1). The first two reactions demonstrate self-propagation and the second the cross-propagation.

Initiation

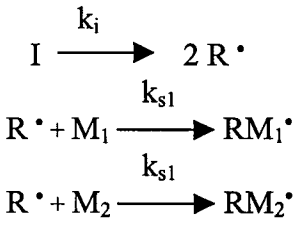

Propagation

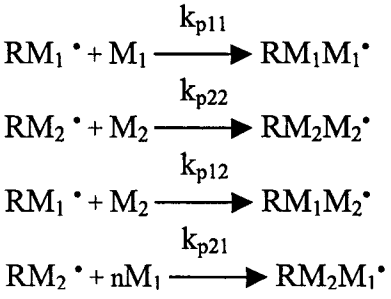

Termination by recombination

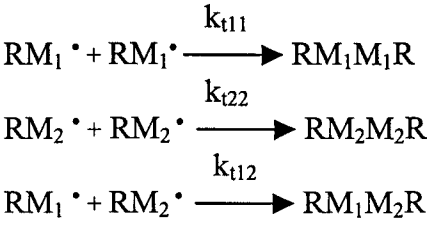

Termination by disproportionation

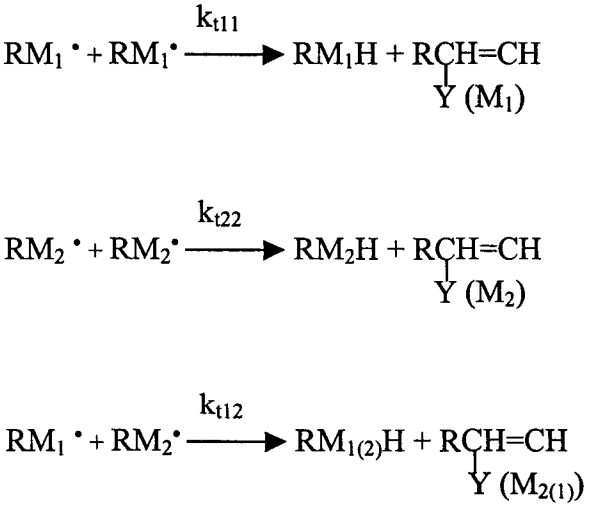

Scheme 1 – Stages of free radical copolymerization.

1.3.2 Formation of Alternative Copolymers

Many radical–initiated copolymerizations give near-random copolymers. In contrast, certain monomers, such as styrene and maleic anhydride are known to undergo alternating copolymerization regardless of the feed composition. The composition of the polymer prepared from two monomers M_1 and M_2 is determined by the relative reactivity ratios of the monomers, which is defined as follows,

$$r_1 = \frac{k_{p11}}{k_{P12}} \qquad r_2 = \frac{k_{p22}}{k_{P21}} \qquad (1.13)$$

where r_1 and r_2 are the relative reactivity ratios of monomers 1 and 2, and k_{p11}, k_{p22}, k_{p12}, k_{p21} are the propagation rate constants. In copolymerization of maleic anhydride and styrene crossed propagations dominate, and the values of the reactivity ratios accordingly are close to zero. The cross-propagations lead to a largely alternating structure of the formed copolymer. This behavior is characteristic of monomers with different electron donor (ED) – electron acceptor (EA) character. Alternating copolymerization of maleic anhydride (EA) and styrene (ED) was the focus of the intensive investigation since the mid-1940s. Several controversial theories to explain the mechanism of alternating copolymerization were developed. The most recent and widely accepted theory postulates that the alternating tendency arises from the partitioning of the charge-transfer complex (CTC) formed from maleic anhydride and styrene (Figure 1.15).[70]

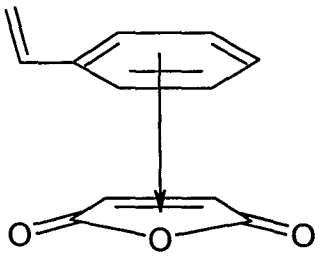

Figure 1.15 – CT complex of styrene and maleic anhydride.

According to this theory, ED and EA monomers can spontaneously form CTC's according to the equilibrium below:

$$ED + EA \rightleftharpoons \underbrace{[(ED\text{-}EA) + (ED^{+}EA^{-})]}_{\text{complex}}$$

nonbonded bonded

The concentrations of these CT complexes have been measured using both UV absorption and ^{1}H-NMR studies.[71] The styrene-maleic anhydride CT complexes are considered to be of the π-donor-π-acceptor type. The complex concentrations are influenced by the properties of the donor-acceptor pair itself, as well as by reaction conditions such as polymerization solvent and temperature.

There are two different mechanisms by which the CT complex can be added to the growing polymer chain.[72] The first is the so-called complex addition mechanism according to which both monomers add simultaneously to the propagating radical. The other mechanism is called complex dissociation mechanism. In this case, addition of the monomers does not take place at the same time; rather one monomer from the complex reacts with the chain end and the other monomer dissociates to become free monomer.

1.3.3 Random SMA Copolymers

To prepare a random, homogeneous copolymer with < 50 mol % of maleic anhydride groups, the concentration of maleic anhydride must be kept low during the reaction, and maleic anhydride must be added under controlled conditions. Continuous bulk polymerization techniques has been developed for the preparation of non equimolar styrene-maleic anhydride copolymers.[73] These copolymers are typically brittle, low molecular weight materials, that are soluble only in polar solvents such as acetone, methanol, and ethyl acetate. Copolymerization of styrene with maleic anhydride improves the physiochemical properties of the polymer by providing increased polarity, rigidity, glass transition temperature, and functionality.

1.4 Thesis Objectives

Hydrophobic building blocks or wall formers in encapsulation technology can be divided into two groups; monomers and preformed polymers. Monomers are used as building blocks in bond-forming, polycondensation encapsulation methods, while preformed polymers are utilized for the preparation of microcapsules based on physiochemical methods. An analogous division exists for hydrophilic wall formers, where water-soluble monomers such as urea and formaldehyde are used in bond-forming encapsulations, while preformed polymers such as gelatine and other polyelectrolytes are used to form walls by primarily electrostatic and hydrophobic interactions.

This thesis studies the formation and properties of capsule walls formed from several novel, preformed hydrophobic polymers. Both interfacial covalent, and photo-induced homogeneous dipolar bonding, are used to deposit these polymers at the interface and form capsule walls.

In particular, the thesis addresses the effect of hydrophobic polymer / core-oil interaction on the mechanism of the polymer microencapsulation, morphology of the formed particles, and the release from these particles.

During the course of this study two new methods of encapsulation were developed: interfacial encapsulation based on preformed styrene-maleic anhydride

(SMA) type copolymers as a new type of wall former, and photoinduced phase-separation encapsulation.

The interfacial encapsulation of SMA type copolymers involves the cross-linking reaction between an oil-soluble SMA copolymer and a water-soluble polyamine, or alternatively the hydrolysis reaction of *tert*-butylstyrene-maleic anhydride copolymers to produce non-cross-linked microcapsules. These methods are described in Chapter 2.

One of the most important aspects in interfacial encapsulations is the internal morphology of the produced microcapsules. The structure and porosity of the formed membrane affect not only the rate and conversion of the encapsulation reaction but also the release properties of the formed microcapsules. Chapter 3 investigates the factors that affect morphology transitions observed in SMA encapsulation systems and addresses the correlation between wall morphology and rate of the release from the SMA microcapsules.

In Chapter 4 the SMA microencapsulation was investigated on the molecular level. The issues of chemical conversion, rates of reaction, and the possibility of side reactions were addressed in this Chapter, as well as the development of a method for interfacial encapsulations at constant pH.

The last chapter of this thesis describes a physical, "pure" solvency based approach to capsule wall formation. The work presented in Chapter 5 was designed to test the possibility for the internal photoinduced phase-separation encapsulation.

This approach entirely removes the need for selective evaporation of a solvent component, or addition of a cross linking reagent. It is based on reducing the solubility of azobenzene-containing polymers in near *theta* core solvents by a reversible photochemical reaction of the polymer itself.

References

1) Proceeding of the American Chemical Society. *Symposium on Microencapsulation: Processes and Aplications* Chicago 1973.

2) Arshady, R. Manufacturing Methodology of Microcapsules in Microspheres Microcapsules and Liposomes Volume 1: Preparation and Chemical Apllications Archady R. (Ed), Citus Books, London 1999.

3) Chang, T. M. S.; Poznansky, M. J. *Nature*, **1968**, *218(5138)*, 243-245.

4) Chang, T. M. S. Recent advances in artificial cells with emphasis on biotechnological and medical approaches based on microencapsulation, in Donbrow M. (Ed), Microcapsules and Nanoparticles, CRC Press, Boca Raton, FL 1992, 323-359.

5) Scher, S. B. *Controlled Release Pesticides*, American Chemical Society 1977.

6) Kwolek, S.L. *J. Polym.. Sci.: Part A: Polym. Chem.* **1996**, *34*, 517-518.

7) Wittbecker, E. L.; Morgan, P. W. *J. Polym. Sci.* **1959**, *XL*, 289-297.

8) Chatzi, E. G.; Kiparissides, C., *Chem. Ing. Sci.* **1992**, *47*, 445-456.

9) Poncelet de Smet, B.; Poncelet, D.; Neufeld, R. J. *Can. J. Chem. Eng.*, **1990**, *68*, 443-448.

10) Tan, H. S.; Ng, T.H.; Mahabad, H. K. *J. Microencapsulation*, **1992**, *8*, 525-536.

11) Yan, N.; Zhang, M.; Ni, P. *J. Microencapsulation,* **1994**, *11*, 365-372.

12) Yan, N.; Ni, P.; Zhang, M., *J. Microencapsulation,* **1993**, *10*, 375-383.

13) Shigeri, Y.; Kondo, T. *Chem. Pharm. Bull.* **1969**, *17*, 1073-1075.

14) Langner, F.; Moritz, H.-U.; Reichert, K. H. *Chem .Ing. Technol.,* **1979**, *51*, 746.

15) Bachtsi, A. R.; Costas, J. B.; Kipararissides, C., *J. Appl. Polym. Sci.* **1996**, *60*, 9-20.

16) Sanghvi, S.P.; Nair, J. G., *J. Microencapsulation* **1992**, *9*, 215-227.

17) Sanghvi, S.P.; Nair, J. G., *J. Microencapsulation* **1992**, *10*, 181-194.

18) Arshady, R. *J. Microencapsulation* **1989**, *6*, 13-28.

19) Morgan, P.W.; Kwolek, S.L. *J. Polym. Sci* **1959**,. *XL*, 299-327.

20) Zydowicz, N.; Chaumont, P.; Soto-Portas, M. L., *J. Membrane Sci.,* **2001**, *189*, 41-58.

21) Jansen, L.J.J.M.; Nijenhuis, K., *J. Membrane Sci.,* **1992**, *65*, 59-68.

22) Cowie, J.M.G. *Polymers: Chemistry and Physics of Modern Materials;* Blackie: New York, 1991.

23) Hildebrand, J.H., Scott, R.L., "Solubility of Non Electrolytes", Reinhold, New York, 1950.

24) Scatchard, G., *Chem. Revs.,***1931,** *8*, 321-334.

25) Guettaf, H.; Iayadene, F.; Bencheikh, Z.; Saggou, A.; Rabia, I. *Eur. Polym. J.* **1998,** *34*, 241-246.

26) Grulke, E.A. In *Polymer Handbook;* Brandrup, J., Immergut, E.H., Grulke, E.A., Eds.; Wiley-Interscience: New-York, 1999; pp 675-714.

27) Okubo, M.; Ichikawa, K.; Tsujihiro, M.; He, Y., Colloid and Polym. Sci. **1990,** *268*, 791-796.

28) Barret, K.E. J. *Dispersion Polymerization in Organic Media;* John Wiley and Sons: Toronto, 1975.

29) Mathiowitz, E.; Cohen M.D., *J. Membrane Sci.,* **1989**, *40*, 1-26.

30) Mathiowitz, E.; Cohen M.D., *J. Membrane Sci.,* **1989**, *40*, 27-42.

31) Mathiowitz, E.; Cohen M.D., *J. Membrane Sci.,* **1989**, *40*, 43-54.

32) Mathiowitz, E.; Cohen M.D., *J. Membrane Sci.,* **1989**, *40*, 55-65

33) Mathiowitz, E.; Cohen M.D., *J. Membrane Sci.,* **1989**, *40*, 67-86.

34) Croll, L.M. *Unpublished Results.*

35) Toubeli, A.; Kiparissides, C., *J. Membrane Sci.,* **1998**, *146*, 15-29.

36) Alexandridou, S.; Kiparissides, C.; Fransaer, J.; Cellis, J.P., *Surf. Coatings Technol.* **1995**, *71*, 267-276.

37) Vanbesien, D.W. In Master Degree Thesis, Mc Master University 1999.

38) *Herbicide Handbook*, 4th ed., Weed Science Society of America, Champaign, IL, 1979.

39) Thies, C. in *Encyl. Chem. Technol., Kirk-Othmar,* 4th ed., John Wiley & Sons, New York, **1995**, *16*, 627-651.

40) Hill, I.R.; Wright, S.J.L. *Pesticides Microbiology*, Academic Press, London, **1978**, *16*, 112-120.

41) Dave, A.M.; Mehta, M.H.; Aminabhavi, T.M.; Kulkarni, A.R.; Soppimath, K.S. *Polym.-Plast. Technol. Eng.,* **1999**, *38(4)*, 675-711.

42) Butler, L. I.; McDonough, L.M. *J. Chem. Ecol.* **1981**, *7*, 627-633.

43) Vrkoč, J.; Konečný, K.; Valterová, I.; Hrdý, I. *J. Chem. Ecol.* **1988**, *14*, 1347-1358.

44)Hofmeyr, J.H.; Burger, B. V. *J. Chem. Ecol.* **1991**, *21*, 355-363.

45) Beestman, G.B., U.S. Patent 4046741, **1981.**

46) Beestman, G.B., U.S. Patent 4417916, **1983.**

47) Scher, H.B. U.S. Patent 4046741, **1977.**

48) Scher, H.B. U.S. Patent 4285720, **1981.**

49) Scher, H.B. U.S. Patent 5332584, **1994.**

50) Scher, H.B. U.S. Patent 5223477, **1993.**

51) Polishshuk, A. Ya.; Zaikov, G. E. In *Multicomponent Trasport in Polymer Systems for Controlled Release;* Gordon and Breach Science Publishers, Amsterdam, 1997.

52) Vandenberg, G. B.; Smolders, C.A. *J. Membr. Sci.* **1992**, *73*, 103-118.

53) Yadov, S.K.; Ron, N.; Chandrasekharam, D.; Khilar, K. C.; Suresh, A. K. *J. Macromol. Sci.-Phys.*, **1996**, *B35(5)*, 807-827.

54) Yadov, S.K.; Khilar, K. C.; Suresh, A. K. *J. Membrane Sci.***1997**, *125*, 213-218.

55) Janssen, L.J.J.M.; Boersma, A.; te Nijenhuis, K., *J. Membrane Sci.*, **1993**, *79*, 11-26.

56) Cross, J. H. *J. Chem. Ecol.* **1980**, *6*, 781-787.

57) Bull, D.L.; Coppedge, J. R.; Ridgway, R. L.; Harde, D. D.; Graves, T. M. *J. Econ. Entomol.* **1973**, *2*, 829-835.

58) *Alternative Copolymers*; Cowie, J. M.G., Ed; Plenum Press: New York, 1985, p. 281.

59) Dhathathreyan, A.; Marry, N.L.; Radhakrishnan, G.; Collins, S.J. *Macromolecules* **1996**, *29*, 1827-1829.

60) Dill, D. R.; Pollart, K. A. Surface Sizing. In *The Sizing of Paper,* 2nd ed.; Reynolds, W. F., Ed.; Tappi Press: Atlanta, GA, 1989; p. 63-78.

61) Dubin, P. L.; Strauss, U. P. *J. Phys. Chem.* **1973**, *77*, 1427-1431.

62) Deh-Ying, Chu; Thomas, J. K. *Macromolecules* **1987**, *20*, 2133-2138.

63) Nagasawa, M.; Rice, S. A. *J. Am. Chem. Soc.* **1960**, *82*, 5070-5075.

64) Schultz, A. W.; Strauss, U. P. *J. Phys. Chem.* **1972**, *76*, 1767-1771.

65) Quadrifoglio, F.; Crescenzi, V.; Delben, F. *Macromolecules* **1973**, *6*, 301-303.

66) Delben, F.; Paoletti, S.; Crescenzi, V.; Quadrifoglio, F. *Macromolecules* **1974**, *7*, 538-540.

67) Wulf, G.; Jakoby, K. *Macromolecules* **1996**, *29*, 2776-2782.

68) Dana, M.; Villenave, J. J.; Montaudon, E. *Eur. Polym. J.* **1996**, *32*, 529-533.

69) Kuo, P-L.; Hung, M-N. *J. Appl. Polym. Sci.* **1993**, *48*, 1953-1961.

70) Rzaev, Z.M.O. *Prog. Polym. Sci.* **2000**, *25*, 163-217.

71) Ratzch, M.; Steinert, V. *Macromol. Che,.* **1984**, *185*, 2411-2420.

72) Ratzch, M. *Prog. Polym. Sci.* **1988**, *13*, 277-337.

73) Trivedi, B.C.; Culbertson, B.M., *Maleic Anhydride,* Plenum Press, New York 1982.

CHAPTER 2.1

Polymer Microcapsules by Interfacial Polyaddition between Styrene-Maleic Anhydride Copolymers and Amines

Anna Shulkin, Harald D.H. Stöver

Department of Chemistry, McMaster University

1280 Main St. West, Hamilton, ON, L8S 4M1, Canada

Modified from Journal of Membrane Science, accepted

2.1.0 Abstract

In the present study, styrene-maleic anhydride copolymers (SMA copolymers) were used as wall-forming materials in microencapsulation. The capsule membranes were formed by polyaddition at the interface between styrene-maleic anhydride copolymers dissolved in a dispersed oil phase, and a polyamine dissolved in the continuous aqueous phase. The organic phase consisted mainly of alkyl acetates and aromatic hydrocarbons such as xylene. Two mechanisms of polymer phase separation were observed in the encapsulation of ethyl acetate, depending upon the polymer - core phase interaction, the surfactant used, and the volume ratio of the core-phase to the aqueous phase: solvent-driven phase separation, and reaction-driven phase separation. Microcapsules containing more hydrophobic core oils were prepared by either increasing the ratio of styrene to maleic anhydride groups in the copolymer, or by incorporating *tert*-butyl styrene instead of styrene into the copolymer. Model compounds for insect sex pheromones, such as dodecyl acetate and dodecanol, were encapsulated in such SMA microcapsules, and release from these microcapsules into air was monitored over several weeks at room temperature. The relatively fast rate of release of core materials was attributed to the porous structure of the capsule walls, as confirmed by transmission and environmental scanning electron microscopy.

2.1.1 Introduction

In the area of crop protection, insect sex pheromones are proving to be a biorational alternative to conventional hard pesticides.[1] In particular, attractant pheromones can be used effectively in controlling insect populations by disrupting the mating process.

Mechanical dispensers,[2] hollow fibers,[3] rubber septa,[4] and wax emulsions[5] are some of the delivery devices commonly used to deliver the pheromone throughout the mating period of the insect, typically two to six weeks. Polymer microcapsules, long known as delivery vehicles for conventional pesticides and other hydrophobic agents,[6] have recently been used to encapsulate insect mate attractant pheromones.[7] Polymer microcapsules promise to serve as efficient delivery vehicles, because they are: easily prepared by a number of interfacial and precipitation polymerizations, protect the pheromone from oxidation and irradiation during storage and release, and may in principle be tailored to control the rate of release of the pheromone fill.

In selecting a polymer for the microcapsule wall, the following design criteria must be considered: (1) the capsules should form easily, allow incorporation of large amounts of active agents, and be sufficiently stable during storage and application; (2) the

wall former should not significantly react with the active agent; (3) chemical composition and morphology of the wall should allow for proper diffusion and release of the specific active agent; (4) the capsule wall and its degradation products should be environmentally benign.

One known method of forming pheromone-filled microcapsules relies on the interfacial reaction between a monomer in the oil phase and a matching monomer in the aqueous phase. A typical example involves dispersing a solution of the pheromone and a polyisocyanate in xylenes, into an aqueous solution, followed by addition of a watersoluble polyamine such as tetraethylenepentamine (TEPA). A polyurea membrane forms almost instantly at the surface of the dispersed oil droplets.[7] Although this process forms polymer microcapsules suitable for controlled release, it does have some limitations. Isocyanates react with most nucleophiles, making it difficult to encapsulate nucleophilic active agents such as alcohols. Furthermore, low molecular weight isocyanates are relatively expensive compounds with known allergenic properties.

Other approaches involve capsule formation through deposition of either urea-formaldehyde type condensates or polyelectrolyte complexes (PEC's) from the aqueous phase. Due to their dense wall, and polar walls, respectively, these capsules tend to retain hydrophobic fills for long periods of time. They are hence more suited for applications

involving mechanical release of the fill, than for diffusion release as is required for pheromone applications.[8,9,10]

Only a few reports in the literature describe the preparation of microcapsules involving the use of hydrophobic polymers as wall formers. In a solvent-evaporation system reported by Loxley and Vincent,[9] poly(methylmethacrylate) precipitates from within the droplets of the dispersed phase, a mixture of methylene chloride and octane, upon selective evaporation of the good, low-boiling cosolvent, methylene chloride. This method produces strong, narrow disperse microcapsules, with good control over the shell thickness. However, the need to remove large quantities of a cosolvent would be a significant drawback in an industrial application. In addition, the polymer - cosolvent system has to be chosen such that the wall-forming polymer is driven by interfacial tension to precipitate at the interface, rather than throughout the oil droplet.[11]

Chapter 5 describes an alternate technique for the preparation of capsules using hydrophobic, photo-responsive polymers that are designed to precipitate and form capsule walls under irradiation with 350 nm light.[12]

This chapter describes the development of a new technique for producing oil-containing microcapsules, based on the interfacial reaction between styrene-maleic

anhydride (SMA) copolymers dissolved in a dispersed hydrophobic phase, and water-soluble polyamines dissolved in the continuous aqueous phase.

SMA copolymers were chosen as wall formers as a result of their functionality and easy availability.[13,14,15,16,17] The combination of nonpolar styrene and polar maleic anhydride groups, makes the copolymer soluble in a variety of solvents.[18] The anhydride functional groups are very reactive towards amidation, esterification, and hydrolysis,[19,20,21] forming amphiphilic, interfacially active polymers commonly used in coatings, and as dispersing agents, and emulsifiers.[22,23,24] Their high reactivity, and their significant increase in polarity during the course of the amidation reaction, were essential for the development of the new encapsulation method presented here. In principle, both the cross-linking reaction with multifunctional amines, and the increased polarity of the resulting zwitter-ionic copolymer, can serve to precipitate the copolymer at the interface.

2.1.2 Experimental

2.1.2.1 Materials

Maleic anhydride (99%,Aldrich) was recrystallized from chloroform prior to use. The cosolvents for the encapsulation, ethyl acetate (Fisher Scientific), propyl acetate (Aldrich), butyl actetate (Fisher Scientific), and hexyl acetate (Aldrich) were reagent grade and used as received. Model compounds dodecyl acetate and dodecanol were purchased from Aldrich Chemical Company. The initiator 2,2'-azobis-(2-

methylpropionitrile) (AIBN) was purchased from DuPont and recrystallized from methanol prior to use. Surfactants, poly(vinylalcohol) (PVA, 87% hydrolyzed, 10,0000 Da) and nonyl-phenyl-oligo-ethylene glycol (IGEPAL CA-630) were purchased from Aldrich and Sigma, respectively. All of the polymers except for the *tert*-butylstyrene-maleic anhydride copolymer were obtained from commercial sources listed in Table 2.1. 1.

2.1.2.2 Copolymer Synthesis

Maleic anhydride (1.5 g, 1.53 mmol), *t*-butylstyrene (2.45 g, 1.53 mmol), and AIBN (0.05 g, 0.03 mmol) were dissolved in 40 mL methyl ethyl ketone in a 100 mL round bottom flask fitted with a nitrogen bubbler, magnetic stir bar, and condenser. After bubbling with nitrogen for 30 minutes, the reaction mixture was heated 70°C for 5 hours under stirring. The copolymer was isolated by precipitating the cooled reaction mixture into a five fold excess of cold diethyl ether. The copolymer was filtered, washed with diethylether, and dried at 40 °C under reduced pressure for 48 hours (yield: 3.2 g, 81%). FT-IR spectra showed the expected strong carbonyl absorptions at 1850 and 1780 cm^{-1} due to the anhydride. The very weak absorptions at 1720 cm^{-1} due to succinic acid, confirmed a low degree of hydrolysis in the final copolymer. ^{1}H-NMR (Bruker AF300, deuterioacetone, TMS standard): 3.25 ppm (m, 2H, succinic anhydride), 7.32 ppm (m, 4H, ar.) and 1.1 - 1.8ppm (12H, ali.). The molecular weight, M_n, of the copolymer, determined by gel-permeation chromatography relative to narrow disperse polystyrene

standards, and using tetrahydrofuran as mobile phase, was 25,000 with a polydispersity of 1.8.

2.1.2.3 Encapsulation Procedure

The typical procedure for the preparation of styrene/maleic anhydride capsules was as follows: 0.4 g IGEPAL was dissolved in 30 mL deionized water in a 200mL beaker, while stirring with an overhead paddle stirrer at 400 rpm for 20 min. 1.0 g copolymer (5.1 mmol of maleic anhydride groups) was dissolved in 11 mL of a cosolvent such as ethyl acetate. After complete dissolution of the copolymer, 4 mL of dodecyl acetate or dodecanol were added to the copolymer solution. The resulting oil phase was then added dropwise over 1 min. to the aqueous phase to form an oil-in-water emulsion. After emulsifying for 5 min. at a stirring speed of 400rpm, the stirring speed was reduced to 200 rpm and a solution of 1.01 g (5.1 mmol) of tetraethylenepentamine (TEPA) in 15 mL of distilled water was added dropwise over 3 min. The resulting dispersion of microcapsules was stirred at 200 rpm for a further 30 min., and then stored in polypropylene screw cap vials.

2.1.2.4 Characterization

FT-IR analyses were performed on a Bio-Rad FTS-40 FT-IR spectrometer. Copolymer spectra were taken as films cast from chloroform onto NaCl discs. All capsule samples used for FT-IR analysis were first washed three times with water, crushed by

sonication, extracted five times with THF, and dried at 40°C under reduced pressure for 48 h. They were then prepared as pellets using spectroscopic grade KBr.

The internal morphology of the capsules was studied using a JEOL 1200EX transmission electron microscope (TEM). For TEM analysis, microcapsules were embedded in Spurr's epoxy resin, microtomed to ~100nm thickness, and stained with uranyl acetate.

A Philips-2020 Environmental Scanning Electron Microscope (ESEM) was used to characterize the surface morphology. Dilute dispersions of microcapsules were deposited on aluminum stubs, dried at room temperature and sputter-coated with a 5 nm layer of gold.

Optical microscopy was performed using an Olympus BH-2 microscope, equipped with a Kodak DC 120 Digital Camera.

Capsule sizes and capsule size distributions were determined using a Coulter LS230 particle sizer, which operates on the principles of Fraunhofer diffraction for large particles (> 0.4 μm) and polarization intensity differential scattering (PIDS) for small particles (< 0.4 – 0.8 μm).

2.1.2.5 Release Measurements

Approximately 100 μL sample of the concentrated capsules dispersed in water was placed on the aluminum pan and rolled around to spread out the microcapsules into a mono-layer. Once a mono-layer had been produced the sample was placed in a fume hood used only for release measurements. The sample was weighed every 15 min for the first two hours, depending on the amount water in the slurry. After the slurry had dried on the pan (the slope of the release curve changes dramatically) and the 100 weight % point (time zero) was established, the sample was weighed twice a day for the first week, and subsequently once a day. The humidity and the temperature of the environment were measured using a standard humidity meter.

2.1.3 Results and Discussion

Styrene and maleic anhydride are known to form alternating copolymers, poly(styrene-*alt*-maleic anhydride) (SMA50), by virtue of their low reactivity ratios.[25] Copolymers incorporating more than 50 mol% styrene may be prepared by semi-batch copolymerizations, where the reaction is starved of maleic anhydride. A series of alternating as well non-stoichiometric styrene-maleic anhydride copolymers were obtained from commercial suppliers, and are listed in Table 2.1.1. In addition, poly(*t*-butylstyrene-*alt*-maleic anhydride) (*t*-BuSMA50) was prepared by free radical solution copolymerization.

Table 2.1.1 - Molecular weights and suppliers of the SMA copolymers used.

Polymer	M_n	Supplier
SMA 50[a]	350,000	Aldrich
SMA 50[a]	50,000	Scientific Polymer Products
SMA 50[a]	1,600	Scientific Polymer Products
SMA 32[a]	1,700	Aldrich
SMA 14[a]	150,000[b]	Aldrich
t-BuSMA 50[c]	25,000[b]	Prepared in this work

[a] the number indicates the nominal weight % maleic anhydride
[b] measured by size exclusion chromatography, calibrated with narrow disperse polystyrene standards. Other molecular weights are as provided by the supplier.
[c] the number indicates the nominal mol % maleic anhydride

Xylenes and other aromatic solvents are often used in interfacial polyurea encapsulation, due to their ability to dissolve organic monomers, their immiscibility with water and their relatively high boiling points (>100 °C). In our initial experiments we explored the use of ethyl acetate as a core solvent for the preparation of SMA50 capsules, as it is polar enough to dissolve SMA50, yet still fairly water immiscible, and environmentally benign. In some encapsulations, the pheromone model compounds dodecyl acetate or dodecanol were added to the core phase, in order to both test their effect on encapsulation, and to measure their rate of release into air.

2.1.3.1 SMA 50 Capsules

The first attempt to encapsulate ethyl acetate in SMA microcapsules was carried out at a 1 to 5 volume ratio of organic to aqueous phases, and with 1 vol % PVA in the aqueous phase. Under these conditions, immediate phase separation and copolymer precipitation were observed during the emulsification period, even before amine addition, leading to the formation of white, stringy aggregates of copolymer. This rapid precipitation was attributed to the relatively high mutual miscibility of ethyl acetate and water.[26] During emulsification, ethyl acetate partitions into the aqueous phase while water diffuses into the ethyl acetate phase. The copolymer, while soluble in pure ethyl acetate, precipitates within the resulting water-saturated ethyl acetate phase. As well, the surface tension at the ethyl acetate / water interface is too low to drive the copolymer to precipitate at the interface. As a result, this solvent-induced precipitation leads to irregular precipitate structures.

In a second experiment the organic phase, consisting of SMA50 and ethyl acetate, was added directly to an aqueous solution of hexamethylenediamine (HMDA) under stirring. Immediate capsule formation was observed and the size of the capsules exactly reflected the size of the parent droplets, approximately 2000 - 4000 micrometer. This indicates immediate wall formation around each droplet, resulting from the fast interfacial reaction between the anhydride units and the diamine.[17] This reaction-driven

phase separation leads to the formation of a polar addition polymer that either forms directly at the interface, or migrates to the interface prior to crosslinking (Figure 2.1.1).

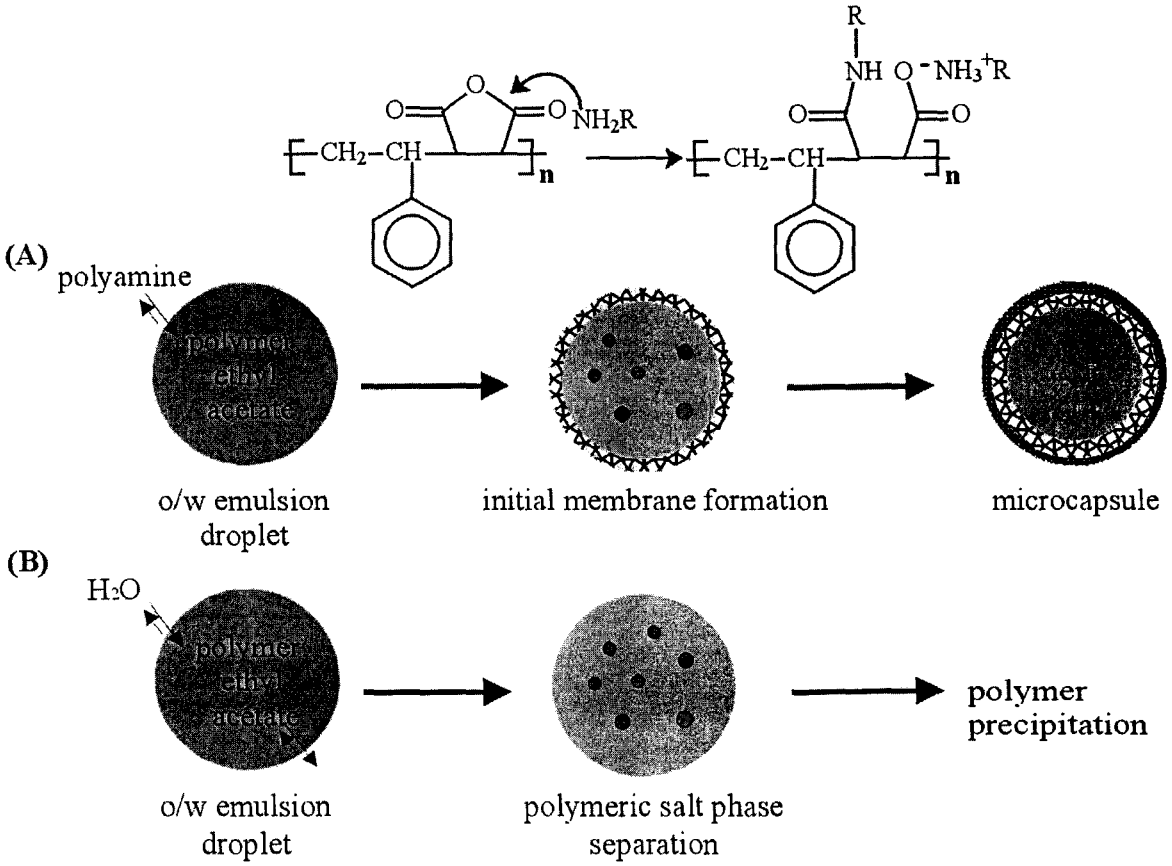

Figure 2.1.1 - Proposed mechanisms of SMA50 copolymer precipitation in ethyl acetate/water system: (A) Reaction driven mechanism – precipitation at the interface/capsule formation (B) change in oil phase properties driven mechanism – precipitation.

The resulting capsules possess a thick wall (Figure 2.1.2), reflecting the high volume-to-surface ratio of these large capsules. The high rigidity of the wall was attributed to the solvent driven phase separation, since the formed capsules may continue to lose ethyl acetate from the cross-linked polymer wall to the aqueous medium, and hence become denser.

These results indicate that while the partial miscibility of ethyl acetate and water is sufficient to cause copolymer precipitation, only the reaction with the amine causes the copolymer to form a shell at the interface.

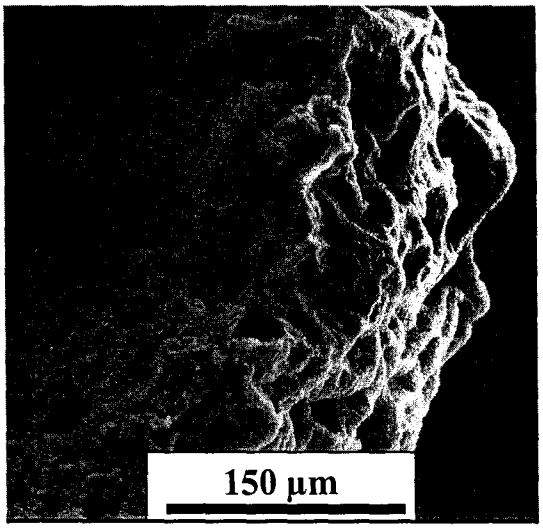

Figure 2.1.2 - ESEM micrograph of a crushed SMA50 microcapsule wall.

Several experiments were subsequently carried out in order to understand and control the solvent-driven phase separation encapsulation of ethyl acetate in SMA50 capsules.

Saturating the aqueous phase with ethyl acetate prior to addition of the organic phase limited the out-diffusion of the ethyl acetate from the 'oil' droplets. This made it possible to disperse the oil phase into the water phase without precipitation of the copolymer. After stirring for 10 minutes, the diamine was added drop-wise and capsules were formed. The capsules produced in these experiments were smaller in size (~500 micron in diameter) compared to those prepared by direct addition of the organic phase to an amine solution that had not been saturated with ethyl acetate (Figure 2.1.3a). This indicates that the oil phase had been sheared by the stirring action prior to polymer precipitation at the interface. The capsules formed had soft, malleable walls. Ethyl acetate, which now remains inside of the capsule wall, swells the capsule membranes making them extremely soft.

However, for many purposes including spray-applications, smaller microcapsules with 20 - 50 micrometer diameter are desirable. Reducing the oil to water ratio to 1 : 2 to avoid having to pre-saturate the aqueous phase with ethyl acetate, and using a better surfactant, IGEPAL, allowed for better oil phase dispersal and resulted in formation of capsules in the desired size range (Figure 2.1.3b).

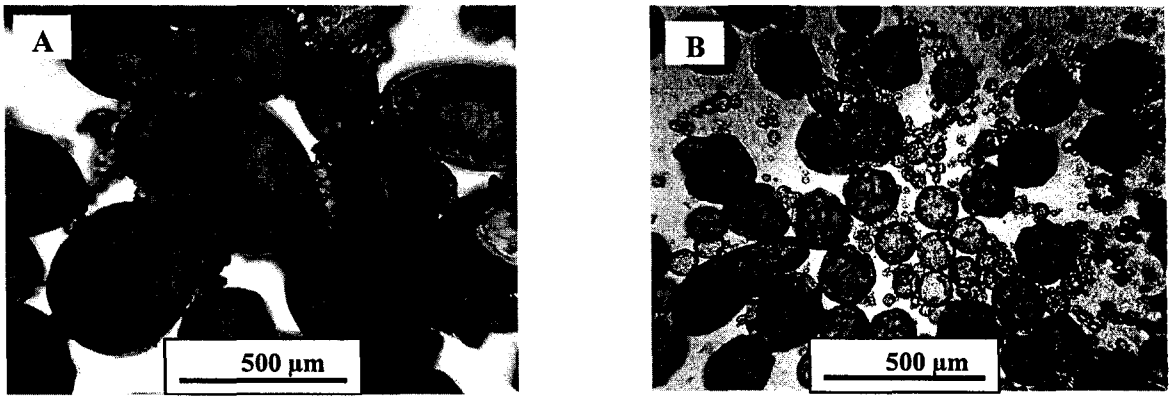

Figure 2.1.3 - Optical photomicrographs of dry microcapsules prepared from SMA50 at room temperature, stirring speed 450 rpm. Ethyl acetate was used as a core-oil: (A) with SDS as emulsifier, aqueous phase saturated with ethyl acetate; (B) with IGEPAL as emulsifier, ratio between o/w 1:2.

2.1.3.2 Effect of Copolymer Structure

To study the effect of copolymer structure on the encapsulation process, and to find ways to suppress the solvent-induced phase separation, copolymers containing less than 50 % maleic anhydride groups (SMA 32 and SMA 14) and a 1:1 *t*-butyl styrene-maleic anhydride copolymer (*t*-BuSMA 50) were investigated. The Hildebrand solubility parameter for these polymers are shown in Table 2.1.2. The Hildebrand or δ-parameter is a measure for the cohesive energy density of a material, and can be used to estimate the

polymer - solvent interaction. A good solvent for a particular polymer typically will have a δ-parameter that lies within about 4 $MPa^{1/2}$ of that of the polymer[27, 28]

According to this guideline, ethyl acetate is already a marginal solvent for SMA50 polymer, and experiments showed that it becomes a non-solvent for SMA 50 upon saturation with water.

Table 2.1.2 - Solubilities and solubility parameters of SMA copolymers and core-solvents.

Solvent	δ ($MPa^{1/2}$)[a]	SMA14 δ(18.8 – 19.9 $MPa^{1/2}$)[b]	SMA32 δ(20.3 $MPa^{1/2}$)[c]	*t*-BuSMA50 δ(22.9 $MPa^{1/2}$)[d]	SMA50 δ(26.0 $MPa^{1/2}$)[d]
butyronitrile	21.5	s	s	s	s
dichloromethane	19.0	s	s	s	s
ethyl acetate	18.6	s	s	s	s
toluene	18.2	s	i	i	i
p-xylene	18.0	s	i	i	i
propyl acetate	18.0	s	s	s	i
butyl acetate	17.4	s	i	s	i
methyl isobutyl ketone	17.2	s	i	s	i
hexyl acetate	-	s	i	s	i
octyl acetate	-	s	i	s	i
dodecyl acetate	-	i	i	i	i

[a] ref 28 ; [b] ref 30 ; [c] ref. 30 ; [d] δ estimated using group contribution method Ref. 28; s = soluble; i = insoluble

On the other hand, ethyl acetate is expected to be a very good solvent for SMA32, SMA14, and *t*-BuSMA50 (Table 2.1.2), and accordingly, may be able to dissolve these polymers even in presence of small amounts of water.

Accordingly, encapsulations were conducted using these copolymers. The organic phases containing these copolymers and ethyl acetate were successfully dispersed into aqueous phase to produce stable emulsions without any visible polymer precipitation. The microcapsules prepared from these copolymers using ethyl acetate as a core-solvent were small, 30 – 70 microns in diameter, as measured by the Coulter LS230 particle sizer. Their relatively narrow size distribution indicates that solution-driven phase separation was indeed suppressed (Figure 2.1.4). These results correlate well with the predictions made on the basis of the solubility parameters of the copolymers and ethyl acetate.

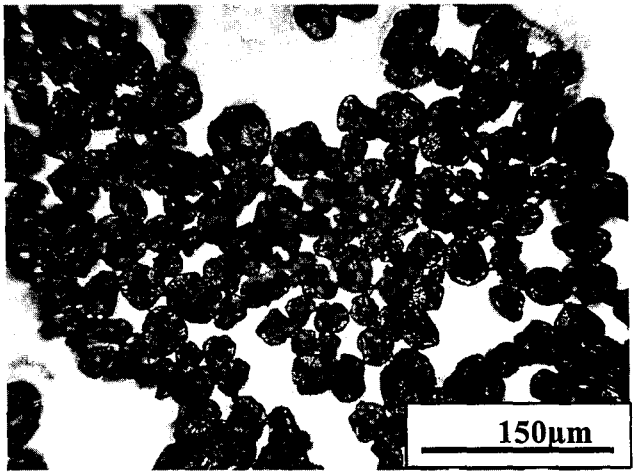

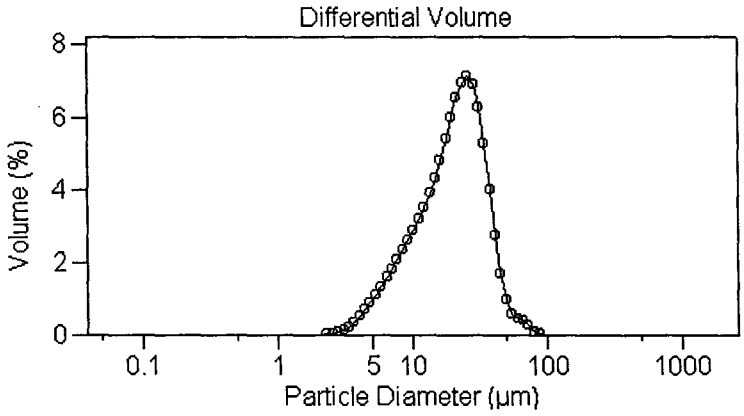

Figure 2.1.4 - Optical micrograph of wet microcapsules prepared from SMA32 copolymer, at room temperature, stirring speed 450 rpm. Ethyl acetate was used as a core-oil, IGEPAL as surfactant. Microcapsule diameter measured by Coulter LS230 particle sizer.

2.1.3.3 Encapsulation of Model Compounds

Model compounds for the insect sex pheromones, such as dodecyl acetate and dodecanol, were successfully encapsulated in SMA microcapsules. It was possible to incorporate up to 60 % of the model compound into the organic phase when ethyl acetate was used as a cosolvent. Model compounds are non-solvents for the SMA copolymers. The copolymer was dissolved in ethyl acetate prior to mixing with the model compound, which reduced the problem of copolymer solubility in the ethyl acetate / model compound mixture. Figure 2.1.5 illustrates the appearance of the SMA32 microcapsules prepared with dodecyl acetate / ethyl acetate (26.6 vol. % dodecyl acetate) as the core oil. Similar to the single solvent encapsulation process, the isolated microcapsules had diameters of 20 – 50 microns, with relatively narrow size distribution.

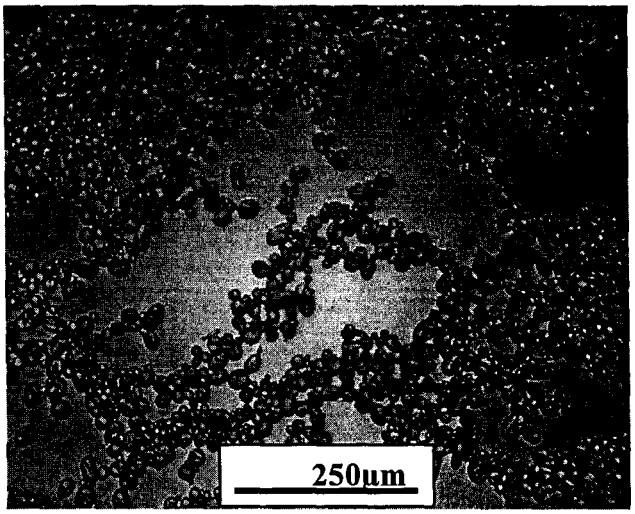

Figure 2.1.5 - Optical micrograph of microcapsules prepared from SMA32 copolymer, at room temperature, stirring speed 450 rpm. Ethyl acetate / dodecyl acetate was used as a core-oil, IGEPAL as surfactant.

2.1.3.4 Effect of Core Oil

Other solvents besides ethyl acetate were also investigated, in particular those solvents commonly used in interfacial encapsulation. As discussed earlier, such solvents should dissolve the starting polymer, be largely water-immiscible, and preferably have boiling points at or above 100°C, and low toxicity. The use of hydrophobic solvents would eliminate the solvent-driven phase separations described above for ethyl acetate, and permit the study of wall formation under a pure interfacial reaction mechanism.

Table 2.1.2 shows the solubilities of the different SMA copolymers in a group of suitable solvents. It can be seen that the SMA50 is soluble only in polar solvents having solubility parameters higher than 18.6 $MP_a^{1/2}$. SMA14, on the other hand, is soluble in traditional encapsulation solvents such as toluene and xylenes, and *t*-BuSMA50 is soluble in hydrophobic solvents such as hexyl and octyl acetate.

The encapsulation procedure for SMA32, SMA14 and t-BuSMA50, with core solvents other than ethyl acetate, differed from that used for SMA50 in three aspects: the amount of surfactant was reduced to 0.3% relative to the aqueous phase, the emulsification time was increased to 30 minutes, and the oil to water ratio was decreased to 1 :3-5. Even at an o/w ratio of 1 :5, no polymer precipitation was observed during emulsification.

2.1.3.5 Conversion

The conversion resulting from the reaction of the maleic anhydride groups of *t*-BuSMA50 copolymer with polyamine during encapsulation was estimated by FT-IR. While the intensity of the peak at 832 cm^{-1}, characteristic of di-substituted aromatic compounds, does not vary with the encapsulation reaction, the intensity of the peak at 1782 cm^{-1}, corresponding to residual maleic anhydride (MA), decreases with reaction. The conversion of reaction p is defined by the following equation:

$$p = 1 - \frac{r}{r_0}$$

where r is the area ratio of FT-IR bands of MA residues and *t*-butyl styrene residues in the formed capsule, and r_0 is the area ratio between the same bands in the starting copolymer. As can be seen in Table 2.1.3, the conversions of the encapsulation reaction performed in different core-solvents, are independent of the core-solvent composition and molecular weight of the copolymer used. The conversion of the reaction with HMDA is limited to about 80 % in all cases.

Table 2.1.3 - Conversion of the *t*-BuSMA50 - HMDA encapsulation reaction in different core – solvents.

M_n	Core-solvent	Conversion (%)
25,000	ethyl acetate	80
25,000	propyl acetate	79
25,000	butyl acetate	76[a]
25,000	hexyl acetate	82
5,000	hexyl acetate	83

Similar conversions were obtained for SMA32 and SMA50 microcapsules (Table 2.1.4). In these cases r was defined as the area ratio of FT-IR bands of MA residues and styrene residues, with a peak at 703 cm^{-1} characteristic of the mono-substituted aromatic compounds, in the formed capsule, and r_0 is the area ratio between the same bands in the starting copolymer.

Table 2.1.4 - Conversions of the SMA encapsulation reaction.

Copolymer	Solvent	Conversion (%)
SMA50 M_n 50,000	ethyl acetate	78
SMA32	propyl acetate	86

2.1.3.6 SMA14 Capsules

The capsule walls prepared from SMA14 are only lightly cross-linked, due to the presence of only 14 weight % anhydride groups in the starting SMA copolymer. For the same reason, the copolymer polarity should increase only slightly during the interfacial reaction. As a result, the capsule walls formed from SMA14 are expected to be quite permeable to non-polar core-oils. Figures 2.1.6a, 2.1.6b and 2.1.6c show capsules

prepared from SMA14 with toluene, methyl isobutyl ketone, and methyl isobutyl ketone / dodecyl acetate mixture as core-oils, respectively. The microcapsules were deposited in form of their aqueous suspensions onto microscopy slides, and dried in air. It can be seen that the capsules prepared with toluene as a core-oil have largely released their contents after drying for 15 minutes on the microscopy slide (Fig. 2.1.6a). The capsules prepared with methyl isobutyl ketone as core-oil retain some fill after 15 min. on the slide (Fig. 2.1.6b), while those made with the methyl isobutyl ketone/dodecyl acetate mixture retained some of their content even after having been dispersed on a glass slide and dried for two weeks (Fig. 2.1.6c).

Toluene and xylene are excellent solvents for the SMA14 copolymer (Table 2.1.2), and swell even the cross-linked shell of the capsules prepared from this copolymer. The shell material is hence extremely permeable to toluene and xylene, so that their rate of release from these capsules is fast. Methyl isobutyl ketone on the other hand possesses a lower solubility parameter than both toluene and xylene, and dodecyl acetate is a non-solvent for the SMA14 copolymer. Thus, methyl isobutyl ketone or mixtures of methyl isobutyl ketone /dodecyl acetate swell the capsule shell to a lesser extent, which explains the better retention of their fill.

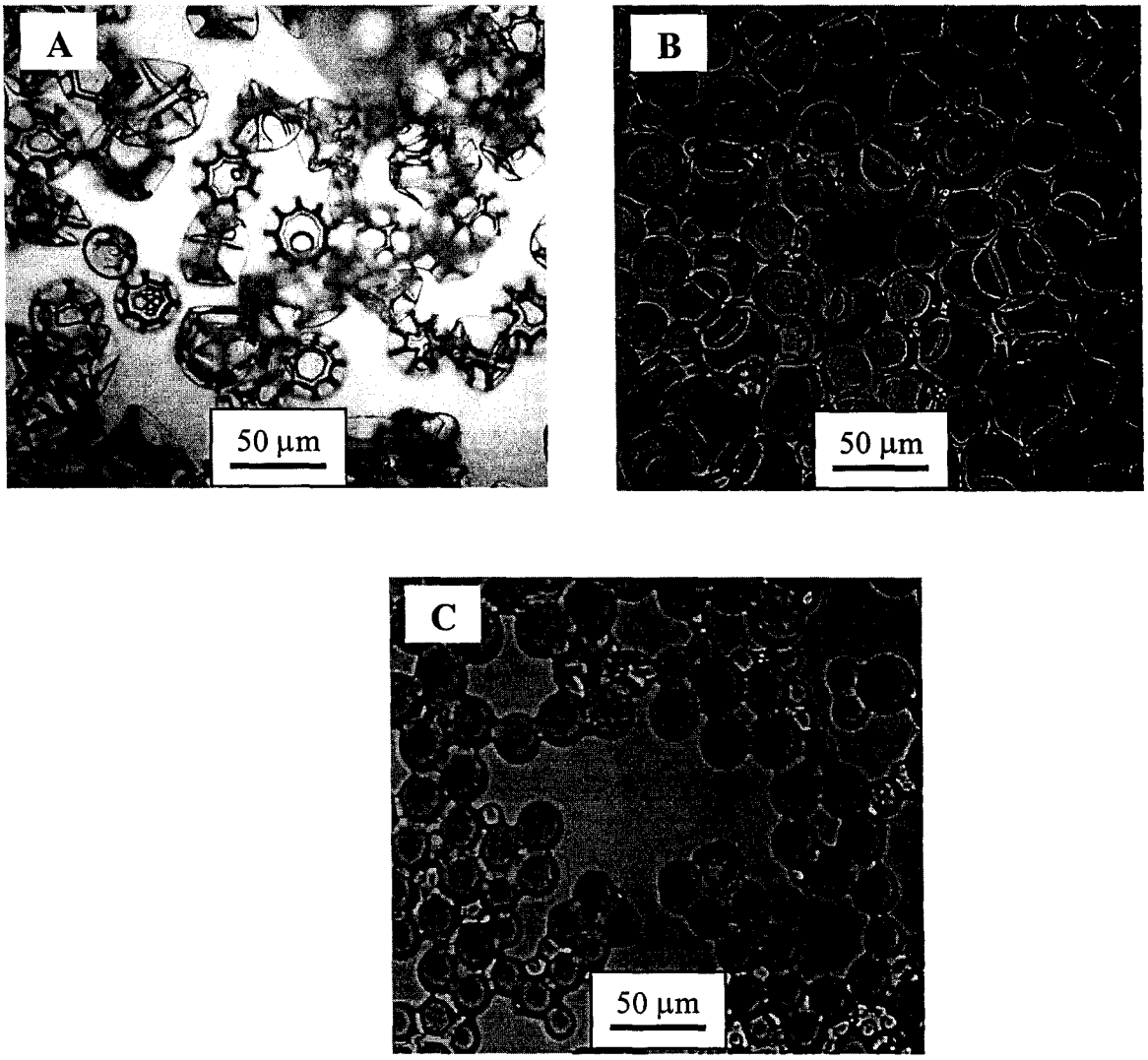

Figure 2.1.6 - Optical micrographs of the dry microcapsules prepared from SMA14 copolymer, at room temperature, with SDS as emulsifier, stirring speed 450 rpm. Core-oil: (A) toluene (B) methyl isobutyl ketone (C) methyl isobutyl ketone / dodecyl acetate mixture 7:3 mL.

This highlights the requirement for the core oil to be a marginal solvent for the copolymer. The core oil should be able to dissolve the original linear polymer, however, the shell material of the capsules should be able to contain the solvent inside the capsules for a reasonably long period of time. This apparent contradiction illustrates the need for polymer chemical modification and / or efficient crosslinking during wall formation.

2.1.3.7 Release from Microcapsules

Release of ethyl acetate / dodecyl acetate mixtures from SMA microcapsules was monitored gravimetrically at room temperature. In all cases, the ethyl acetate evaporates almost instantly upon exposure to air, such that the actual weight loss shown in the release curves reflects the loss of the higher boiling dodecyl acetate.

Figures 2.1.7-9 show that most microcapsules lose their contents within about three weeks at room temperature. The release from microcapsules was compared with the evaporation of a corresponding ethyl acetate / dodecyl acetate mixture from filter paper. It was found that the release of dodecyl acetate was significantly reduced by encapsulation in SMA capsules.

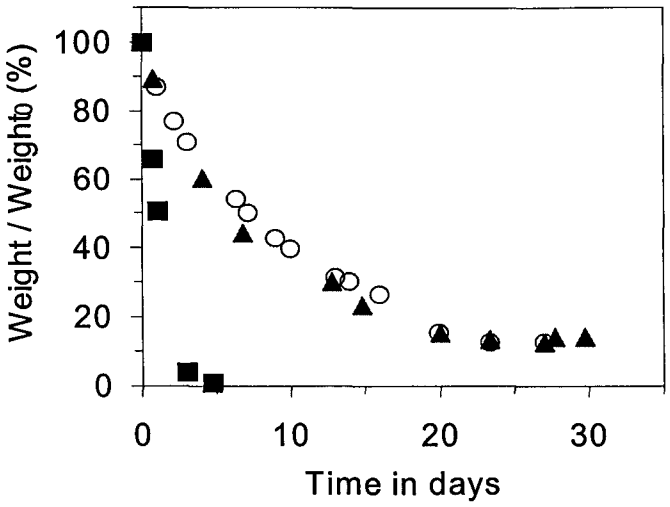

Figure 2.1.7 - Normalized weight at room temperature vs. time. SMA50 microcapsules of 50-60 μm prepared with 11 mL ethyl acetate / 4 mL dodecyl acetate mixture as core oil, IGEPAL as emulsifier. Polymer loading in the core oil: (▲) 3.3 %, (o) 6.6 %. Unencapsulated dodecyl acetate (■).

For potential applications in pheromone encapsulations, longer release periods of 4 – 6 weeks are desirable in order to cover an entire breeding season of target insect populations. In principle, diffusional release from microcapsules should vary inversely with the capsule wall thickness. Shell thickness for microcapsules made from hydrophobic polymers usually increases with the overall capsule diameter, and depends on the concentration of polymer in the oil phase.[9] Therefore, increasing the polymer loading in the oil phase and /or increasing the capsule size (decreasing surface area) should bring about an increase in capsule wall thickness and hence slow down the rate of release.

However, increasing the copolymer loading in the core oil phase from 3.3 to 6.6 weight/vol% did not change the rate of release from the resulting SMA microcapsules (Figure 2.1.7). Furthermore, SMA50 microcapsules at 3.3% polymer loading, and with nominal diameters ranging from 25 to 200 microns were prepared by changing the amount of IGEPAL surfactant in the aqueous phase from 0.3 to 1.2% while keeping the stirring speed constant at 450 rpm. Figure 2.1.8 shows that their release rates are nearly equally rapid, with only the largest ones, at 180 micrometer diameters, retaining some of their fill for up to four weeks.

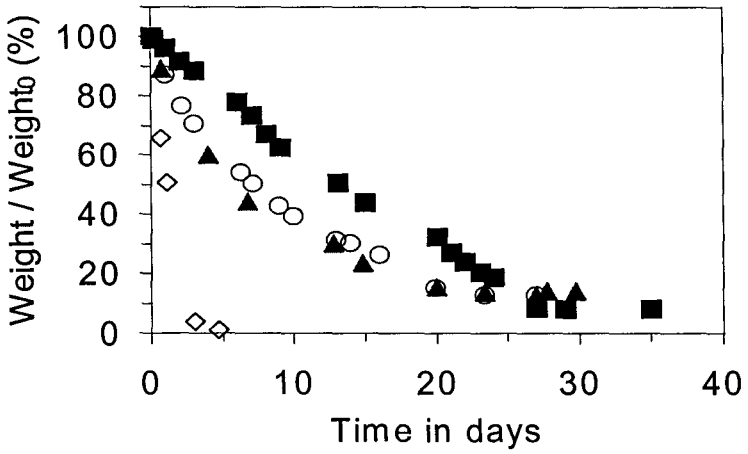

Figure 2.1.8 - Normalized weight at room temperature vs. time. SMA50 microcapsules prepared with 11 mL ethyl acetate / 4 mL dodecyl acetate mixture as core oil, IGEPAL as emulsifier, 3.3 % polymer loading in the oil. Microcapsule size: (■) 181 μm, (▲) 57 μm, (o) 29 μm. Unencapsulated dodecyl acetate (◊).

The observed rapid release at room temperature from SMA microcapsules correlates well with the results obtained by transmission electron microscopy (TEM). The TEM micrograph of SMA32 capsules prepared using ethyl acetate / dodecyl acetate (11 : 4 mL) as core-solvent revealed porous, gel-like microcapsule walls (Figure 2.1.9).

Figure 2.1.9 -TEM micrograph of a SMA microcapsule wall.

Figure 2.1.10 shows that there is no marked difference in the release profiles between *t*-BuSMA50 capsules and SMA14 capsules, even though the SMA14 capsule walls should be less cross-linked than the *t*-BuSMA50 capsule walls. Similar release profiles from these two capsule types suggests that core oil is released via macropores.

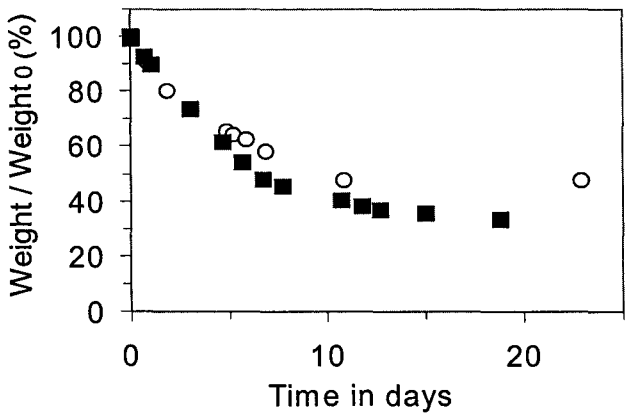

Figure 2.1.10 - Normalized weight at room temperature vs. time. Microcapsules of 50-60 μm diameter prepared with 11 mL ethyl acetate / 4 mL dodecyl acetate mixture as core oil, IGEPAL as emulsifier, 3.3 % polymer loading in the core-oil. Type of the copolymer: SMA32 (■), *t*-BuSMA50 (o).

The ability of SMA microcapsules to release the core material was found to critically depend on the level of humidity. Figure 2.1.11 shows weight loss profiles of SMA32 microcapsules at two different humidity conditions: less than 20 %, and between 60 to 75 % relative humidity, at constant temperature. The total release period was increased by a factor of three at high humidity levels. This is likely due to the hydrophilic nature of the microcapsule membrane that can absorb water from the air.

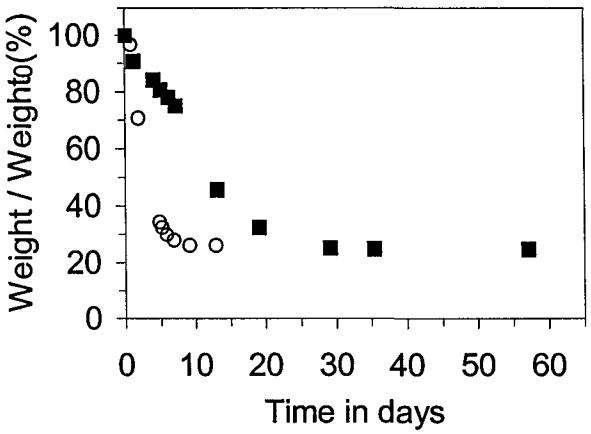

Figure 2.1.11 - Normalized weight at room temperature vs. time. SMA32 microcapsules of 50-60 μm diameter prepared with 11 mL ethyl acetate / 4 mL dodecyl acetate mixture as core oil, IGEPAL as emulsifier, 3.3 % polymer loading in the core-oil. Low humidity level (less than 20 %) (o), high humidity level (between 60 to 75 %) (■).

2.1.3.8 Encapsulation of Reactive Fills

One ongoing challenge in microencapsulation is the containment of reactive fills, i.e. fills that can react with the wall forming polymer in the oil phase. In the pheromone family, linear aliphatic alcohols such as dodecanol and its analogs, can be difficult to encapsulate in classical polyurea capsules, due to their tendency to form urethanes with the wall forming isocyanates, and perhaps also due to their interfacial activity. It was thought that the present anhydride wall formers might be less sensitive to such undesired side reaction with alcoholic fills, and would permit efficient encapsulation and release of compounds such as dodecanol.

Figure 2.1.12 shows the weight loss profile of *t*-BuSMA50 microcapsules prepared with ethyl acetate / dodecanol as a core-oil. The rate of release from these microcapsules is slower than that from *t*-BuSMA50 microcapsules prepared with an ethyl acetate / dodecyl acetate mixture. This is attributed to the higher boiling point of dodecanol, and the interaction of alcohol with a carboxyl groups of the wall material. This interaction represents the basic hydrogen-bonding interactions that occur between a carboxyl group and a hydroxyl group.[29]

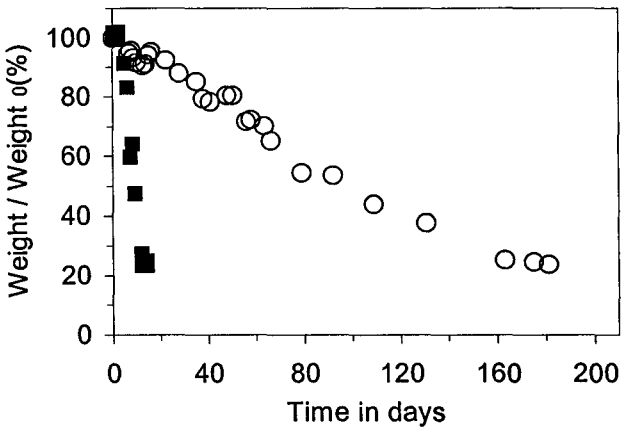

Figure 2.1.12 - Normalized weight at room temperature vs. time. *t*-BuSMA50 microcapsules prepared with 11 mL ethyl acetate / 4 mL dodecanol mixture as core oil, IGEPAL as emulsifier, 3.3 % polymer loading in the oil. Microcapsules 50-60 μm (o). Unencapsulated dodecanol (■).

The effect of the core-solvent and the balance between reaction driven and solution driven phase separation on the capsule morphology and release profile will be discussed in a forthcoming article.

2.1.4 Conclusion

This chapter describes a novel method of encapsulation through an interfacial reaction between styrene-maleic anhydride copolymers and polyamines. It has been demonstrated that in the presence of a polar core solvent, such as ethyl acetate, two mechanisms were responsible for the copolymer precipitation: interfacial reaction and solvent-driven phase separation. Of these two mechanisms, only the reaction-driven process causes the copolymer to form a durable shell at the interface.

The balance between the interfacial reaction and solvent-driven phase separation can be controlled by changing the ratio between the organic and aqueous phases, by adjusting the amount of surfactant used, by saturating the aqueous phase with the organic phase, or by changing the copolymer used. When SMA copolymers with either low maleic anhydride content or with alkylstyrene groups were used, hydrophobic core oils such as octyl acetate and toluene could be encapsulated.

It was shown that the rapid evaporation of model compounds was reduced by encapsulating dodecyl acetate and dodecanol in SMA capsules. However, the desirable 4 – 6 weeks release could not be achieved in the case of the dodecyl acetate due to the high porosity of the formed microcapsule wall. The rate of release of dodecanol from the SMA microcapsules was slower due to the possible hydrogen-bonding interaction between the

model compound and capsule wall. Finally, humidity was shown to have a significant effect on the release rate of the core oils from the SMA microcapsules.

Acknowledgements

We would like to thank 3M Canada Inc., in particular M. Wicki and R. Frank, for their valuable discussions. We would also like to thank 3M Canada and the Natural Sciences and Engineering Research Council of Canada for funding this research. In addition, A. Shulkin would like to acknowledge McMaster University for her Centennial Scholarship, and the Government of Ontario for an Ontario Graduate Scholarship.

References

1) Kydonieus, A. F., Beroza, M. *Insect Suppression with Controlled Release Pheromone SystemVol. I*; Zweig, G., Ed.; CRC Press, Inc.: Boca Raton, Florida 1982; p 4.

2) Hofmeyr, J. H.; Burger, B. V. *J. Chem. Ecol.* **1995**, *21*, 355-363.

3) Weatherston, I.; Miller, D., Lavoie-Dornik, J. *J. Chem. Ecol.* **1985**, *11*, 1631-1641.

4) Butler, L. I.; McDonough, L. M. *J. Chem. Ecol.* **1981**, *7*, 627-633.

5) Delwiche, M.; Krochta, J.M.; Rice, R.E.; Atterholt, C. Sustained-Release Pheromone Formulation with Biodegradable wax carrier, US patent 6,001,346, issued Dec. 14, 1999.

6) Seitz, M.E.; Brinker, R.J.; Travers, J.N. Safened Herbicide Microcapsules with Readily-Adjustable Release Rates. US patent 5,925,595, issued June 20, 1999.

7) Sengupta, A.; Nielsen, K.K.; Barinshteyn, G.; Li, K.; Banovetz, J.P. Adherent Microcapsules Containing Biologically Active Ingredients, US patent 6,080,418, issued June 27th, 2000.

8) Arshady, R. *Polym. Eng. Sci.* **1990**, *30*, 905-914.

9) Bachtsi, A. R.; Boutris, C. J.; Kiparissides, C. *J. Appl. Polym. Sci.* **1996**, *60*, 9-20.

10) Burgess, D. J. *J. Colloid Interface Sci.***1990**, *140*, 227-238.

11) Loxley, A.; Vincent, B. *J. Colloid Interface Sci.***1998**, *208*, 49-62.

12) Stöver, H. D. H.; Shulkin, A. Canadian Patent Application, filed: June 2000.

13) Alfrey, T.; Lavin, E. *J. Am. Chem. Soc.***1945**, *67*, 2044-2045.

14) Heckler, G. E.; Newlin, T. E.; Stern, D. M.; Stratton, R. A.; Witt, J. R.; Ferry, J. D. *J. Colloi Sci.* **1960**, *15*, 294-306.

15) Endo, R.; Hinokuma, T.; Takeda, M. *J. Polym. Sci. Part A-2* **1968**, *6(4)*, 665-673.

16) Brown, P. G.; Fujimori, K.; Brown, A. S.; Tucker, D. J. *Makromol. Chem.* **1993,** *194*, 1357-1370.

17) Lee, S-S.; Ahn, T. O. *J. Appl. Polym. Sci.,* **1999**, *71*, 1187-1196.

18) Ratzsch, M.; Chomiakov, K. *Acta Polym.***1979**, *30*, 577-589.

19) Ratzsch, M.; Steinert, V. *Macromol. Chem,.* **1984**, *185*, 2411-2420.

20) Ratzsch, M. *Prog. Polym. Sci.,* **1988**,*13*, 277-337.

21) Hu, G. H.; Lindt, J. T. *J. Polym. Sci. Part A,* **1993**, *31*, 691-700.

22) Akhmedov, U. K.; Tukhtaeva, M.U.; Abdylova, K. M., *Colloid Journal of the USSR,* **1989**, *50*, 838-841.

23) Chien-Cho, L. Process for The Preparation of Microcapsules Using a Salt of a Partial Ester of a Styrene-Maleic Anhydride Copolymer, U.S. Patent 5,310,721, **1994**

24) Benoff, B. E.; Dexter, R. W. Process for The Preparation of Microcapsule Compositions, U.S.Patent 5,705,174, **1998**

25) Greenley, R. Z. Free Radical Copolymerization Reactivity Ratios; In *Polymer Handbook*; Brandrup, J., Immergut, E. H., Grulke, E. A., Eds. Wiley-Interscience: New York, 1999; p 321.

26) Solubility of ethyl acetate in water is 9.7 vol % at 25 °C.

27) Rudin, A. Polymer Mixtures; In *The Elements of Polymer Science and Engineering*; Academic Press, Inc.: Toronto, 1982; p 428.

28) Grulke, E. A. Solution Properties: Solubility Parameter Values; In *Polymer Handbook*; Brandrup, J., Immergut, E. H., Grulke, E. A., Eds. Wiley-Interscience: New York, 1999; p 675.

29) Vogt, A. D.; Beebe, Jr., T. P. *Langmuir* **1999**, *15*, 2755-2760.

30) Schneier, B. *J. Polym. Sci. Part B*, **1972**, *10(4)*, 245-251.

CHAPTER 2.2

Polymer Microcapsules by Hydrolysis of Styrene-Maleic Anhydride Copolymers

Anna Shulkin, Harald D.H. Stöver

Department of Chemistry, McMaster University

1280 Main St. West, Hamilton, ON, L8S 4M1, Canada

Manuscript in Preparation

2.2.1 Introduction

Release characteristics of liquid-containing microcapsules prepared by interfacial encapsulation largely depend on their morphology, the nature of the wall forming materials and the properties of the encapsulated material. Despite the array of interfacial encapsulation technologies available, there is an intense interest in approaches to form non-toxic, pH-responsive capsules and wall membranes.[1] We have previously demonstrated that the maleic anhydrid based polymers can be used as building blocks in interfacial wall formation. The method is based on the interfacial reaction between stryrene-maleic anhydride based copolymers (SMA) as a hydrophobic component and polyamines, such as TEPA and HMDA, as water-soluble reagents. [2] The resulting polymer phase separation and the precipitation at the interface are driven by the significant increase in the polymer polarity during the polyaddition reaction. The anhydride ring opens upon amidation to form amide and carboxylic acid groups. The carboxylic acid converts to the carboxylate salt upon reaction with a second equivalent of the amine. This polymeric salt phase separates and precipitates at the oil – water interface as well as inside the oil droplet. Thus, the formed capsule wall gains polyelectrolyte properties, with its charge controlled i.e. by the pH.

Properties, reactivity and behaviour of the styrene-*alt*-maleic anhydride copolymer (SMA50) solutions are well described.[3] Recently it was shown that this

copolymer offers a great potential as a polymer surfactant and dispersant.[4, 5] The polyelectrolyte behaviour of hydrolysed styrene maleic anhydride copolymers in aqueous solutions is influenced by the structural characteristics of maleic acid copolymers such as the presence of two neighbouring carboxylic groups in one monomer unit, the hydrophobic character of the comonomer, and the polymer configuration.[6] Thus, a pH dependent self-association and conformation transition of SMA in solution was reported by several authors.[7, 8] On the other hand, *t*-butyl-styrene-*alt*-maleic anhydride copolymers (t-BuSMA50) have been little studied in the past, probably due to the limited applications of this copolymer as a result of its insolubility in water even under alkaline conditions.

In the current study, we have extended our capsule/matrix system preparation approach to non-crosslinked microcapsules prepared from *t*-BuSMA50 copolymer. Instead of using amine as the hydrophilic reagent, we have here taken advantage of the water-immiscibility of the hydrolysed copolymer, and are using sodium hydroxide as aqueous reagent to cause interfacial hydrolysis. The resulting, drastic change in polymer polarity during hydrolysis causes the copolymer to phase separate and precipitate at the interface during the addition reaction, due to the fact that polymer-polymer interactions are more favorable than polymer-solvent interactions on either side of the membrane. This approach was utilized for the preparation of microcapsule and matrix particles.

The pH-responsive properties of the formed capsule/matrix systems were studied and compared to their cross-linked, amine containing analogs.

2.2.2 Experimental

2.2.2.1 Materials

Maleic anhydride (99%, Aldrich) was recrystallized from chloroform prior to use. The cosolvents for the encapsulation, ethyl acetate (Fisher Scientific), propyl acetate (Aldrich), butyl actetate (Fisher Scientific), and hexyl acetate (Aldrich) were reagent grade and used as received. Model compound dodecyl acetate was purchased from Aldrich Chemical Company. The initiator 2,2'-azobis-(2-methylpropionitrile) (AIBN) was purchased from DuPont and recrystallized from methanol prior to use. Surfactant, Nonyl-phenyl-oligo-ethylene glycol (IGEPAL CA-630) was purchased Sigma.

2.2.2.2 Polymerization

t-BuSMA50 copolymer (M_n = 25,000) was prepared according to the general procedure for the free radical polymerization reported elsewhere.[2]

2.2.2.3 Encapsulation procedure

The typical procedure for the preparation of *t*-BuSMA50 capsules was as follows: 0.1 g IGEPAL was dissolved in 30 mL deionized water in a 200 mL beaker, by

stirring with an overhead paddle stirrer at 400 rpm for 20 min. 1.00 g of *t*-BuSMA50 (3.9 mmol of maleic anhydride groups) was dissolved in 11 mL of a co-solvent such as hexyl acetate. After complete dissolution of the copolymer, 4 mL of dodecyl acetate or dodecanol were added to the copolymer solution. The resulting oil phase was then added dropwise over 1 min. to the aqueous phase to form an oil-in-water emulsion. After emulsifying for 5 min. at a stirring speed of 400 rpm, the stirring speed was reduced to 200 rpm and a 75 mL of 0.1N NaOH solution were added dropwise. The addition of NaOH solution was controlled and monitored by automatic in some cases. The resulting dispersion of microcapsules was stirred at 200 rpm for a further 10 min., and then stored in polypropylene screw cap vials.

2.2.2.4 Characterisation

All capsule samples used for FT-IR analysis were usually first acidified, washed three times with water, and dried at 40°C under reduced pressure for 48 h. They were then prepared as pellets using spectroscopic grade KBr.

The internal morphology of the capsules was studied using a JEOL 1200EX transmission electron microscope (TEM). For TEM analysis, microcapsules were embedded in Spurr's epoxy resin, microtomed to ~50nm thickness, and stained with uranyl acetate.

Optical microscopy was performed using an Olympus BH-2 microscope, equipped with a Kodak DC 120 Digital Camera.

2.2.3 Results and Discussion

The cross-linked SMA microcapsules were prepared using HMDA or TEPA as the water-soluble monomers for the interfacial encapsulation. These amines partition sufficiently well into organic phases used in SMA encapsulation procedures to form microcapsules in high yields.[9] However, to adapt the SMA encapsulation technique to the preparation of non–crosslinked microcapsule was not expected to be straight forward, due to the very low partitioning of sodium hydroxide into any organic solvent. Therefore, the first step in these experiments was to study the formation, morphology and yields of non-crosslinked *t*-BuSMA50 microcapsules. Figure 2.2.1 shows optical microscope images of the formed microcapsules prepared with hexyl acetate as a core solvent. The images show that these microcapsules are relatively narrow dispersed with fairly strong walls and spherical shape when wet (Figure 2.2.1a). However, upon drying on the microscopy slide they completely release their content (Figure 2.2.1b and 2.2.2c). The presence and quality of microcapsule walls can be clearly seen from the image of the dry capsules. The high permeability of the microcapsules was attributed to the non-cross-linked nature of the formed walls.

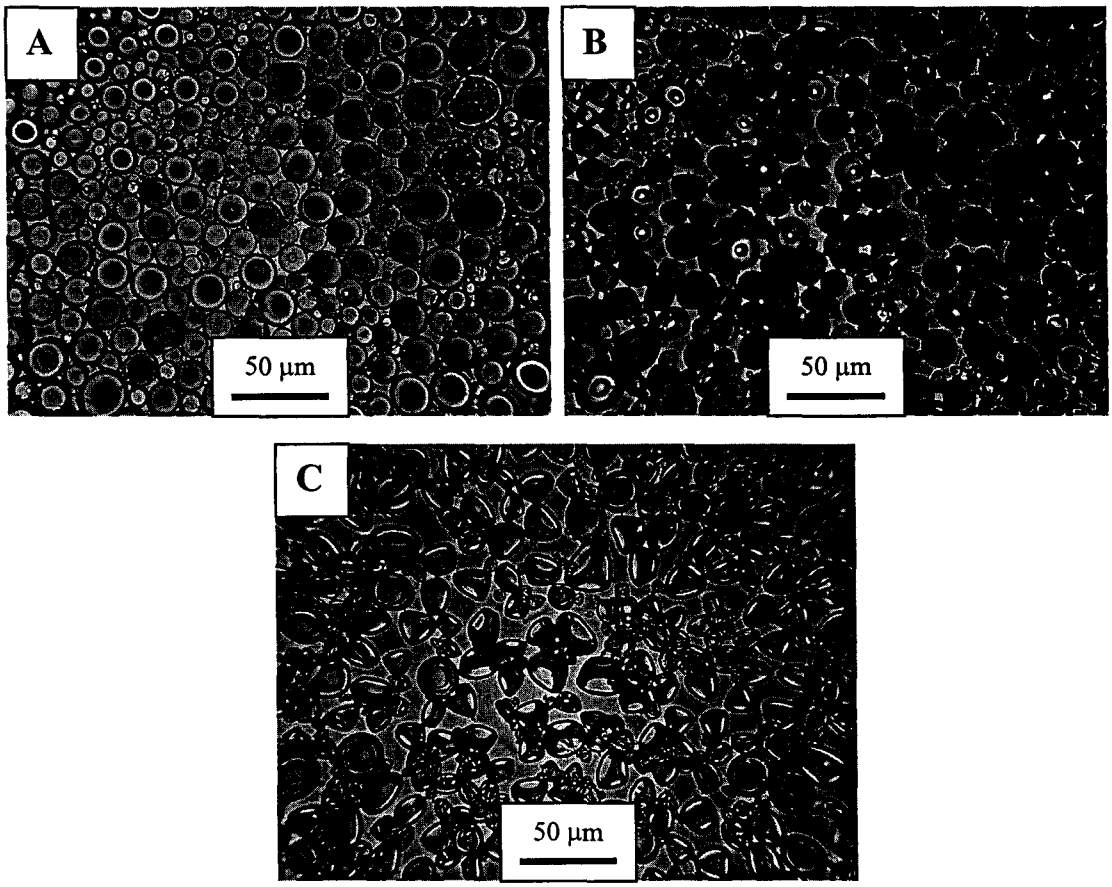

Figure 2.2.1 - Optical micrographs of the microcapsules prepared from t-BuSMA50 copolymer by hydrolysis. (A) wet microcapsules; (B) 15 min. on the slide; (C) 30 min on slide.

The conversion of the encapsulation reaction was estimated by FT-IR based on the method described in Chapter 4.[2] Surprisingly, the conversion of the encapsulation reaction with sodium hydroxide was high, at about 78 %, and comparable to the anhydride conversion in the similar encapsulation with HMDA.[2] The high conversion of

the encapsulation reaction can be explained by the increased hydrophilicity of the *t*-BuSMA50 copolymer upon hydrolysis which facilitates the partitioning of the sodium hydroxide into the interfacial region and inside of the oil phase. The ability of the sodium hydroxide to penetrate into organic phase was also supported by the investigation of the internal capsule morphology. Figure 2.2.2a shows the transmission electron microscopy (TEM) image of 50 nm thick cross-sections of *t*-BuSMA50 non-crosslinked microcapsules prepared with hexyl acetate as a core-oil. The gel–like microcapsules with relatively thick and porous walls were obtained. Increasing the polymer loading from 3.3 to 6.6 weight % brought about the formation of the non-crosslinked gel particles (Figure 2.2.2b). The polymer precipitation and entrapment inside of the oil droplet was attributed to the drastic change in polymer polarity during hydrolysis. Physical cross-linking of the hydrolysed polymer due to the so-called ionomer behaviour can also play an important role in the formation of network morphology instead of capsule. Such behaviour of the polyelectolytes in non-polar regime was observed and studied by several authors.[10, 11, 12] In media of low polarity, the counterions condense on the corresponding co-ions forming ion pairs. The formation of ion pairs leads to the physical cross-linking due to aggregation of ion pairs into multiplets.[13, 14]

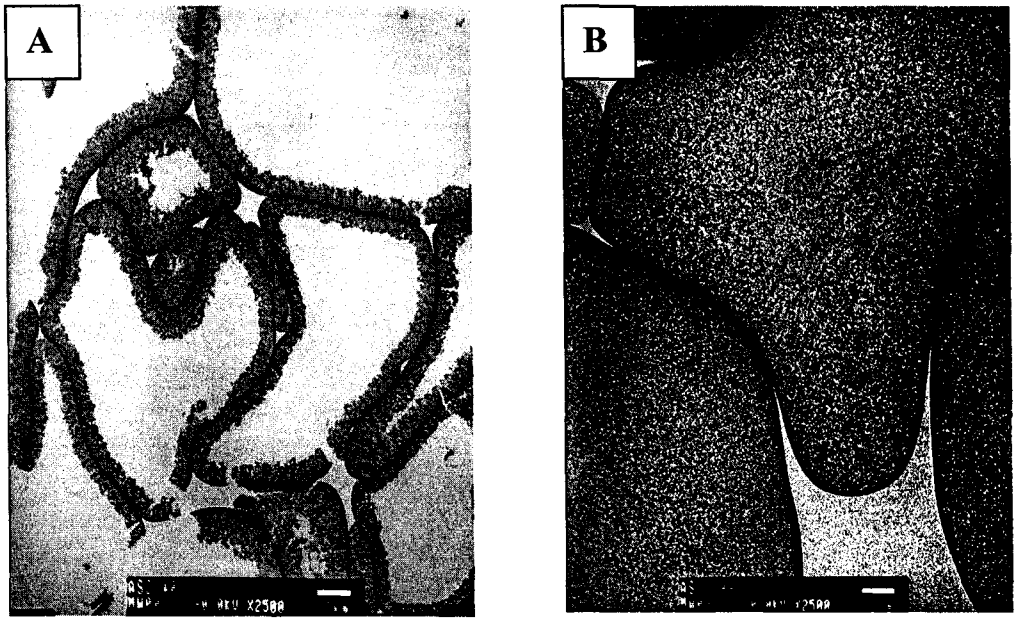

Figure 2.2.2 - TEM micrograph of a non-crosslinked SMA microcapsule wall; (A) 3.3 % polymer loading; (B) 6.6 % polymer loading

pH-responsive behaviour of *t*-BuSMA50 microcapsules was studied by titration of the formed microcapsules with 1 N HCl solution using a PC-Titrate automated titrator and the change in the appearance of the wet microcapsules was captured using optical microscopy. Figure 4 shows a series of optical microscope images of *t*-BuSMA50 non-crosslinked microcapsules prepared with hexyl acetate as core-oil. Figure 2.2.3a

demonstrates the exterior morphology of the original wet microcapsules at pH around 12. Decreasing the pH of the capsule dispersion to pH 5–5.5 resulted in the weaker microcapsules which felled apart upon transfer to the microscope slide and/or immediately on the slide (Figure 2.2.3b). These microcapsules had a tendency to aggregate into bigger agglomerates. The partial release of the encapsulated oil was also observed. Further decrease of pH to 3-3.5 caused complete capsules disappearance (Figure 2.2.3c) and brought about the full phase separation between encapsulated material, polymer and aqueous phase.

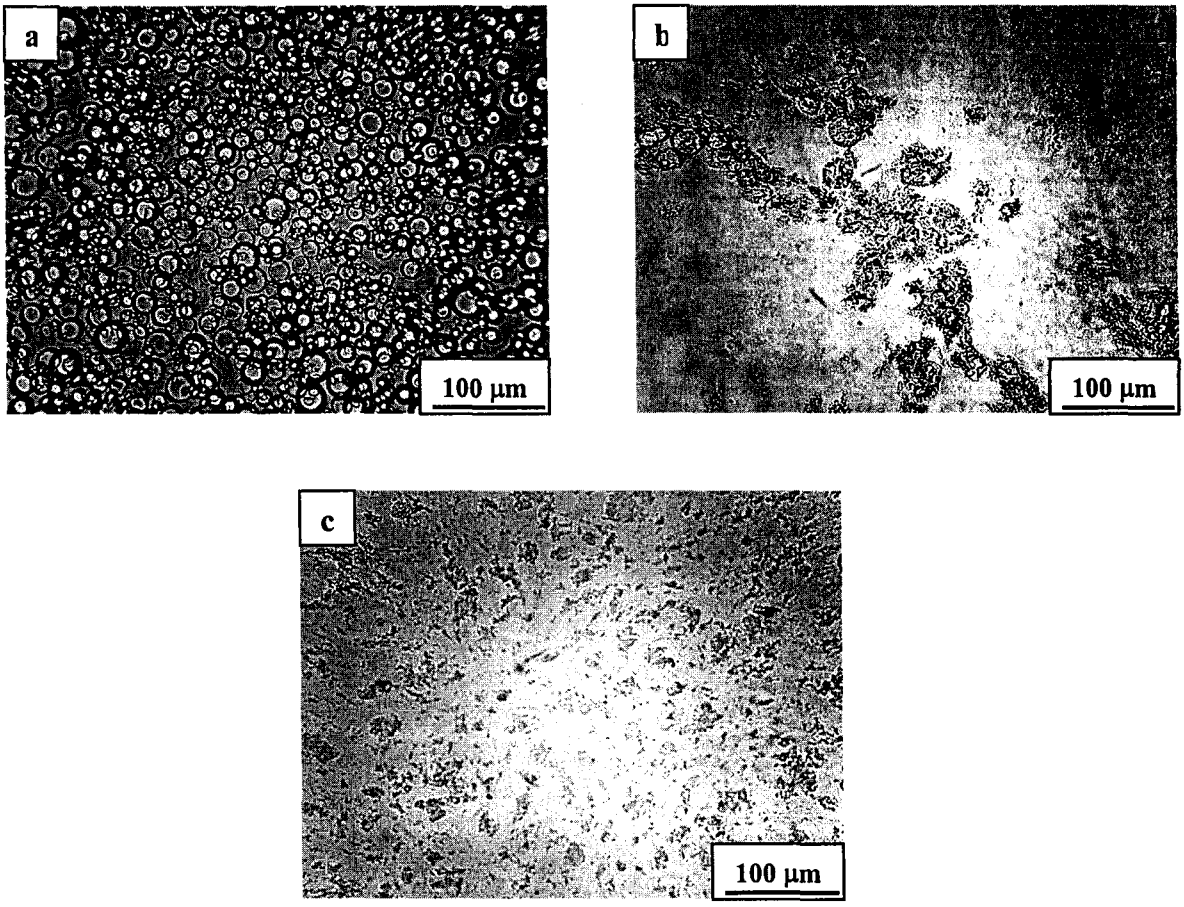

Figure 2.2.3 - Optical micrographs of the microcapsules prepared from *t*-BuSMA50 copolymer by hydrolysis. pH: (A) pH 12; (B) pH 5-5.5; (C) pH 3-3.5

The pH of the solution controls the charge of the polymer chains by affecting its degree of dissociation. The dissociation of the two carboxyl groups of maleic acid characterized by two dissociation constants pK_{a1} and pK_{a2} suggesting the stabilization of the mono-anion by intramolecular hydrogen bonding. The primary carboxylic group of maleic acid copolymers exhibits pK_s value around 2.7-3.9, while the secondary carboxylic acid displays pK_s value around 6.4-8.8 depending on the volume of the substituents of the maleic acid comonomer.[3, 15] Thus, at pH 12.5 the dicarboxylic acid *t*-BuSMA50 copolymer is expected to be completely deprotonated and the balance between hydrophobic *t*-butyl groups and extremely hydrophilic deprotonated carboxylic groups assists not only in the polymer precipitation at the interface and inside the oil, but also in the stabilization of the particles. We postulate that hydrolysed copolymer substitutes the molecules of the surfactant (Igepal) at the interface and provides the particles stabilization due to electrostatic repulsion. This hypothesis was supported by the observation that the microcapsules lose their colloidal stability in sodium chloride solutions. At pH 5.5 one of the carboxylic acid groups in each succinic unit became protonated resulting in the formation of the monosodium salt of the dicarboxylic acid. We believe that microcapsules start aggregating at this pH due to the decrease of the charge density at the interface, and also as a result of the formation of strong inter- and intra-hydrogen bonding. It should be mentioned that under these conditions SMA50 copolymers exhibit maximum agglomeration in aqueous solution.[7] At pH 3-3.5 t-BuSMA50 copolymer is neutral and non-effective as a surface stabilizer. It is also

rendered more hydrophobic and prone to internal hydrogen bonding. Under these conditions microcapsules are falling apart and core-oil is released (Figure 2.2.4).

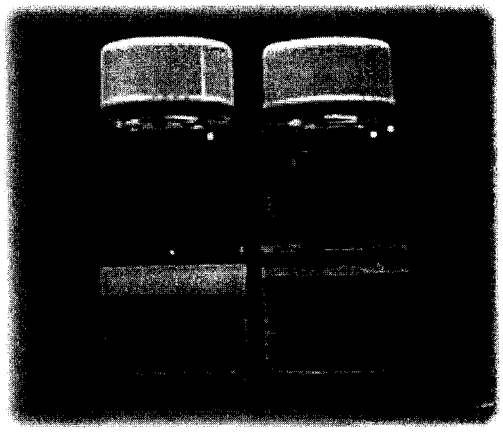

Figure 2.2.4 – Optical image of microcapsules dispersion at high and low pH

It was interesting to compare the colloidal behaviour of non-crosslinked SMA particles (prepared by hydrolysis) and crosslinked SMA particles (prepared using oligoamines), under different pH conditions. The crosslinked *t*-BuSMA50 gel particles were prepared by reacting the copolymer with HMDA. The resulting particle dispersion at the end of the interfacial reation was pH 11. Titration of this dispersion with 1N HCl, showed no difference in the appearance of the gel particles until the pH of the solution reached the value of pH 3.5, where the particles started to aggregate together. At pH 2.5-3 the particles released their content and precipitated out at the bottom of the beaker. The

reaction between anhydride groups of the polymer and amine caused the formation of the monocarboxylic acid copolymer with only one pK_s value of approximately 4.5. Therefore, no significant change in the particles properties was observed until at lower pH values the particles lost their colloidal stability due to protonation.

The complete phase separation between matrix particles and encapsulated oil at low pH was attributed to strong polymer-polymer interactions through hydrogen bonding between the protonated carboxylic aid goups. Figure 6 shows a TEM image of a 50 nm thick cross-section of *t*-BuSMA50 gel particles prepared with hexyl acetate as a core-oil. Figure 2.2.5a demonstrates the internal morphology of the original particles directly after the encapsulation. Figure 2.2.5b shows the internal morphology of the same gel particle at low pH. The internal polymer phase separation can be clearly visible in this image.

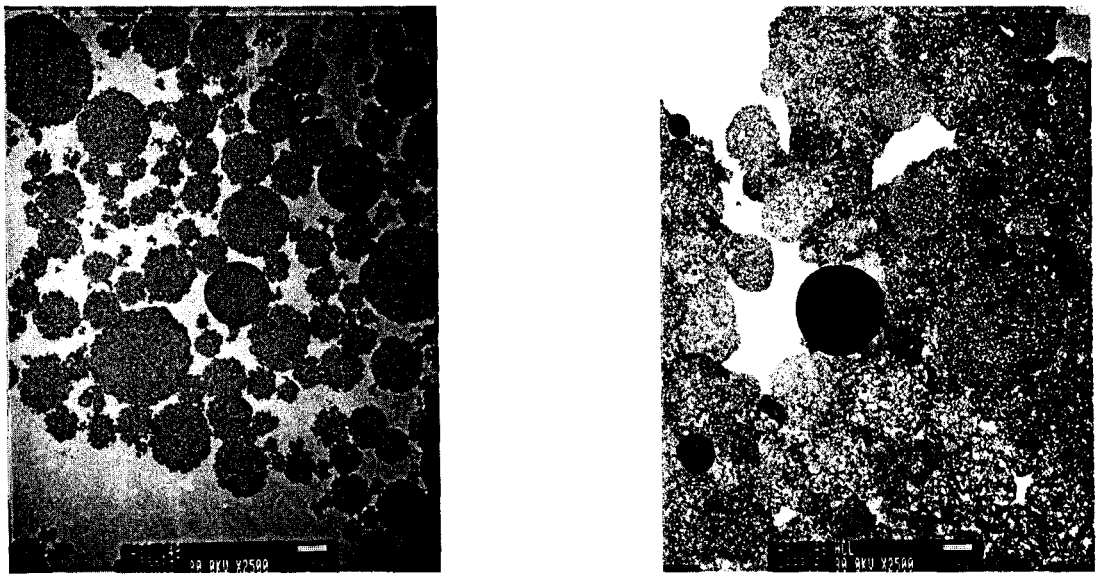

Figure 2.2.5 - TEM micrograph of a non-crosslinked SMA microcapsule wall; (A) original microcapsules; (B) microcapsules at low pH

This hypothesis is based on the assumption that the copolymer in the gel particles or microcapsule membrane microphase-separates into hydrophobic (t-butyl styrene) and hydrophilic (succinic acid) micro-domains, swollen by core –oil and water, respectively. This hypothesis also explains the rapid interfacial hydrolysis reaction, enabled by penetration of the sodium hydroxide through the aqueous microdomains. Upon protonation, the hydrophilic domains became less polar, polymer-polymer interaction increase and the hydrogel components collapse causing larger scale polymer / core-oil phase separation. This hypothesis is supported by the theory postulated in the literature according to which the SMA molecules in aqueous solution associate to form

macrocoils by a zipperlike association-induced mechanism.[7] The polymer molecules can link via hydrophobic interactions between phenyl groups. The alternate theory of isolated ion clusters crosslinking the polymer in a continuous hydrophobic matrix is less likely given the rapid interfacile reaction with sodium hydroxide.

2.2.4 Conclusion

Hydrolysis-induced microcapsule and matrix particle formation from *t*-butylstyrene-*alt*-maleic anhydride copolymers presents an interesting alternative to similar encapsulations using reactive amines. The highly amphiphilic nature of the hydrolysed copolymer forces it to form a separate interpenetrating network of hydrophilic and hydrophobic microdomains, that depending on polymer loading may form discrete capsule walls, or fill the entire interior of the matric particles. Due to the porous, and perhaps bi-continuous, nature of this micro-phase separated material, release profiles of volatile fills are expected to follow the desirable reservoir-type characteristics.

References

[1] Kidchob, T.; Kimura, S.; Imanishi Y.

[2] Shulkin A.; Stöver, H.D.H *Submitted to J. Mebrane Science*

[3] Rätzsch, N. *Prog. Polym. Sci.*, **1988**, *13*, 277-337

[4] Akhmedov, U.K.; Tukhtaeva, M. U. ; Adulova, K. M. *Colloid J. USSR* **1988**, *50*, 838-841

[5] Kuo, P.-L.; Ni, S.-C.; Lai, C.-C. *J. App. Polym. Sci.*, **1992**, *45*, 611-617.

[6] Shimizu, T.; Minakata A. *Polymer* **1980**, *21*, 1432-1437.

[7] Garnier, G.; Duskova-Smrckova, M.; Vyhnalkoa, R.; van de Ven, T. G. M.; Revol, J-F. *Langmuir* **2000**, *16*, 3757-3763

[8] Ohno, N.; Nitta, K.; Makino, S.; Sugai S. *J. Polym. Sci.* **1973**, *11*, 413-425

[9] Shulkin, A.; Stöver, H.D.H *Submitted to J. Membrane Sci.*

[10] Philippova, O.E.; Sitnikova, N. L.; Demidovich, G. B.; Khokhlov, A. R. *Macromolecules* **1996**, *29*, 4642-4645.

[11] S. G. Starodoubtsev, A. R. Khokhlov, E. L. Sokolov, B. Chu, Macromolecules 28 (1995) 3930-3936.

[12] Kawaguchi, D.; Satoh M. *Macromolecules* **1999**, *32*, 7828-7835.

[13] Khokhlov, A. R.; Kramarenko, E. Yu. *Macromolecules* **1996**, *29*, 681-685.

[14] Morawetz, H.; Wang,Y. *Macromolecules* **1987**, *20*, 194-195.

[15] Garett, E. D.; Guile, R. L. *J. Am. Chem. Soc.* **1951**, *73*, 4533

CHAPTER 3

Microcapsules from Styrene - Maleic Anhydride Copolymers: Study of Morphology and Release Behavior

Anna Shulkin and Harald D. H. Stöver

Department of Chemistry, McMaster University

1280 Main St. West, Hamilton, Ontario, Canada L8S 4M1

Modified from Journal of Membrane Science, accepted

3.0 Abstract

Both microcapsules and matrix particles were formed by interfacial polycondensations of styrene-maleic anhydride copolymers and polyamines in oil in water (o/w) suspension systems. The morphologies formed depend on composition, molecular weight and loading of the styrene-maleic anhydride copolymer, as well as on amine partitioning and on the rate of amine addition. The organic phase was comprised of mixtures of ethyl acetate (good solvent) and dodecyl acetate (non-solvent). Dodecyl acetate served both as a co-solvent, and as a model compound for controlled release of insect sex pheromones. The dependence of the release characteristics of the particles on the morphology is discussed as well.

3.1 Introduction

The control of the polymer capsule wall morphology prepared by interfacial encapsulation method has been an intensive area of research for the last 20 years. Chemical properties of reacting monomers, the monomer concentration, the type of organic co-solvent, as well as the nature of active compound control the morphology and properties of polymer membranes formed by interfacial polycondensation. In addition, the pH of the surrounding aqueous medium, particularly in cases where the membrane forming material is a polyelectrolyte may also affect the membrane properties.[1]

Controlling the polymer capsule morphology is important since the permeation characteristics of the capsule membranes can depend quite strongly on the membrane structure. For example, Mathiowitz and Cohen[2] reported that the rate of azobenzene diffusion from the polyamide microcapsules decreases both with increasing wall thickness, and upon addition of a silane coupling agent. They also showed that the capsule morphology and physical properties depend on the type of amine used in the encapsulation.[3] Frére et *al.* reported the preparation of polyurethane capsules from isocyanates and diols. [4] Though no release data were reported, they found that the wall flexibility and porosity can be controlled through the choice of diols. Many studies of controlled morphology and structure-permeability correlation are reported in the polyurea microcapsule literature. Yadav et *al.* showed the strong influence of the degree of

crystallinity and thickness of the polymer shell on the release from polyurea microcapsules.[5] Hong *et al.* investigated the effects of different diisocyanates on the morphology and release behavior of microcapsules, and proposed a correlation between the type of isocyanate used, the surface roughness and the release rate. [6]

Polymer-solvent interactions have probably the strongest effect on morphology and properties of the particles prepared by a two phase interfacial polycondensation process.[7,8,9] The mechanism of capsule formation by interfacial polycondensation consists of several aspects:[7] partitioning of amine into the organic phase, reaction with isocyanates to form oligomer, oligomer phase separation and precipitation at the interface, formation of a primary membrane and subsequent growth of this membrane to the final capsule wall thickness. Each of these steps is affected by the solvency. In order to form a distinct polymer membrane, the solvent should favor the precipitation of the polymer at the early stage of the reaction. On the other hand, it should also allow the continuing diffusion of the water-soluble monomer through the existing membrane into the organic phase. This diffusion depends on the membrane permeability.[4,5,6,10] Typically, mixtures of good and poor solvents are often used to balance these solvency requirements for the interfacial encapsulation.[11,12]

Recently, we have shown that styrene-maleic anhydride type copolymers (SMA) can be used as building blocks in interfacial encapsulation.[13] The capsule membrane

formed by polycondensation at the interface between an oil-soluble styrene-maleic anhydride copolymer and a water-soluble polyamine to produce amide and carboxylic acid. Carboxylic acid converts to the salt upon the acid-base reaction with a second amine group; therefore the produced polymeric membrane is a crosslinked polysalt. The precursor, poly(styrene-*alt*-maleic anhydride) is relatively polar and hence soluble only in polar solvents, such as ethyl acetate. To encapsulate more hydrophobic core oils, styrene maleic anhydride copolymers with less than 50 weight % of maleic anhydride groups in the copolymer, or the analogous poly(*tert*-butylstyrene-*alt*-maleic anhydride) were used. Model compounds for insect sex pheromone such as dodecyl acetate and dodecanol were encapsulated in these SMA microcapsules and weight loss from these microcapsules was monitored over several weeks at room temperature. Relatively fast release of these core materials was attributed to the porous structure of the membrane, as confirmed by TEM and ESEM.[13]

The goal of the present study is to study the effects of solvent, the rate of amine addition, polymer loading, and type of copolymer used, on the capsule wall morphology, with the aim of preparing capsules with dense walls containing model compounds. In addition, the effect of this morphology on release into air will be described.

3.2 Experimental

3.2.1 Materials

Maleic anhydride (99%, Aldrich) was recrystallized from chloroform prior to use. The co-solvent for the encapsulation, ethyl acetate (Fisher Scientific) was reagent grade and used as received. Model compound, dodecyl acetate was purchased from Aldrich Chemical Company. The initiator 2,2'-azobis-(2-methylpropionitrile) (AIBN) was purchased from DuPont and recrystallized from methanol prior to use. Surfactant, nonyl-phenyl-oligo-ethylene glycol (IGEPAL CA-630) was purchased from Sigma. Styrene-*co*-maleic anhydride copolymer with 32 weight % maleic anhydride units (SMA32) was purchased form Aldrich. Amines, tetraethylenepentamine (TEPA) and hexamethylenediamine (HMDA) were purchased from Aldrich.

3.2.2 Encapsulation Procedure

The typical procedure for the preparation of styrene/maleic anhydride capsules was as follows: 0.4 g IGEPAL was dissolved in 30 mL deionized water in a 200mL beaker, by stirring with an overhead paddle stirrer at 400 rpm for 20 min. 1.00 g of *t*-BuSMA50 (3.9 mmol of maleic anhydride groups) was dissolved in 11 mL of a cosolvent such as ethyl acetate. After complete dissolution of the copolymer, 4 mL of dodecyl acetate or dodecanol were added to the copolymer solution. The resulting oil phase was then added dropwise over 1 min. to the aqueous phase to form an oil-in-water emulsion. After emulsifying for 5 min. at a stirring speed of 400 rpm, the stirring speed was reduced

to 200 rpm and a solution of 0.49 g (2.6 mmol) of tetraethylenepentamine (TEPA) in 2 mL of distilled water was added dropwise over 30 sec. The resulting dispersion of microcapsules was stirred at 200 rpm for a further 10 min., and then stored in polypropylene screw cap vials.

3.2.3 Characterization

FT-IR analyses were performed on a Bio-Rad FTS-40 FT-IR spectrometer. Copolymer spectra were taken as films cast from chloroform onto NaCl discs. All capsule samples used for FT-IR analysis were first washed three times with water, crushed by sonication, extracted five times with THF, and dried at 40°C under reduced pressure for 48 h. They were then prepared as pellets using spectroscopic grade KBr.

The internal morphology of the capsules was studied using a JEOL 1200EX transmission electron microscope (TEM). For TEM analysis, microcapsules were embedded in Spurr's epoxy resin, microtomed to ~50nm thickness, and stained with uranyl acetate.

Optical microscopy was performed using an Olympus BH-2 microscope, equipped with a Kodak DC 120 Digital Camera.

3.2.4 Determination of Apparent Partition Coefficient of HMDA and TEPA

The apparent partition coefficient of HMDA and TEPA between different organic solvents and water used in this study were determined in the same way as in the preparation of microcapsules by the following method. The organic phase (15 mL) was added to 30 mL of a 0.13 M aqueous solution of HMDA, or a 0.09 M solution of TEPA, respectively, containing 0.4 g IGEPAL. The mixture was then mechanically emulsified at 400 rpm for 5 min to yield an o/w emulsion. Immediately after stirring was stopped, the emulsion was centrifuged at 3500 rpm for 10 min to separate the aqueous phase from the organic phase. The concentration of the polyamine in the aqueous phase was then determined by titration with 0.1N HCl in case of HMDA, and with 1N HCl in case of TEPA. The partition coefficient of the polyamines was then calculated from their initial and final concentration in the aqueous solution.

3.2.5 Release Measurements

Approximately 100 μL sample of the concentrated capsules dispersed in water was placed on the aluminum pan and rolled around to spread out the microcapsules into a mono-layer. Once a mono-layer had been produced the sample was placed in the fume hood and weighed every 15 min for a period of approximately two hours, depending on the amount water in the slurry. The point at which all the water had evaporated from the pan was taken as the 100 weight % point (time zero). Subsequently the sample was

weighed twice a day for the first week, and then once a day until constant weight had been reached. The humidity and the temperature of the environment were measured using a standard humidity meter with thermometer.

3.3 Results and Discussion

Two types of SMA copolymers were used in this study; SMA32 (32 weight % of maleic anhydride groups) and *t*-butyl styrene-*alt*-maleic anhydride (t-BuSMA50, 50 mol % of maleic anhydride groups). SMA32 copolymer was obtained from a commercial supplier and had a molecular weight about 1,700. Low molecular weight *t*-BuSMA50 copolymer (M_n = 4,000) was prepared by free radical polymerization in the presence of 4-*tert*-butylcatecol as a chain transfer agent. Higher molecular weight *t*-BuSMA50 copolymer (M_n = 25,000) was prepared according to the general procedure for the free radical polymerization reported elsewhere.[13]

3.3.1 Effect of Core Solvent Composition on Microcapsule Wall Morphology

First, we will consider the changes in SMA32 capsule morphology observed as a result of varying the core oil composition from ethyl acetate to binary mixtures of ethyl acetate and dodecyl acetate. Ethyl acetate and dodecyl acetate are good and poor solvents, respectively, for the starting copolymer, with solubility parameters of δ = 18.6 $MPa^{1/2}$ (ethyl acetate)[14] and 17.2 $MPa^{1/2}$ (dodecyl acetate).[15] These microcapsules were

prepared according to the general procedure, with TEPA used as a polyamine. Besides being a suitable co-solvent, dodecyl acetate is also a component of several insect sex pheromones, and is hence a good model compound for release studies.

Figure 3.1 shows a typical series of transmission electron microscopy (TEM) images of 50 nm thick cross-sections of SMA32 microcapsules prepared in ethyl acetate and ethyl acetate / dodecyl acetate mixtures and the optical image of the same microcapsule to demonstrate the external capsule morphology (Figure 3.1a). Polymer loading was kept constant at 6.6 weight % in all experiments. Matrix systems without distinct outer skin were obtained in solvents ranging from neat ethyl acetate to 65 vol % ethyl acetate / 35 vol % dodecyl acetate (Figure 3.1b). Presence of 40% dodecyl acetate brings about an intermediate matrix /capsule morphology, consisting of very porous matrix particles with a distinct outer skin (Figure 3.1c). At 50 vol % dodecyl acetate capsules are formed, with porous walls containing areas of precipitated polymer (Figure 3.1d). And finally, at the 60 vol % of dodecyl acetate, capsules with thin and dense walls were obtained (Figure 3.1e). In some cases precipitated polymer was still observed within these capsules. Further increasing the amount of dodecyl acetate to 70 vol % caused the SMA32 copolymer to precipitate.

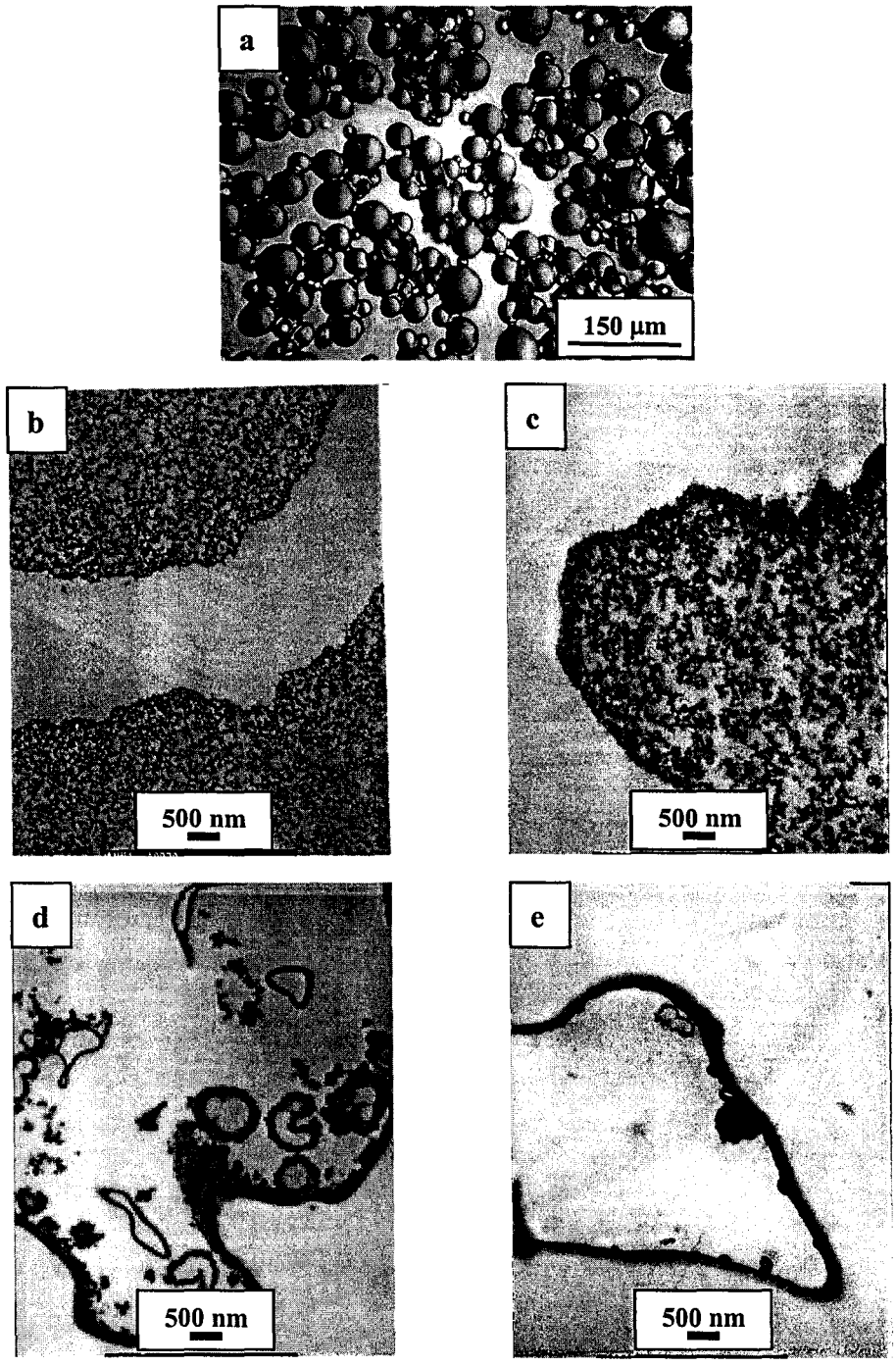

Figure 3.1 - (a) Optical micrograph of microcapsules prepared from SMA32 copolymer. Transmission electron cross-sectional micrograph of capsule internal morphology prepared from SMA32 copolymer and TEPA. Polymer loading in the core oil is 6.6 weight %. Core-oil: (b) 70:30, (c) 60:40, (d) 50:50, (e) 40:60 ethyl acetate: dodecyl acetate.

This wide range of observed morphologies arises in response to the reaction medium. The solvency has a two-fold effect on the course of the interfacial polycondensation and consequently on the particle morphology, affecting both thermodynamics and kinetics of the polycondensation reaction.

First, the polymer salt produced by reaction of the anhydride copolymer with amine, is better solvated in a polar solvent such as ethyl acetate. This solvation delays copolymer phase separation, and slows the diffusion of the polymeric salt to the interface. Under these conditions, the reacting copolymer chains become entrapped within the droplets by crosslinking, producing the observed matrix morphology. Late phase separation leads to formation of large pores, in analogy to suspension polymer systems. [16] When addition of dodecyl acetate brings the solvency of the organic phase closer to the *theta* – condition for the starting copolymer, phase separation of the forming polymeric salt occurs at early stages of the reaction, causing polymer diffusion towards, and precipitation at the interface, before significant crosslinking and entrapment can occur. The polymer precipitates at the interface, forming capsule morphology, because polymer-polymer interactions are more favorable than polymer-solvent interactions on either side of the membrane. Table 3.1 shows the solubility parameters of the solvent mixtures used in this study and observed morphology of SMA32 microcapsules.[17]

Table 3.1 - Solubility parameters of core mixtures and observed morphologies.

Organic Phase (% ethyl acetate)	δ_m [a] MPa $^{1/2}$	Observations (SMA32 δ = 20.3 MPa $^{1/2}$)[b]
100-70	18.6 - 18.1	matrix
60	18.0	porous matrix / capsule
50	17.9	capsule with porous wall
40	17.8	capsule

[a] δ_m approximated using $\delta_m = \phi_1\delta_1 + \phi_2\delta_2$ where ϕ is the volume fraction
[b] Ref. 17

Secondly, the diffusion of the polyamine into the oil phase influences the rate of the reaction. This diffusion depends not only on the membrane permeability but also on the partition coefficient of amine in the two phases, particularly in case of porous membranes.[4] High polyamine partition into more polar core oils leads to a higher possibility for the cross-linking reaction inside the oil droplet.[12] This effect slows the migration, and the precipitation of the polymeric salt at the interface and leads to matrix particles and capsules with porous, solvent swollen shells. Aliphatic polyamines such as TEPA are hydrophilic, and hence usually show low partitioning into hydrophobic core solvents such as xylene.[18] Our core solvents are mixtures of acetates, and we decided to measure the partitioning of polyamines between the aqueous and the organic phase under the same conditions as those in the preparation of microcapsules (Table 3.2). The apparent partition coefficients were determined under the same conditions as used in the preparation of microcapsules. The K value for HMDA measured for our systems was at

least 10 times smaller than that reported for water/cyclohexane-chloroform (3:1) and water/toluene systems.[11,18] However, direct comparison with literature partition coefficients are difficult, since in addition to the different solvents, different ratios between organic to aqueous phases, different surfactants, and different stirring speeds were used in the encapsulation literature.[11,12]

Table 3.2 - Partition coefficients of HMDA and TEPA between water and different core oil mixtures.

Organic phase EA/DA (%)[a]	IGEPAL (% in aqueous phase)	Partition Coefficient K (C_{aq}/C_{org}) HMDA	Partition Coefficient K (C_{aq}/C_{org}) TEPA
100	0	2.1	4.7
100	1.3	2.1	4.7
60/40	0	2.2	-
60/40	1.3	2.2	5.7
40/60	0	2.4	-
40/60	1.3	2.4	7.9
33/67	0	2.5	-
33/67	1.3	2.5	8.6

[a] EA – ethyl acetate, DA – dodecyl acetate

In our system, TEPA shows a larger partition coefficient than HMDA, in agreement with the more hydrophilic nature of the TEPA compares with HMDA. The partition coefficients for TEPA increase significantly with increasing hydrophobicity of the organic phase. The presence of IGEPAL in the aqueous phase has no effect on the partition coefficient values of either HMDA or TEPA.

3.3.2 Effect of Type of Polyamine on SMA32 Capsule Morphology

The significant difference in the partition coefficients of HMDA and TEPA motivated an investigation of the effect of amine on the capsule morphology formed from SMA32. Figure 3.2 shows TEM images of the microcapsules prepared with HMDA in ethyl acetate / dodecyl acetate mixtures. Matrix/capsule morphology was observed at 60 vol. % ethyl acetate (Figure 3.2a), and distinct capsule morphology at 40 vol. % ethyl acetate (Figure 3.2b). The transition from matrix to capsule morphology occurs at the similar solvency as for SMA32 microcapsules prepared with TEPA (Fig. 3.1). It appears that, although the two amines have very different partition coefficient values, particularly for the solvent mixtures with high content of dodecyl acetate (Table 3.2), the partitioning of TEPA into the organic phase is still sufficiently high and faster than polymer phase separation and diffusion to the interface, thus replacing TEPA by HMDA had no apparent effect on the capsule morphology under investigated conditions.

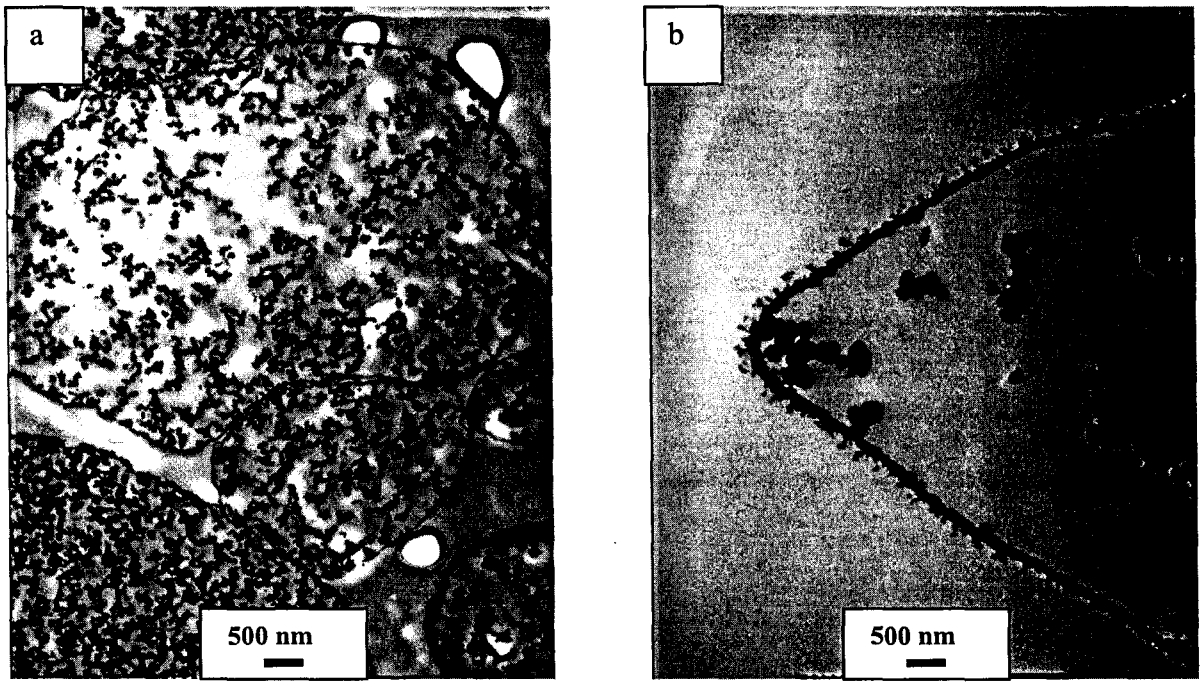

Figure 3.2 - Transmission electron cross-sectional micrograph of capsule internal morphology prepared from SMA32 copolymer and HMDA. Polymer loading in the core oil is 6.6 weight %. Core-oil: (a) 60:40, (b) 40:60 ethyl acetate: dodecyl acetate.

3.3.3 Effect of Type of Copolymer on Capsule Morphology

To investigate the effect of the type of copolymer on the capsule morphology t-BuSMA50 copolymer (4,000 Da) was used instead of SMA32 copolymer of comparable molecular weight (1,700) Da. *t*-BuSMA50 is soluble in a wider range of hydrophobic solvents compared with SMA32.[13] Thus, *t*-BuSMA50 is soluble in octyl acetate (17.3 $MPa^{1/2}$). As a consequence, the transition from capsule to matrix morphology was expected to occur at a higher percentage of dodecyl acetate for *t*-BuSMA50 compared with SMA32. However, the transition from matrix to capsule morphology was observed at exactly the same solvency condition as in the case of SMA32. At 60/40 ethyl acetate / dodecyl acetate, porous matrix structures and capsules with porous walls were observed (Figure 3.3a), while in 40/60 ethyl acetate/dodecyl acetate, capsules with thin and dense walls were obtained (Figure 3.3b).

This result can be explained based on the chemical composition difference between these two copolymers. *t*-BuSMA50 copolymer, although more hydrophobic, contains a higher amount of anhydride groups than SMA32. These groups react with polyamine to produce charged polyelectrolyte. The presence of a high concentration of charges facilitate polymer phase separation and diffusion to the interface.

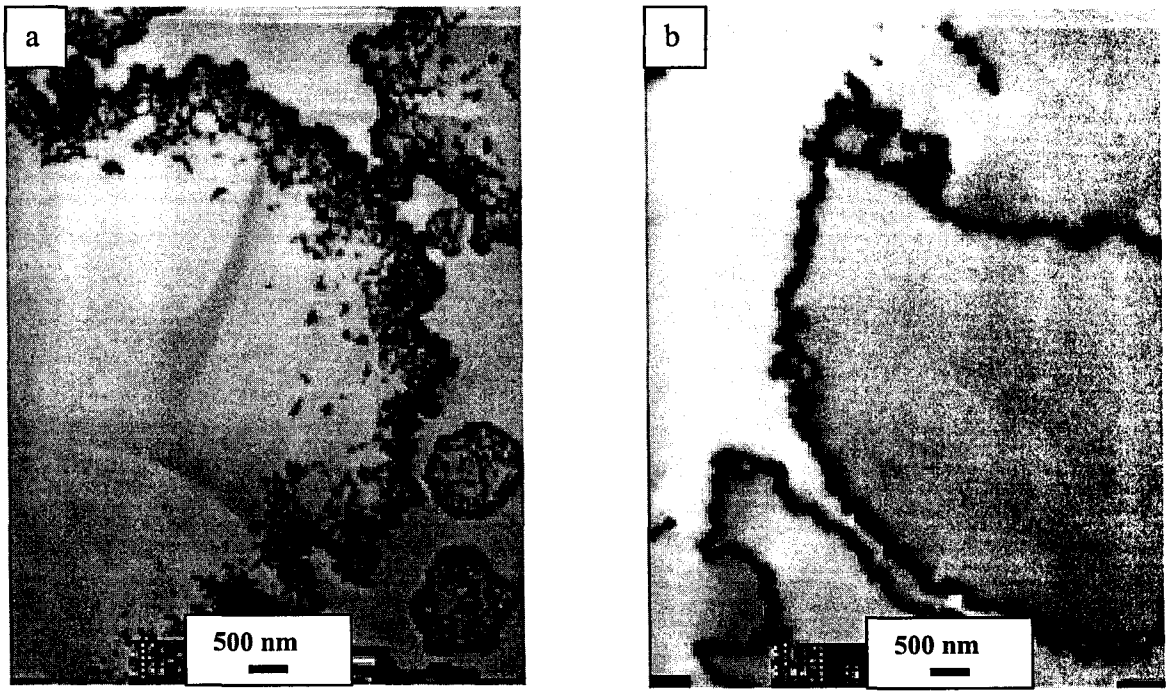

Figure 3.3 - Transmission electron cross-sectional micrograph of capsule internal morphology prepared from *t*-BuSMA50 (4,000) copolymer and TEPA. Polymer loading in the core oil is 6.6 weight %. Core-oil: (a) 60:40, (b) 40:60 ethyl acetate: dodecyl acetate.

3.3.4 Effect of Molecular Weight of Copolymer on Capsule Morphology

Another factor likely to influence the rate of the diffusion and the precipitation of the polymer chains at the interface is the molecular weight of the starting copolymer. In general, increasing molecular weight should slow its migration to the interface.[19] It should therefore be possible to control the particle morphology by using starting copolymers of different molecular weight. To evaluate this hypothesis, we compared the morphologies obtained in encapsulations using *t*-BuSMA50 copolymers of 4,000 Da (see above) and 25,000 Da (Fig. 3.4), respectively. The solvency of the system was adjusted as before by diluting ethyl acetate with dodecyl acetate. The two copolymers gave identical matrix morphologies in neat ethyl acetate. However, the transition from matrix to capsule morphology occurs at a later stage, or higher dodecylacteate content, for the higher molecular weight copolymer. At 60 vol. % ethyl acetate matrix morphology continues to be observed for the particles made from higher molecular weight *t*-BuSMA50 copolymer (Figure 3.4a), and at 40 vol. % ethyl acetate capsules with porous walls are obtained (Figure 3.4b). Denser walls were observed only at 33 vol. % ethyl acetate (Figure 3.4c). This is in contrast to the particles made with low molecular weight *t*-BuSMA50 copolymer, which show the transition from matrix to capsule with dense, thin walls at 40 vol. % of ethyl acetate (Figure 3.3b).

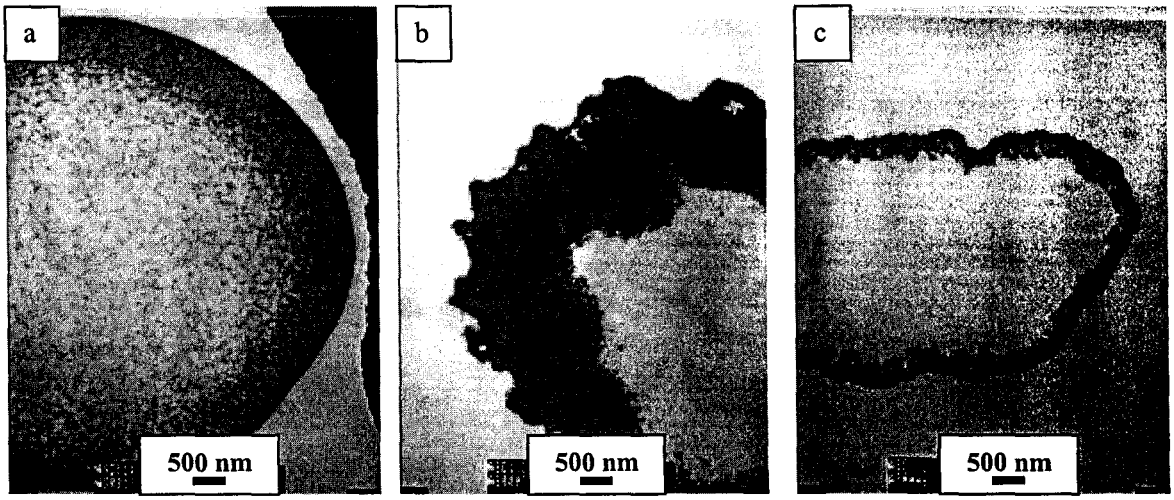

Figure 3.4 - Transmission electron cross-sectional micrograph of capsule internal morphology prepared from *t*-BuSMA50 (25,000) copolymer and TEPA. Polymer loading is 6.6 weight %. Core-oil is: (a) 60:40, (b) 40:60, (c) 33:67 ethyl acetate: dodecyl acetate.

3.3.5 Effect of Polymer Loading

Initial polymer loading should also affect the viscosity of the organic medium and consequently the diffusion of the polymer and its precipitation at the interface. We have reported earlier that an increase in the polymer loading does not bring about a decrease in the rate of release.[13] However, the produced particles were stronger and did not break apart under sonication. Figure 3.5 shows a series of TEM images of SMA32 particles prepared with 73 / 27 ethyl acetate / dodecyl acetate, with copolymer loading increasing from 3.3 to 9.9 weight %. The transition from microcapsule with porous walls to matrix morphology is clearly visible in these images. If the starting polymer loading exceeds approximately 6 weight %, the phase-separated polymer fills the entire particle leading to a microdomain structure.

The exact polymer loading required for matrix morphology is dependent on the nature of the core solvent as discussed above. Thus, in poor solvency conditions (60 vol. % of dodecyl acetate) an increase in polymer loading from 6.6 to 9.9 weight % causes an increase in thickness of the capsule wall instead of matrix formation.

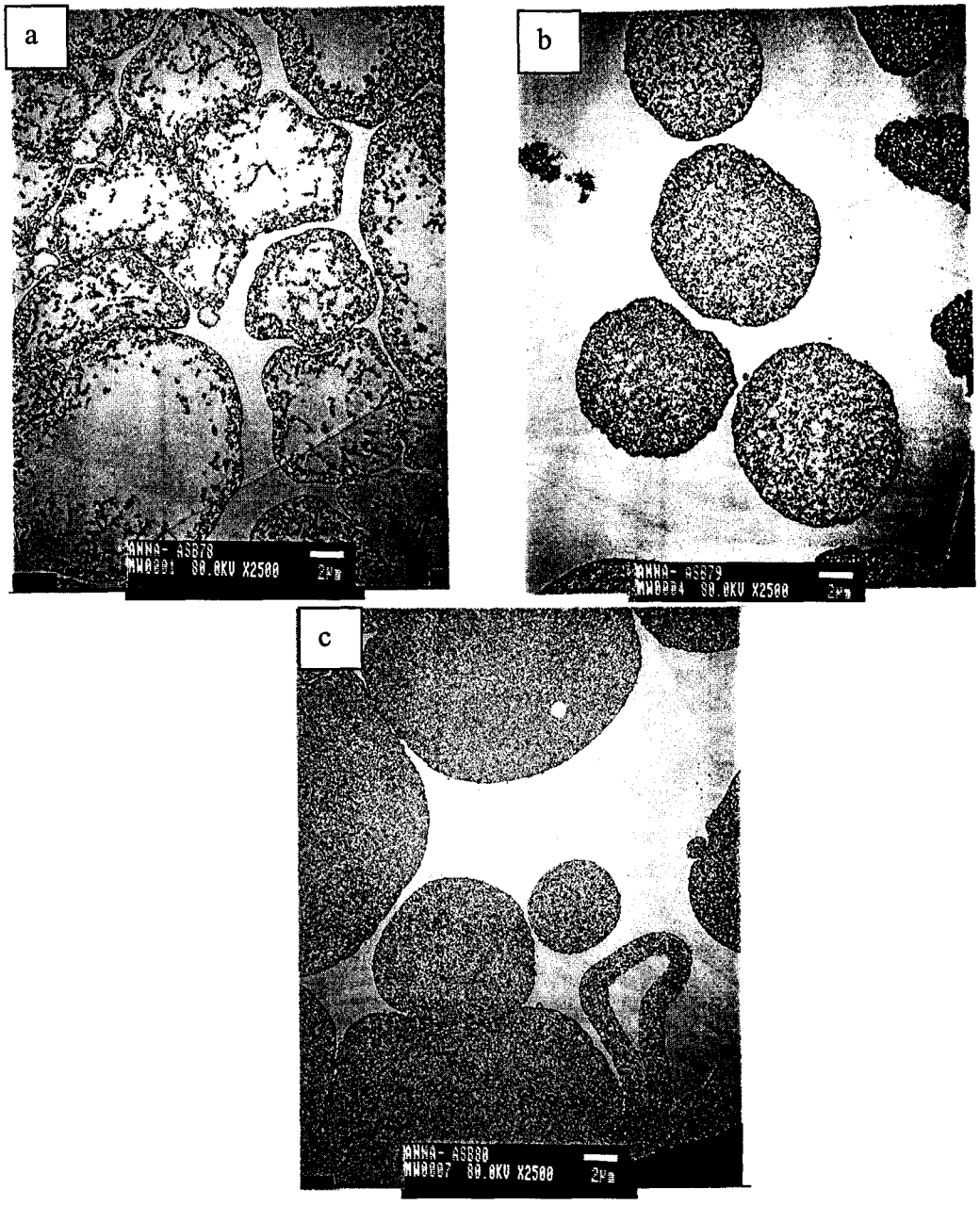

Figure 3.5 - Transmission electron cross-sectional micrograph of capsule internal morphology prepared from SMA32 copolymer and TEPA Core-oil is 73:27 ethyl acetate: dodecyl acetate. Polymer loading in the core oil: (a) 3.3 weight %, (b) 6.6 weight %, (c) 9.9 weight %

3.3.6 Effect of Rate of Amine Addition on Microcapsule Wall Morphology

As mentioned previously, we propose that amine partitioning into the organic phase is one of the main factors that controls capsule wall morphology. In an attempt to separate the effects of amine partitioning and polymer/solvent interactions on the capsule morphology, we carried out encapsulations at constant core solvent compositions, but with varying rates of amine addition. The solvent mixture chosen for this study, 74 vol % ethyl acetate / 27 vol. % dodecyl acetate, leads to a matrix system. The rate of TEPA addition was adjusted using an automated titrator. Two amine addition regimes were used; in the first experiment, the aqueous solution of TEPA was added over 30 seconds, as described in the general encapsulation method, and in the second, the same amount of amine was added over 3 hours, at a rate of 0.001 mL/sec. It was expected that slowing the rate of amine addition would cause morphology changes equivalent to those observed upon changing the core oil composition. Figure 3.6 shows TEM images of SMA32 particles prepared with different rates of amine addition. Particles made with fast amine addition have the matrix morphology typical for polar core oils. However, the microcapsules prepared with slow amine addition have a thin and dense wall. The amount of amine partitioning inside of the oil drop is now controlled by the rate of amine addition and not by the partition coefficient of amine between organic and aqueous phases.

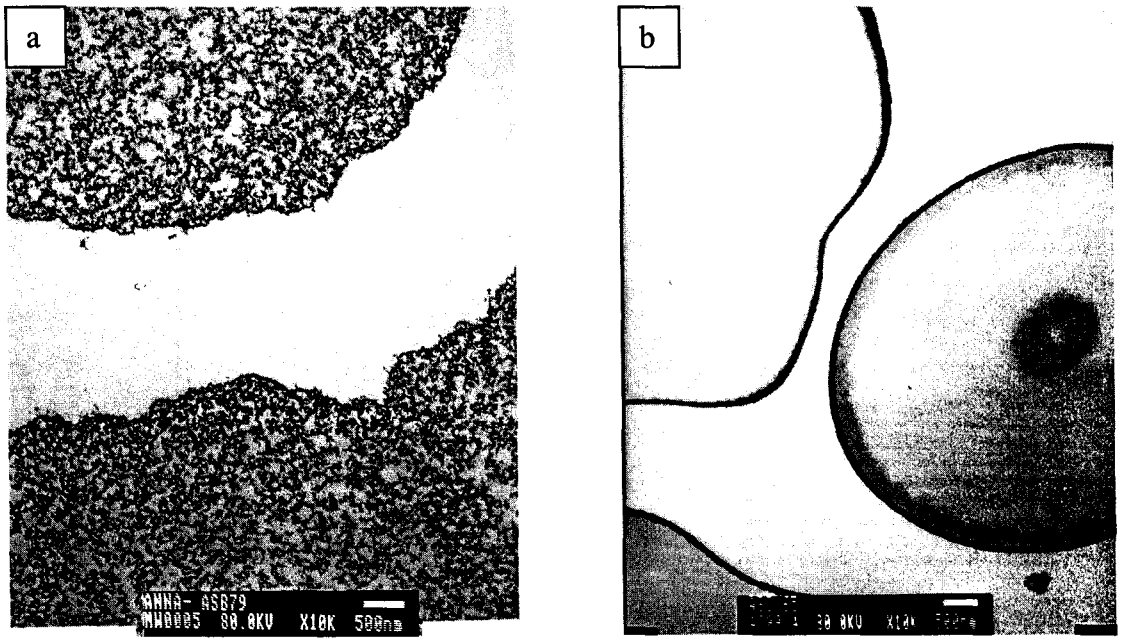

Figure 3.6 - Transmission electron cross-sectional micrograph of capsule internal morphology prepared from SMA32 copolymer and TEPA Core-solvent is 73:27 ethyl acetate: dodecyl acetate. Polymer loading in the core oil is 6.6 weight %. Rate of amine addition: (a) 30 sec., (b) 3 hr.

3.3.7 Effect of Morphology on Release

The release from SMA microcapsules prepared with various core co-solvents and with different rates of amine addition was monitored gravimetrically at room temperature. In all cases, the ethyl acetate evaporates almost instantly upon exposure to air, such that the actual weight loss shown in the release curves reflects the loss of the higher boiling dodecyl acetate. To check method reproducibility all release measurements were carried out in triplicates.

Figure 3.7 shows the release profiles from SMA particles having capsule morphology (thin, dense walls) prepared from three different polymers; SMA32, *t*-BuSMA50 (low molecular weight) and *t*-BuSMA50 (high molecular weight). There is no marked difference in the release profiles between the microcapsules prepared with *t*-BuSMA50 copolymers of different molecular weight. On the other hand, microcapsules prepared with SMA32 released their content two times faster than those prepared with either of the *t*-BuSMA50 copolymers. These results correlate well this the fact that the SMA32 polymer has a lower density of cross-linking sites than the *t*-BuSMA50 copolymers.

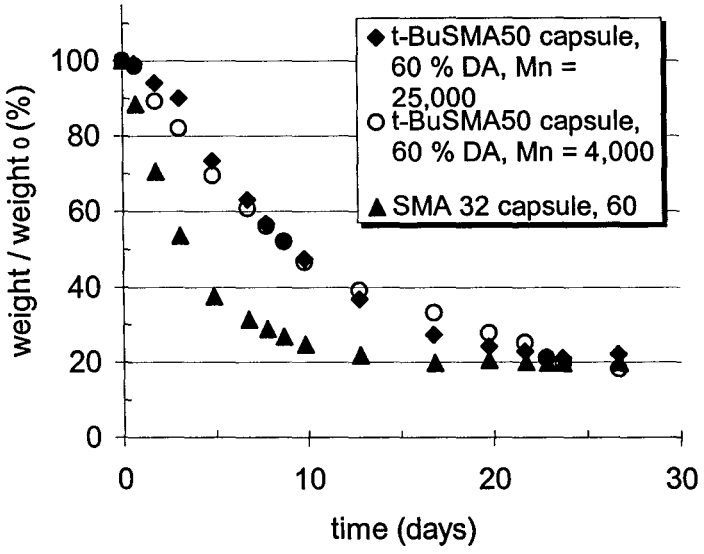

Figure 3.7 - Normalized weight at room temperature vs. time. Microcapsules of 50-60 μm with dense walls. Polymer loading in the core oil is 6.6 %. Copolymer used: (♦) t-BuSMA50 (25,000), (o) t-BuSMA50 (4,000), (▲) SMA32.

However, the matrix particles prepared from the same three polymers demonstrated identical permeation properties regardless the type of polymer used (Figure 3.8). These results also correlate well with our previous observations.[13] In all cases the matrix particles released their contain at the slower rate than capsules particles.

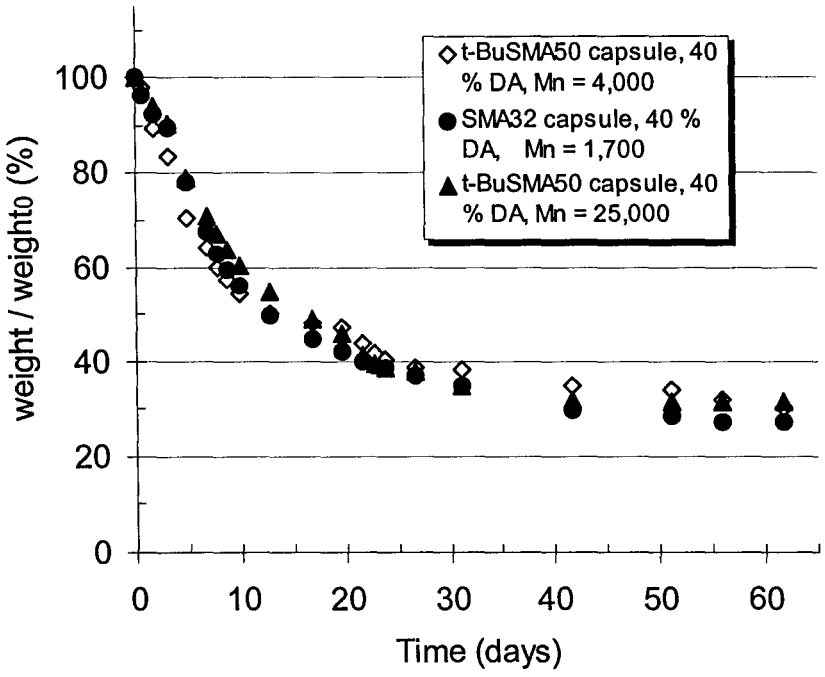

Figure 3.8 - Normalized weight at room temperature vs. time. Microcapsules of 50-60 μm with porous thick walls / matrix morphology. Polymer loading in the core oil is 6.6 %. Copolymer used: (◊) t-BuSMA50 (4,000), (•) SMA32, (▲) t-BuSMA50 (25,000).

Figure 3.9 shows the release rates from SMA32 microcapsules prepared with different rates of amine addition. In this case core oil composition was kept constant, and the release rate can be directly correlated to the microcapsule morphology. It was found that microcapsules prepared with fast amine addition, which have porous walls release their contents slowly relative to the SMA32 microcapsules prepared with slow amine addition which have a dense skin.

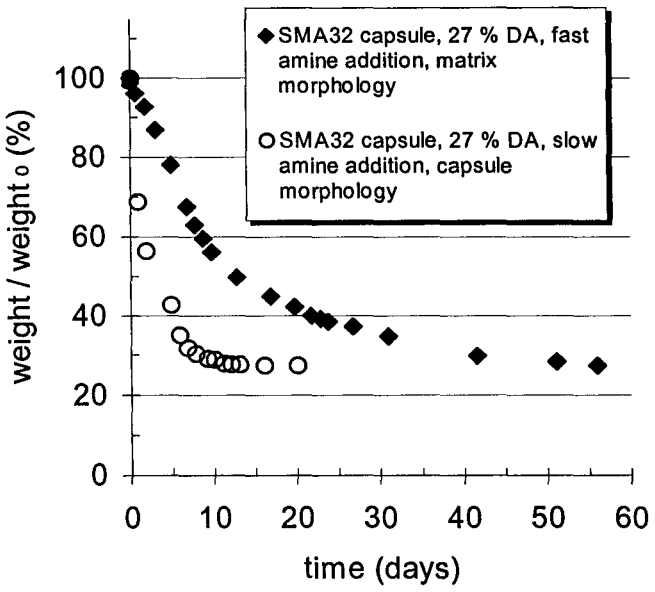

Figure 3.9 - Normalized weight at room temperature vs. time. Microcapsules of 50-60 μm. Polymer loading in the core oil is 6.6 %. Copolymer used is SMA32. (o) slow TEPA addition (capsule morphology), (♦) fast TEPA addition (matrix morphology).

We reported that the ability of SMA microcapsules with porous and thick walls to release the core material was found to critically depend on the level of humidity.[13] The total release period was increased by a factor of three at high humidity levels. This release trend was attributed to the hydrophilic nature of the microcapsule membrane that can absorb water from the air.

It is possible that the same effect plays a key role in the release from the microcapsules with different wall morphology. Active hydrophobic compounds can penetrate the thin and dense wall easily whereas the penetration through the thick wall in which pores are saturated with water, is much more difficult. To support this hypothesis, the release from SMA32 microcapsules prepared with different amine addition regimes was measured in dry conditions. Figure 3.10 demonstrates that the rate of release from microcapsules with thick wall increased and became identical to the rate of release from the microcapsules with thin walls, which has not changed in dry conditions.

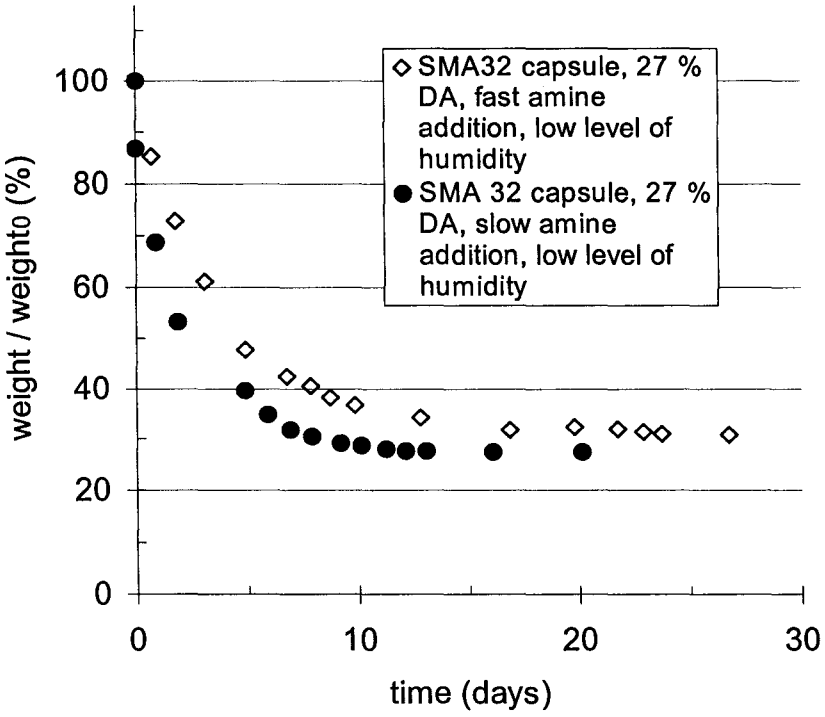

Figure 3.10 -Normalized weight at room temperature vs. time. Microcapsules of 50-60 μm. Polymer loading in the core oil is 6.6 %. Copolymer used is SMA32. (•) slow TEPA addition (capsule morphology), (◊) fast TEPA addition (matrix morphology). Humidity level is 20 –30 %.

3.4 Conclusion

Interfacial reaction between maleic anhydride copolymers and water soluble polyamines can be utilized to prepare particles with different morphologies, by varying several parameters including starting polymer loading and molecular weight of the starting copolymer. However, the main factors that affect particle morphology are the nature of the core oil solvent, and the rate of amine addition. Solvency strongly influences polymer/ solvent interactions and polyamine partitioning into the organic phase. Neat ethyl acetate, a good solvent for the starting copolymer and a marginal solvent for the formed polymeric salt, leads to the formation of matrix particles. Dodecyl acetate is a non-solvent both for the starting copolymer and the formed polymeric salt. In a mixture of ethyl acetate and dodecyl acetate there is transition between matrix and capsule morphologies, at a point where the core solvent mixture was still a good solvent for the starting copolymer, but a non-solvent for the formed polymer salt. Partition coefficient measurements indicated that the solvency of the organic phase was still sufficient for the polyamine partitioning even when only 40 vol % of ethyl acetate was used. Varying the polymer molecular weight had little effect on the capsule morphology under conditions of good solvency. Conversely, under conditions of poor solvency, i.e. 60 / 40 vol. % ethyl acetate / dodecyl acetate, the transition in particle morphology shifts when high molecular weight copolymer was used.

The rate of polyamine addition strongly affects the particle morphology, even under good solvency conditions. Thus, capsules with thin and dense wall were obtained in almost 80 vol. % of ethyl acetate, when polyamine was added slowly.

The relationship between capsule morphology and the permeation properties was also established. It was found that microcapsules that have thick, porous walls release their content slowly relative to those that have a thin, dense wall. The observed slow release at room temperature from microcapsules having porous and thick wall was attributed to the nature of the copolymer.

Acknowledgements

We would like to thank Marcia West for helping in the preparation of TEM samples. We would also like to thank 3M Canada and the Natural Sciences and Engineering Research Council of Canada for funding this research. In addition, A. Shulkin would like to acknowledge McMaster University for her Centennial Scholarship, and the Government of Ontario for an Ontario Graduate Scholarship.

References

1) Toubeli, A.; Kiparissides, C. *J. Membrane Sci.*, **1998**, *146*, 15-29.

2) Mathiowitz, E.; Cohen, M. D. *J. Membrane Sci.*, **1989**, *40*, 43-54.

3) Mathiowitz, E.; Cohen, M. D. *J. Membrane Sci.*, **1989**, *40*, 1-26.

4) Frére, Y.; Danicher, L.; Gramain, P. *Eur. Polym. J.* **1998**, *34*, 193-199.

5) Yadav, S. K.; Khilar K. C.; Suresh, A. K. *J. Membrane Sci.*, **1997**, *125*, 213-218.

6) Hong, K.; Park, S. *J. Mater. Sci.* **1999**, *34*, 3161-3164.

7) Arshady, R. *J. Microencapsulation* **1989**, *6(1)*, 13-28.

8) Morgan, P. W.; Kwolek, S. L. *J. Polym. Sci.* **1959**, *XL*, 299-327.

9) Vanbesien, D. Synthesis and Properties of Polyurea Microcapsules, M. Sc. Thesis, McMaster, 1999.

10) Wittbecker, E. L.; Morgan, P. W. *J. Polym. Sci.* **1959**, *XL*, 289-297.

11) Zydowicz, N.; Chaumont, P.; Soto-Portas, M. L. *J. Membrane Sci.*, **2001**, *189*, 41-58.

12) Koishi, M.; Fukuhara, N.; Kondo, T. *Chem. Pharm. Bull.*, **1969**, *17*, 804-809.

13) Shulkin, A.; Stöver, H. D. H., Submitted to *J. Membrane Sci.*

14) Grulke, E. A. Solution Properties: Solubility Parameter Values; In *Polymer Handbook*; Brandrup, J., Immergut, E. H., Grulke, E. A., eds. Wiley-Interscience: New York, 1999; pp 675-714.

15) The solubility parameter value was estimated using group contribution method.

16) Guyot, A.; Bartholin, M. *Prog. Polym. Sci.* **1982**, *8*, 277-332.

17) Culbertson, B. M. Maleic and Fumaric Polymers; In *Encyclopedia of Polymer Science and Engineering* H. F. Mark, N. M. Bikales Eds., Interscience Publishers, New York,1976, 9, 225.

18) Tsukahara, S.; Satake, S.; Suzuki, N. *Solvent Extraction and Ion Exchange* **1997**, *15(6)*, 961-973.

19) Lovell, P. A.; El-Aasser, M. S. In *Emulsion Polymerization and Emulsion Polymers*, John Wiley and Sons, Chichester, 1997.

CHAPTER 4

Reactivity of Maleic Anhydride Based Copolymers in Encapsulation Procedures

Anna Shulkin and Harald D. H. Stöver

Department of Chemistry, McMaster University

1280 Main St. West, Hamilton, Ontario, Canada L8S 4M1

To Be Submitted to The Journal of Membrane Science

4.1 Introduction

As discussed in the first three chapters, the preparation of microcapsules using styrene-maleic anhydride (SMA) microcapsules has posed a number of new challenges and behaviours that were not encountered with traditional polyurea or polyamide systems. These behaviours originate from utilizing preformed polymers instead of monomers as the starting blocks in the encapsulation procedure, and from the extremely hydrophilic nature of the formed polymer membrane. In this work, a comprehensive experimental study is performed of the final conversion, time and rates of the interfacial SMA reaction, under the conditions of the SMA microencapsulation. In addition, the competition of amidation versus hydrolysis in interfacial SMA encapsulations has been studied.

4.1.1 Effect of Solvent on Conversion of Amidation Reaction

The degree of conversion in reactions on polymers in solutions is slowed and sometimes incomplete, due to steric hindrance and to chain conformation. This "polymer effect" is directly related to the solution state of the polymer. In some cases no reaction medium can be identified as a good solvent for the polymer. In other cases, a good solvent for the starting polymer can turn out to be a poor solvent for the product of the reaction. [1] In this case the solution state of the polymer is changing during the reaction, from an expanded coil to a more compact form, reducing the accessibility of the residual

functional groups. This phenomenon is important for amidation reactions of styrene-maleic anhydride based polymers since there are only a few standard solvents such as DMF and DMSO that dissolve the starting polymer and the reaction product equally well.[2] Rätzsch and Hue reported that this reaction proceeds to 100 % conversion in the case of *n*-butyl amine in DMF.[3] However, when THF, a precipitant for the product polymer was added to the solvent mixture, the conversion of the reaction with amines was reduced to 40.5% in a DMF : THF (1:9) solvent mixture.

4.1.2 Steric Effect and Effect of Polymer Molecular Weight on Conversion of Amidation Reaction

It is well known that the reactivity of the amines in the aminolysis reaction of anhydrides is determined by their basicity (pK_B value) and their steric hindrance.[4,5,6] However, in the reaction between maleic anhydride based copolymers and amines a steric influence of the copolymer itself was reported.[1] Thus, the reaction rate constants for the reaction of a series of maleic anhydride based copolymers with amines were reported to follow the order of comonomers: norbornene < styrene < cyclopentene < propene < ethene. The absolute values of the rate constants vary with the amine but this sequence remains. The screening of the anhydride group by the comonomer has also been observed in polymer hydrolysis and esterification reactions.[7]

The rates of reaction of anhydride-containing polymers with amines are also dependent on the molecular weight of the polymer used. A minimum molecular weight of 50,000 has to be reached before the reaction is retarded due to the polymer effect.[1]

In the first part of this paper the conversions and rates of the interfacial reaction between SMA copolymers and amine is discussed. It should be mentioned, that in the present interfacial reaction between anhydride and amine, both reaction rate and ultimate conversion depend not only on the properties of polymer, amine and solvent but also on the rate of partitioning of amine into organic phase, and on the morphology of the initially formed membrane.

4.1.3 Hydrolysis as a Side Reaction During Amidation Process

The uncatalyzed hydrolysis of maleic anhydride copolymers is a relatively slow process. Thus, the complete hydrolysis of poly(propylene-*alt*-maleic anhydride) in a DMF/water mixture takes about 22 hr, at 65°C.[1] The rate of reaction of maleic anhydride based copolymers with water in organic solvents has been shown to be an order of magnitude slower than the corresponding reaction with amine.

Table 4.1- Reaction rate constants k (L mol^{-1} hr^{-1}) for the amidation reaction with aniline, and for hydrolysis.[1]

Polymer	Amidation	Hydrolysis
Pr/MAn copolymer	0.605 (45 °C)	0.024 (45 °C)
St/MAn copolymer	2.7 (45 °C)	1.14 (65 °C)

However, the possibility of hydrolysis as a side reaction during the amidation process in organic solvent/water mixtures still exists since the rate and conversion of the hydrolysis reaction can be significantly increased in the presence of catalyst and/or at high pH values.[8] Thus, it was shown that the yield of covalent immobilisation of biological molecules to maleic anhydride based copolymers in DMSO/ water mixtures (5 volume % water) was high, around 93 % at pH 9.3, however it significantly decreased at higher pH.[9] These results were attributed to the fact that the rate of hydrolysis of the anhydride moieties was faster than that of the coupling reaction of the DNA probe onto the polymer at the high pH values. When the immobilization of proteins onto poly(maleic anhydride–*alt*-methyl vinyl ether) was performed in a DMSO / water mixture containing a much higher water content, 95 %, a very low grafting efficiency that exhibited no dependence on pH was observed.[10] The low yield of the reaction (about 7 – 17 %) is as a result of elevated hydrolysis in this water-rich (95 %) binary solvent system.

Therefore, the reactivity of maleic anhydride copolymers towards amines and water during encapsulation procedures still remains an open question and will be discussed in the second part of this paper. This issue becomes pertinent in SMA encapsulation where relatively hydrophilic core oils are usually used and the capsule shell consists of polymeric salt. Partitioning of both amine and water into these organic phases can be high, especially when the amine is added slowly to the aqueous phase resulting in long encapsulation times. Consequently, maleic anhydride groups suffer prolonged exposure to water that continually diffuses into the organic phase.

4.2 Experimental

4.2.1 Materials

Maleic anhydride (99%,Aldrich) was recrystallized from chloroform prior to use. The cosolvents for the encapsulation, ethyl acetate (Fisher Scientific), propyl acetate (Aldrich), butyl actetate (Fisher Scientific), and hexyl acetate (Aldrich) were reagent grade and used as received. Nonyl-phenyl-oligo-ethylene glycol (IGEPAL CA-630) was purchased from Sigma.

4.2.2 Conversion Measurements by FT-IR

FT-IR analyses were performed on a Bio-Rad FTS-40 FT-IR spectrometer. All samples used for FT-IR analysis were first acidified with 0.1M solution of HCl washed three times with water, filtered, and dried at 40°C under reduced pressure for 48 h. They were then prepared as pellets using spectroscopic grade KBr.

4.2.3 Measurements of Rates of Encapsulation

Experiments to measure rates of encapsulation were conducted using a modification of the procedure developed by Yadav *et al.*[12] for polyurea microcapsules. In a typical experiment an emulsion was first prepared as following: 0.1 g IGEPAL was dissolved in 25 mL deionized water in a 200 mL beaker, by stirring with an overhead paddle stirrer at 400 rpm for 20 min. 0.25 g of *t*-BuSMA50 (0.96 mmol of maleic

anhydride units) was dissolved in 7.5 mL of a cosolvent such as hexyl acetate. The resulting oil phase was then added to the aqueous phase to form an oil-in-water emulsion. After emulsifying for 5 min. at a stirring speed of 400 rpm, the formed emulsion was transferred into a 80 mL beaker and the original beaker was rinsed with an additional 2 mL of deionized water. The stirring speed was reduced to 60 rpm and the standard six-bladed propeller (50 mm in diameter) was switched to the small automatic titrator propeller. The pH of the continuous phase and the time of the reaction were monitored using an automatic titrator. The readings were taken every 3 or 5 seconds. The pH of the continuous phase before HMDA addition was approximately 3.5. After 5 minutes of stirring, 0.16 g of 70 % HMDA (0.96 mmol) dissolved in 5 mL of deionized water were added. The starting time of the encapsulation was reckoned from the moment when the pH rose to a maximum value of approximately 11.75. When the pH attained a constant value, indicating completion of the reaction, the agitation was stopped and small portion of the microcapsules dispersion was acidified with 0.1M HCl solution, washed, filtered and dried for the FT-IR analysis.

Calibrations of pH as a function of the concentration of HMDA in the range of interest were prepared from actual measurements of the pH of the standard HMDA solutions of known concentration.

4.2.4 Encapsulation Reaction at "Ceiling" pH

In a typical experiment an emulsion was first prepared as follows: 0.1 g IGEPAL was dissolved in 25 mL deionized water in a 200 mL beaker, by stirring with an overhead paddle stirrer at 400 rpm for 20 min. 0.25 g of *t*-BuSMA50 (0.96 mmol of maleic anhydride units) was dissolved in 15 mL of a co-solvent such as hexyl acetate. The resulting oil phase was then added to the aqueous phase to form an oil-in-water emulsion. After emulsifying for 5 min. at a stirring speed of 400 rpm, the formed emulsion was transferred into a 80 mL beaker and the original beaker was rinsed with an additional 5 mL of deionized water. The stirring speed was reduced to 60 rpm and the standard six-bladed propeller (50 mm in diameter) was replaced by a smaller propeller. 0.05 M HMDA or 0.1M butyl amine solutions were prepared and calibrated by titrator, The software of a Mandel Scientific automated titrator running PC-Titrate was modified in order to be able to record time, pH of the continuous phase and volume of the added amine simultaneously. The new titration methods were also developed to permit to run the encapsulation in pH-controlled environment. The instrument was programmed to calculate the rate of pH change over time, and estimate the appropriate volume of amine to be injected based on the previous pH. Thus, at the beginning of each encapsulation the titrator would rapidly inject amine until the system reached the predefined "ceiling" pH, the desired pH at which the reaction was to be carried out. Then, the volume of amine injection would by reduced if the change in pH was greater than 0.05 pH units or if the pH of the aqueous phase was within 0.1 pH units of the "ceiling" pH. The addition of

amine would stop as long as the pH of the continuous phase was higher than or equal to the "ceiling" pH value, and would start again when the pH dropped 0.1 pH units below the 'ceiling' pH value.

4.3 Results and Discussion

4.3.1 Conversion with Time

Wall thickness measurements are commonly used in the encapsulation literature to estimate the rate of reaction.[11] However, this method cannot be used for SMA microcapsules due to the high porosity of the formed capsule walls. Alternative techniques, based on monitoring the change in concentration of one of the monomers would be more suitable for SMA encapsulation. Nevertheless, there is no simple method of measuring the amount of unreacted anhydride groups or polyamine on-line. Experiments using on-line FT-IR to monitor the progress of the reaction failed due to the insensitivity of the fibre optic FT-IR probe in heterogeneous systems. Therefore, the concentration of amine present in the aqueous phase was related to the pH of the continuous phase as was described in the method developed by Yadav and co-workers.[12,13] As well, the concentration of the unreacted anhydride groups at the end of the reaction was estimated by FT-IR.

To be able to monitor the progress of the encapsulation reaction by following the change in pH, an equimolar ratio of *t*-BuSMA50 maleic anhydride groups to amino groups on hexamethylene-1,6-diamine (HMDA) was used. The amount of initial polymer used in this study was 3.3 weight %, which is typical for SMA encapsulation procedures, however the amount of polyamine used was less than usual. In typical encapsulation procedures, a slight excess of amine is usually present. Figure 4.1 shows the change in pH profile of the aqueous phase with time during the encapsulation process using hexyl acetate as core oil. The starting concentration of HMDA was 0.03M. As can be seen from the graph, the pH changes from a value of about 11.8 to about 9 during the encapsulation.

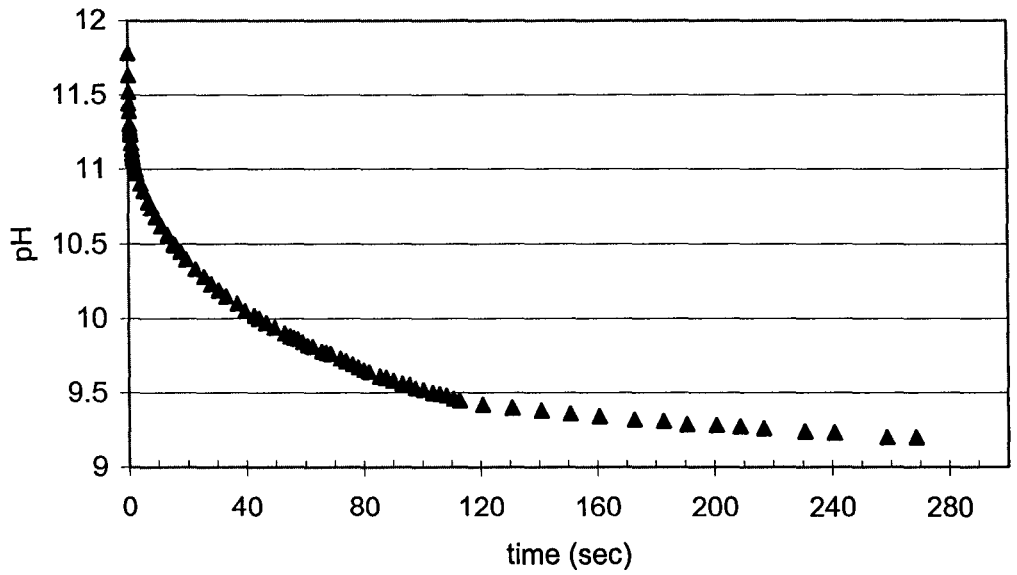

Figure 4.1 - Typical variation in pH during encapsulation procedure; hexyl acetate used as core oil.

An experimental calibration curve, which correlates HMDA concentrations and pH values, was used to convert pH values obtained from the encapsulation to concentrations of HMDA. This calibration curve was obtained from actual measurements of pH in different HMDA solutions with appropriate amounts of emulsifier added to mimic actual encapsulation conditions (Figure 4.2).

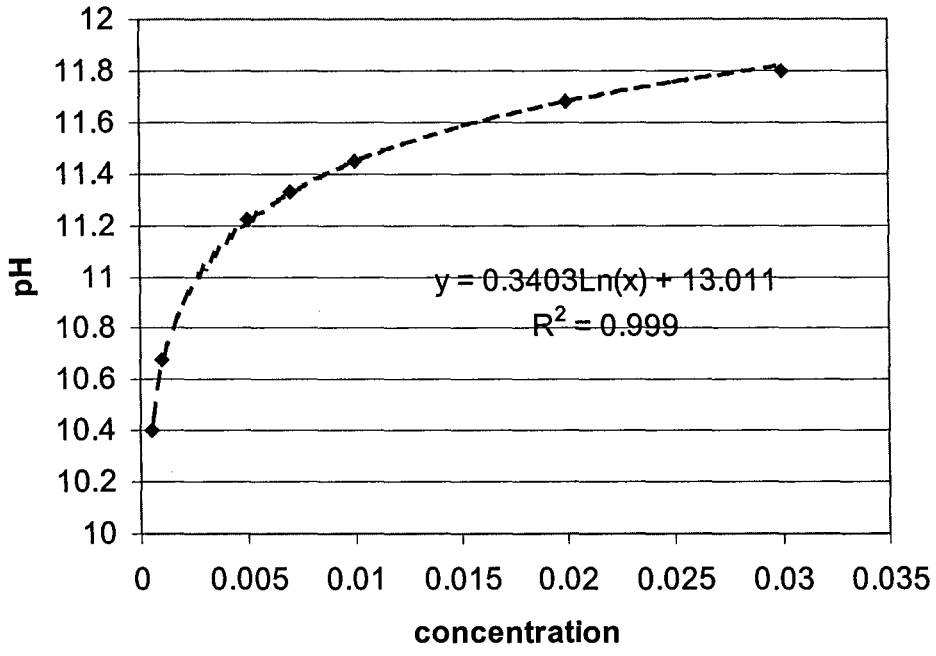

Figure 4.2 - Calibration curve that correlates the pH values and HMDA concentrations

Figure 4.3 shows the dependence of reaction conversion on reaction time for four solvent mixtures: ethyl, propyl, butyl and hexyl acetate. It is clear from these data that the

reaction between HMDA and *t*-BuSMA50 copolymer is fast, as 75 % conversion was achieved at about 15 seconds when ethyl acetate was used as a core solvent, at about 30 seconds when propyl, butyl were used as core solvents, and at about 60 seconds in the hexyl acetate case. It should be mentioned, that the values for the final reaction conversions, estimated from the change in pH values during the encapsulations, were higher than the ones estimated by FT-IR for the ethyl acetate and propyl acetate cases (Chapter 1). This discrepancy is attributed to the fact that after the reaction is complete amine can continue to partition into the polar organic phase without reacting, causing a decrease in the pH of the aqueous phase.

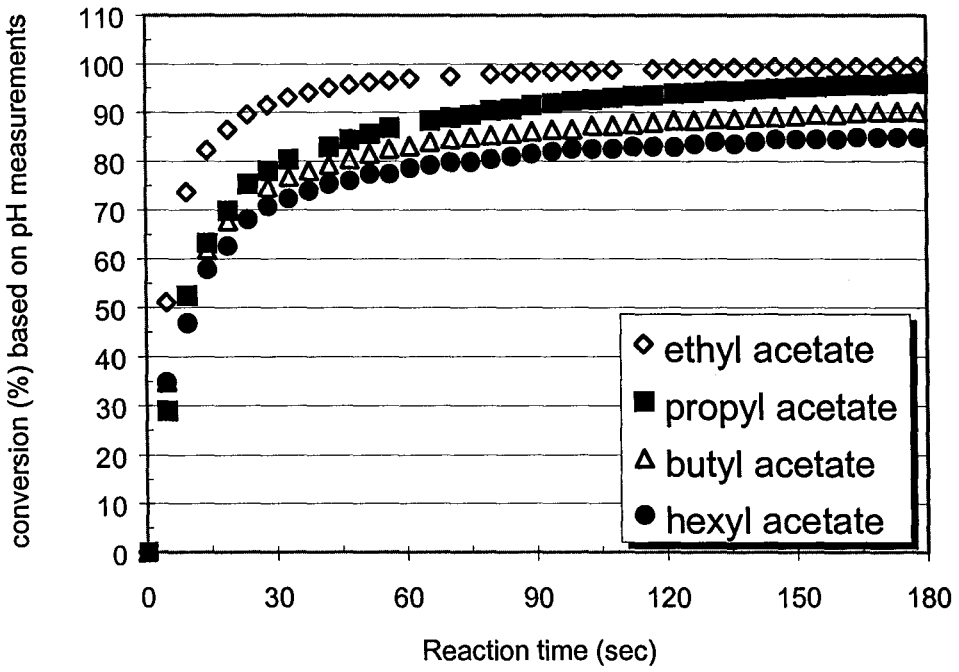

Figure 4.3 – Conversion of encapsulation reactions (*t*-BuSMA50 copolymer and HMDA) measured based on pH variations during encapsulation procedures.

The progress of the encapsulation reaction with time was also followed by FT-IR. The interfacial encapsulation reactions were quenched after 15, 30, and 60 seconds by adding 0.1M HCl solution and bringing the pH of the continuous phase to 2. Subsequently, the microcapsules were filtered, washed with water, vacuum dried overnight. The conversion of anhydride groups to amide and carboxylic acid was estimated from FT-IR spectra as described previously. Figure 4.4 shows the conversion versus time for the encapsulation reaction of *t*-BuSMA50 copolymer with HMDA in hexyl acetate.

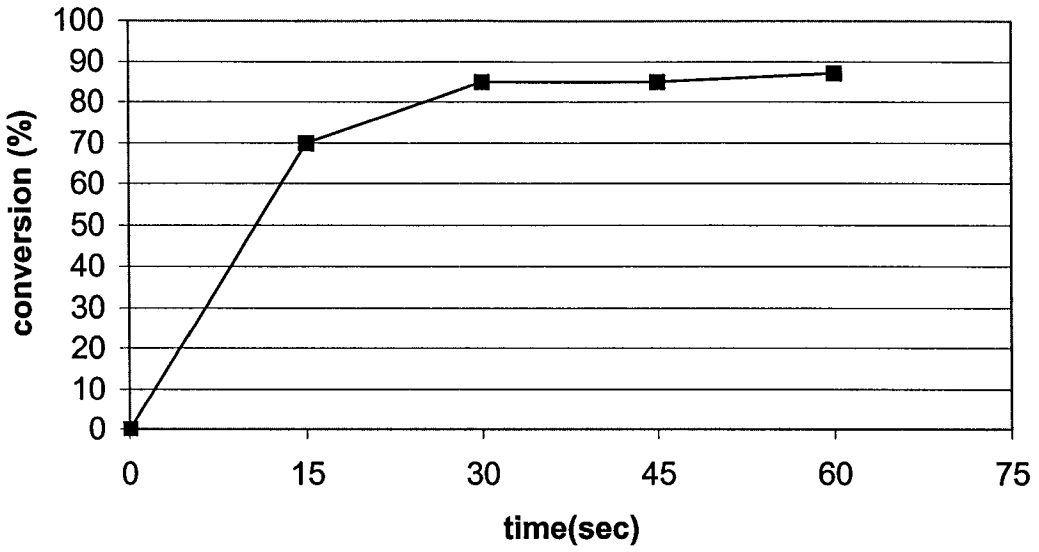

Figure 4.4 - Conversion of encapsulation reactions of *t*-BuSMA50 copolymer and HMDA in hexyl acetate measured by quenching the reaction with 0.1N HCl solution.

These results correlate well with the data obtained from pH measurements. However, the IR method has significant uncertainty in the exact timing of the quenching.

4.3.2 Kinetics

The rate of the present interfacial encapsulations is assumed to be governed by two processes: diffusion of the amine into the organic phase, and subsequently its reaction with the anhydride groups on the polymer. Kinetic control is expected to prevail in SMA encapsulation reaction, since the high conversion of the encapsulation and high porosity of the formed membrane, both suggest that the polymer shell offers no diffusional resistance to amine. The potential rate of the encapsulation reaction can be expressed as follows:

$$\frac{d[P]}{dt} = k_{app}[A_W][B] \qquad (1)$$

where k_{app} = K•k_2, and K is the partition coefficient of amine between aqueous and organic phase, k_2 is the second order reaction rate constant; $[A_W]$ and $[B]$ represent the concentrations of the HMDA and anhydride species in aqueous and organic phase at time *t*, which can both be defined as $[A_W]$ since they where used in equimolar amounts. Integration of eq. (1) from time 0 to *t* for the concentration of A_w decreasing from $[A_W]_0$ to $[A_W]$, one arrives at

$$\frac{1}{[A_W]} = \frac{1}{[A_W]_0} + kt \qquad (2)$$

Thus, a plot of $1/[A_W]$ vs. *t* should give a straight line of slope *k*. The HMDA concentration and conversion data, obtained from pH measurements, were fitted using a simple second order rate expression. The second order plots for the interfacial reaction between HMDA and t-BuSMA50 in three solvents, ethyl, propyl and hexyl acetate are shown in Figure 4.5

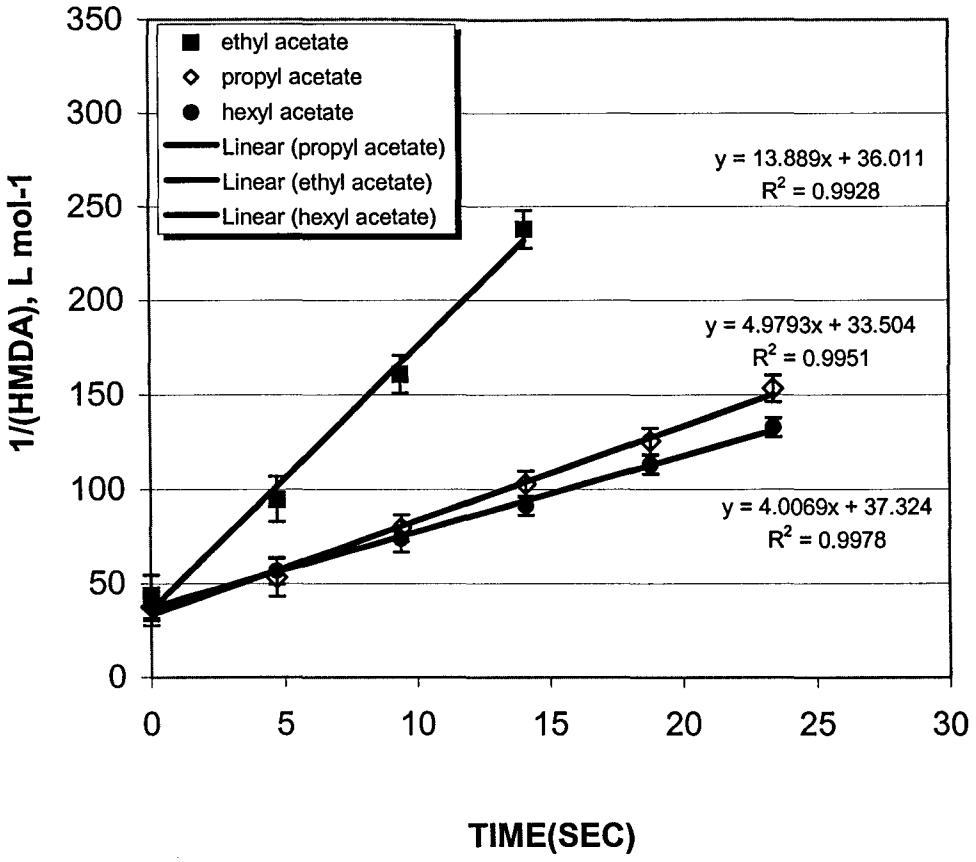

Figure 4.5 - Second order plots and reaction rate constants for reaction between HMDA and *t*-BuSMA50 in heterogeneous encapsulation medium. Error bars reflect the error percent calculated from three independent runs.

. The linearity of these curves show that the second order expression holds for the heterogeneous encapsulation systems, at least up to conversion of 70 – 75 %. Table 4.2 shows the rates of encapsulation in all four different solvents considered above.

Table 4.2 – Overall rates of encapsulation reaction for SMA encapsulation.

Core Solvent	**k_{app} (L $mol^{-1}sec^{-1}$)**	**r^2**
Ethyl acetate	13.9	0.993
Propyl acetate	5.0	0.995
Butyl acetate	4.5	0.996
Hexyl acetate	4.0	0.998

There are two important considerations when comparing these rates of encapsulation: solvent effect on the rate of amidation reaction, and solvent effect on the amine partitioning into organic phase.

The choice of reaction solvent can have a significant effect on the rate of the amidation reaction. For example, the rate of the reaction between succinic anhydride and aromatic amines increases by a factor of 30 when solvent is changed from DMF (high donicity solvent) to dioxane (low donicity solvent).[1] This is opposite to what is observed in Table 4.2, assuming ethyl acetate to have a higher polarity and donicity than hexylacetate.

In the case of reaction on polymers the situation may be more complicated because the solvation state of the polymer also depends on the solvent. Thus, a small addition of DMF to THF causes a drastic reduction of the amidation rate for the polymer,

while for succinic anhydride a nearly linear relation has been found between the rate constant and the volume fraction of DMF in THF.[1] DMF is a better solvent for the polymer than THF, which suggests that the polymer would be in a more extended coil conformation in DMF, and hence that the viscosity of the polymer solution would increase. Since diffusion slows in more viscous solutions, reaction rates decrease, even through better accessibility would be expected. Even considering that the difference in the dielectric constants (donor ability) between the four solvents used in our encapsulation procedures is not as significant as the difference in the dielectric constants in going from DMF to dioxane,[14] still, ethyl acetate would be the better solvent for our starting polymer, and hence would be expected to show a slower reaction, if viscosity were the major criterion. Table 4.2 however, shows that the encapsulation reaction is faster in ethyl acetate than in the other, poorer solvents.

The answer must lie in the interfacial nature of the encapsulation reactions. Here, the polarity of the organic phase plays a key role in the partitioning equilibrium of the polyamine between the aqueous and organic phases. It can be expected that partitioning into the organic phase will increase with its polarity, and that this can strongly affect the rate of encapsulation reactions. When considering the data in Table 4.2, this appears to be the case since the rates of encapsulation reflect the order of polarity of the core-solvents used.

4.3.3 Hydrolysis

In order to study the role of hydrolysis in SMA encapsulation procedures, the encapsulation reactions were carried out at constant pH. However, all attempts to perform the encapsulation reaction in buffer solutions of specific pH failed due to emulsion instability in high ionic strength buffer systems. Therefore, the encapsulation reactions were performed using an automatic titrator, which controlled the pH of the continuous phase. The instrument software was modified to allow simultaneous measurements of time, pH and volume of the added amine. The instrument was also programmed to automatically adjust the rate and volume of amine injection, based on the rate of change of pH. Thus, the volume increments of amine added would be reduced if the change in pH was greater than 0.01 pH units and the addition of amine would stop as long as pH of the continuos phase was higher or equal to the "ceiling" pH value set up specifically for each reaction. Amine addition resumes when pH drops 0.05 pH units below the designated "ceiling" pH value.

The method was tested by carrying out the amidation reaction of SMA50 copolymer in DMF/water (1:2) system with butyl amine as nucleophile. The ceiling pH was 9. This system is as close as possible to homogeneous conditions, since the amidated copolymer is soluble in the DMF:water mixture, and the starting polymeric solution is only slightly turbid. Figure 4.6 and Figure 4.7 illustrate typical pH versus time and volume plots of butyl amine added versus time plots, for the amidation reaction of SMA50 copolymer in DMF/water. The pH at the start of the reaction is acidic (approximately 3- 3.5), normal for SMA copolymer solutions, since a small percentage of

anhydride groups on the copolymer are hydrolyzed and form succinic acid upon storage and/or during mixing. The pH rises sharply up to about 8.5 until a significant amount of the deprotonated, free for the nucleophilic attack amine is generated. From this point forward, the pH remains constant as butyl amine is added, until the end of the reaction is approached (when about 1 eq. of butyl amine is added). During this time, the pH remains constant because the rate in which carboxylic acids produced upon amidation reaction is equal to the rate in which butyl amine is added. At this point, the rate of butyl amine addition reached its maximum (1 mL per 3 sec). Therefore the desirable, "ceiling" pH 9 could not be obtained under these conditions, until much of the anhydride had reacted.

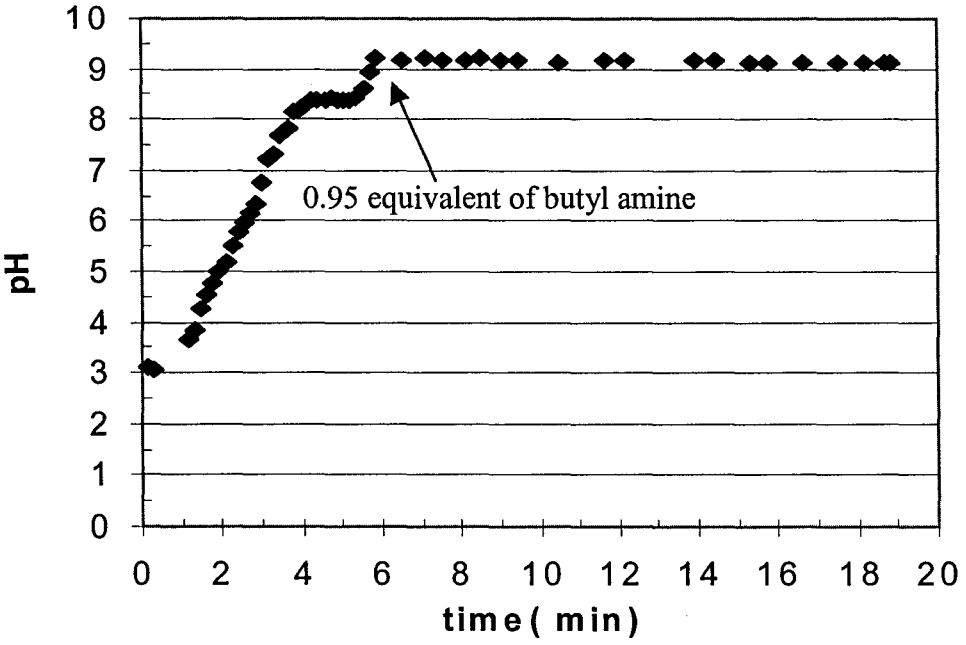

Figure 4.6 – Change of pH with time during amidation reaction of SMA50 copolymer with butyl amine in DMF/water 1:2 mixture.

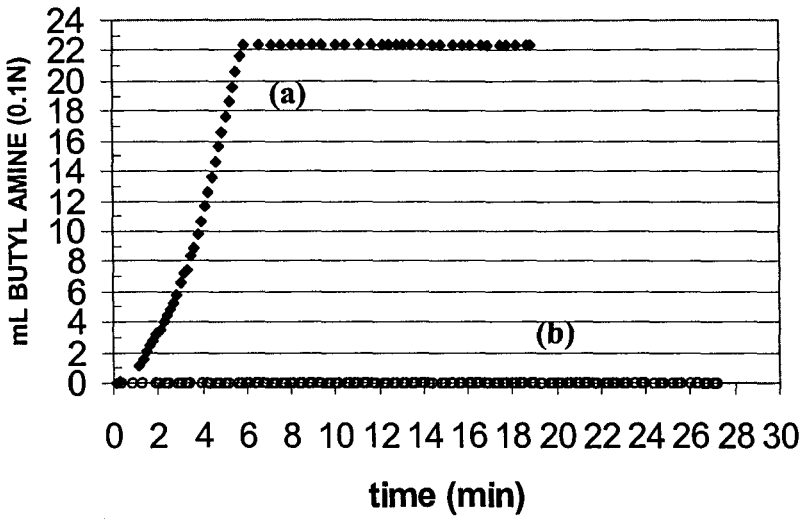

Figure 4.7 – (a) Volume of added butyl amine with time during amidation reaction of SMA50 copolymer with butyl amine in DMF/water 1:2 mixture; (b) in the blank experiment.

In the next step, the same reaction was performed in a heterogeneous ethyl acetate/water 1:2 solvent mixture. The pH and volume versus time curves were identical to the ones obtained in DMF/water system. Similar results were obtained in the system when HMDA was used instead of butyl amine. The results are summarized in Table 4.3. The longer reaction time, and lower amine incorporation in case of the reaction of SMA50 copolymer with HMDA was attributed to decreased accessibility of the anhydride groups due to the crosslinking reaction.

Table 4.3 – Amidation reaction of SMA50 copolymer.

solvent	Nu	reaction time (min.)	amine incorporation (eq.)
DMF : water (1:2)	butyl amine 0.1 M	6	0.95
ethyl acetate : water (1:2)	butyl amine 0.1 M	6	0.93
ethyl acetate : water (1:2)	HMDA 0.05 M	15	0.87

Results of the test experiments showed that the developed method can be used for monitoring the amidation reactions with simultaneous measurements of pH, time and volume values. However, it was impossible to carry out the amidation reaction at constant, high pH due to the extremely high reactivity of the SMA50 copolymers. On the other hand, the *t*-BuSMA50 copolymer should react much slower as a result of steric hindrance due to the presence of the *t*-butyl group. Indeed, as can been seen from Figure 4.8 in the encapsulation reaction of *t*-BuSMA50 copolymer with HMDA using ethyl acetate as a core oil the "ceiling" pH value of 9 was obtained during first 2 minutes of reaction, and was maintained throughout the reaction. After 30 minutes of reaction, the pH stops to drop between amine additions, indicating the end of the reaction. The small fluctuations in pH values after 30 min of reaction were attributed to noise due to the mechanical stirring. 0.9 equivalent of HMDA was incorporated after 30 min.

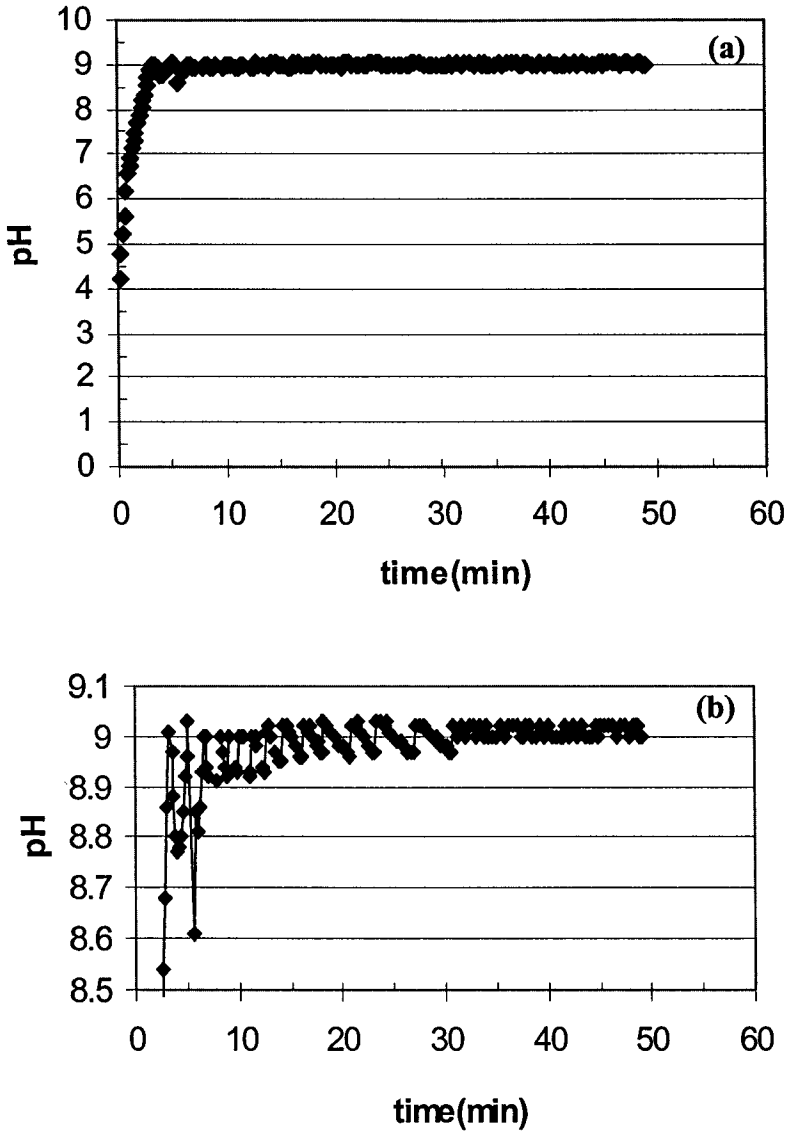

Figure 4.8 - (a) Change of pH with time during amidation reaction of *t*-BuSMA50 copolymer with HMDA in ethyl acetate/water 1:2 mixture, (b) expansion of the pH 8-9 region.

The pH curves of the reaction of *t*-BuSMA50 copolymer with HMDA at constant pH 9 had similar profiles for each of the core - oils used. However, total reaction time and amine incorporation (reaction conversion) varied from one solvent to another (Table 4.4). Thus, the total reaction time was significantly increased in non-polar solvents.

Table 4.4 – Solvent effect on the interfacial encapsulation reaction of *t*-BuSMA50 copolymer with HMDA under constant pH conditions.

Core oil	"ceiling" pH	reaction time (min.)	amine incorporation (eq.)
ethyl acetate	9	30	0.9
propyl acetate	9	45	0.9
butyl acetate	9	75	0.85
hexyl acetate	9	200	0.75

As mentioned previously, the preparations of microcapsules in different buffer solutions failed. Therefore, the key questions here concern the preparation of microcapsule at various "ceiling" pH and the characterization of the produced particles in order to establish the effect of hydrolysis in our encapsulation procedures. Consequently, the *t*-BuSMA50 microcapsules containing hexyl acetate as a core-oil were prepared at "ceiling" pH values of 8, 8.5, 9 and 10. The pH and volume plots have similar profiles for all targeted pH values. Figure 4.9 demonstrates plot of change in pH with time during the

encapsulation reaction carried out at pH 8.5. For more convenient representation only expanded area, near "ceiling" pH values is shown.

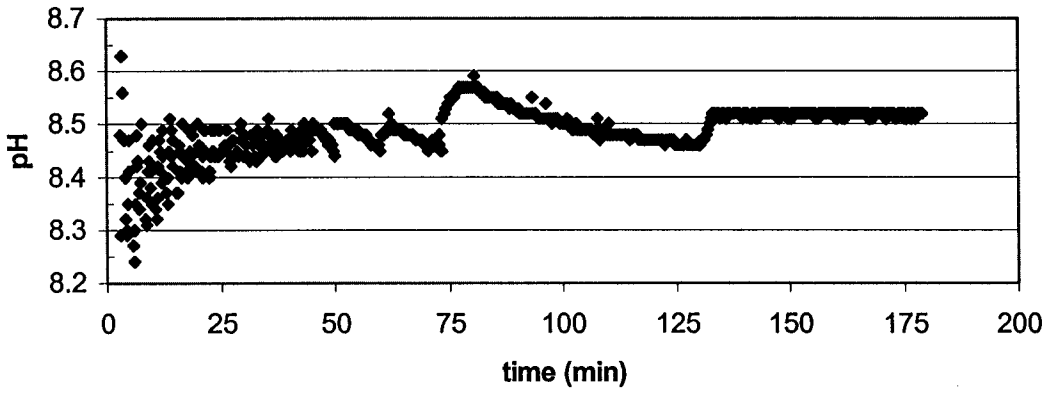

Figure 4.9 – Change of pH with time during amidation reaction of t-BuSMA50 copolymer with butyl amine in hexyl acetate/water 1:2 mixture, "ceiling" pH 8.5.

Tables 4.5 and 4.6 summarised the results from this set of experiments. We can observe from these tables monotonous increase in the reaction time as the "ceiling" pH decreased. The rate of the encapsulation reaction was affected by the type of the amine used. Thus, the rate of reaction was faster when butyl amine was used instead of HMDA. Similar observations were previously made for SMA50 copolymer. The dependence of amine incorporation on the "ceiling" pH value and nature of core-oil (Table 4.4 and 4.5) can be attributed to the difference in capsule morphology. Slow initial rate of the encapsulation reaction caused by poor amine partitioning into organic phase due to high level of amine protonation (at low pH) affects the formed capsule morphology. Upon these conditions capsules with denser outer-skin is produced. At the later stage of the

encapsulation reaction these dense walls can became a physical barrier for the amine diffusion causing decrease in amine incorporation.

Table 4.5 – pH effect on the interfacial encapsulation reaction of t-BuSMA50 copolymer with HMDA (0.05 M aqueous solution) under "ceiling" pH conditions. Hexyl acetate was used a core-oil.

"ceiling" pH	reaction time (min.)	amine incorporation (eq.)
8	350	0.6
8.5	200	0.7
9	180	0.75
10	10	0.85

Table 4.6 – pH effect on the interfacial encapsulation reaction of t-BuSMA50 copolymer with butyl amine (0.1 M aqueous solution) under constant pH conditions. Hexyl acetate was used a core-oil.

"ceiling" pH	reaction time (min.)	amine incorporation (eq.)
8	280	0.6
8.5	130	0.75
9	45	0.8
10	5	0.95

In order to determine extend of hydrolysis in these series of experiments microcapsules prepared by reaction of t-BuSMA50 copolymer with butyl amine were characterized by FT-IR and proton NMR. The choice of this type of microcapsules for the characterisation was dictated by the non-crosslinked nature of the microcapsule walls, which allow dissolving the product of the encapsulation in organic solvents and running simple proton NMR experiments. Upon completion of the encapsulation reaction the reaction mixture was acidified with 0.1N HCl solution, the microcapsules were immediately filtered, washed with water, and vacuum dried overnight. The conversion of these encapsulation reactions was determined by FT-IR as discussed previously.[15] In order to estimate the degree of the incorporation of carboxylic groups into the copolymer during the encapsulation reaction, a model copolymer was prepared by reacting t-BuSMA50 copolymer with butyl amine in dry THF under nitrogen. The conversion of this reaction was 100 % and hydrolysis as a side reaction was prevented by carrying out the reaction in dry conditions. The degree of carboxylic group incorporation is defined by the following equation:

$$c = 1 - \frac{r}{r_0}$$

where r is the area ratio of FT-IR bands of carboxylic acid (1723 cm^{-1}) residues to *t*-butyl styrene residues in the formed capsule, and r_0 is the area ratio for the same bands in the model copolymer. It is worth noting that only acidified samples can be used in these procedures, since the carboxylate ion, which is typically produced at the end of

the encapsulation reaction, gives rise to a strong asymmetrical band near 1650-1550 cm^{-1} that overlaps with the amide carbonyl band.

Finally, butyl amine incorporation into polymer was estimated from integration of proton NMR spectra of the products of encapsulation. The FT-IR spectra in this case gave unreliable results due to the extremely broad nature of the amide band. The extent of the incorporation of butyl amine into the copolymer was calculated from the integration ratio of protons of methyl groups of butyl amine ($\delta = 0.8$) and styrenic protons ($\delta = 6.5 - 7.5$).

Table 4.7 - Characterization of microcapsules prepared by reacting t-BuSMA50 copolymer with butyl amine. Hexyl acetate was used as core-oil.

"Ceiling" pH	Conversion calculated based on amine incorporation from PC-Titrate (%)	Conversion of anhydride groups from FT-IR (%)	Amount of carboxylic groups from FT-IR (%)	Amount of amide groups from ^{1}H-NMR (%)
8	61	75	75	72
8.5	74	78	81	83
9	82	84	85	95
10	95	92	100	100

The results of these experiments are summarised in Table 4.7. The data reported in Table 4.7 show a good correlation between the results obtained from different characterisation methods. Thus, the conversions calculated based on the amine incorporation from PC-Titrate data were in a good agreement with the anhydride groups conversions estimated by FT-IR. The amounts of the carboxylic groups and amide groups in the polymer

estimated from FT-IR and proton NMR respectively were equal to each other, and in a good agreement with the reaction conversions regardless of the "ceiling" pH. Equal amounts of the amide and carboxylic groups in the final polymer suggest that under our experimental conditions at "ceiling" pH rage between 8 to 10 the amidation dominates, and the role of hydrolysis is insignificant.

4.4 Conclusion

The times of the interfacial encapsulation reactions are fast in order of minutes. The rates of the reactions were found to be dependent on the nature of the core oil. Thus, the rate of the reaction decreases in more hydrophobic core-oils.

The method was developed to perform the encapsulation reactions at constant or close to constant ("ceiling") pH. Microencapsulations carried out under different "ceiling" pH conditions ranged from pH 8 to 10 showed gradient in anhydride conversions from 75 to up to 95 % which was attributed to different rates of amine partitioning into organic phase due to the various degrees of amine protonation. The relationship between the reaction conversion and the nature of the core-oil was also showed.

Hydrolysis does not play an important role in the interfacial encapsulation reaction between SMA copolymers and amines under investigated conditions.

References

1) Rätzsch M. *Prog. Polym. Sci.* **1988,** *13*, 277-337.

2) Rätzsch M. *J. Macromol. Sci.-Chem.,* **1987,** *A24(8)*, 949-965.

3) Rätzsch M; Hue, N. T. *Acta Polym.* **1979**, *30*, 93-96.

4) Pitman, I.H.; Uekama, K.; Higuchi, T.; Hall, W. E. *J. Am. Chem. Soc.* **1972,** *94*, 8147-8153.

5) Hall, W. E.; Higuchi, T.; Pitman, I.H.; Uekama, K. *J. Am. Chem. Soc.* **1972,** *94*, 8153-8156.

6) Kluger, R.; Hunt J. C. *J. Am. Chem. Soc.* **1984,** *106*, 5667-5670.

7) Rogne, O. *Perkin Trans. II* **1972**, *4*, 472-474.

8) Eberson, L.; Welinder, H. *J. Am. Chem. Soc.* **1971,** *93*, 5821-5826.

9) Ladavière, C.; Veron, L.; Delair, T. Domard, A.; Pichot, C.; Mandrand, B. *J. Appl. Polym. Sci.,* **1997**, *65*, 2567-2577.

10) Ladavière, C.; Delair, T. Domard, A.; Pichot, C.; Mandrand, B. *J. Appl. Polym. Sci.,* **1999**, *72*, 1565-1572.

11) Jansen, L. J.J.M.; te Nijenhuis, K *J. Membrane Sci.,* **1992**, *65*, 59-68.

12) Yadav, S. K.; Suresh, A. K.; Khilar K. C. *AIChE Journal*, **1990**, *36*, 431-437.

13) Yadav, S. K.; Khilar K. C.; Suresh, A. K. *AIChE Journal*, **1996**, *42*, 2616-2626.

14) Lide, D. R. *CRC Handbook of Chemistry and Physics 76th Edition;* CRC Press: 1995-1996.

15) Shulkin, A.; Stöver, H. D. H., Submitted to *J. Membrane Sci.*

CHAPTER 5

Photostimulated Phase Separation Encapsulation

Anna Shulkin, Harald D.H. Stöver

Department of Chemistry, McMaster University

1280 Main Street West, Hamilton, ON Canada L8S 4M1

Macromolecules, Accepted

5.0 Abstract

Polymer capsules were prepared by photostimulated precipitation of azobenzene-functionalized poly(styrene-*alt*-maleimide) copolymers dissolved in an oil phase and dispersed in a continuous phase. The oil phase is selected to be a near *theta*-solvent for the copolymer, such that the increasing polarity of the polymer due to the photochemical *trans* to *cis* isomerization induces polymer phase separation and migration to the interface. The resulting polymer walls are permanent even during storage in the dark, or irradiation with visible light.

5.1 Introduction

The principle of the hydrophobic polymer phase separation for the formation of hollow particles and microcapsules has been well described in different patents and publications.[1,2,3,4] The key element in these methods is the efficient phase separation of the forming or preformed polymer from the core phase, controlled by polymer /core oil interactions. Two main approaches have been used to date to effect this polymer phase separation: one is based on the difference in the solubility properties between monomers and the polymer formed during encapsulation, and the other is based on changing core oil properties during encapsulation.

Thus, microencapsulation by *in situ* polymerization involves polymerization in a dispersed system in which the monomers are soluble in the core material while the forming polymer is not. Therefore, the forming polymer phase separates from the core mixture and typically spreads at the interface producing microcapsule morphology. An efficient, early polymer phase separation is achieved either by using relatively polar monomers together with non-polar core oils in which the monomers are barely soluble, or by using a mixture of a hydrophobic monomer together with a small amount of a highly hydrophilic comonomer (Figure 5.1a).[1,2,3]

In a second approach a preformed, initially core oil soluble polymer phase separates from the core medium due to a change in the solvent properties of the core oil, and precipitates at the oil/water interface. In an elegant example of this approach, the core oil mixture contains the starting polymer dissolved in a mixture of a low boiling solvent and a high boiling non-solvent for the polymer.[4] The core oil solvency is changed by gradually removing the low-boiling good solvent for the polymer from the emulsion by evaporation. Under these conditions the changing solvent composition causes polymer phase separation at the interface (Figure 5.1b). Other examples of this approach include selective liquid-liquid extraction of a good solvent from a corresponding solvent/non-solvent mixed core oil.

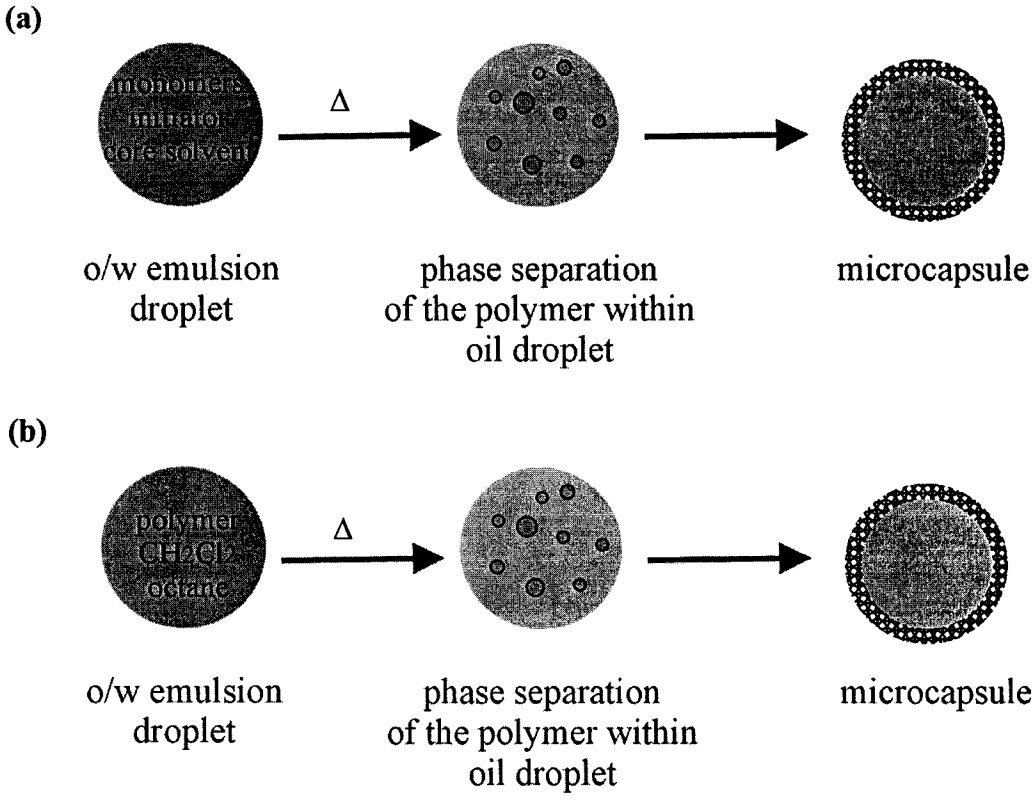

Figure 5.1 – (a) The microcapsules formation by in *situ* polymerization; (b) the microcapsules formation by solvent evaporation method.

In this paper, we describe the use of hydrophobic photoresponsive polymers in a new approach to phase separation encapsulation where the solubility properties of the wall-forming polymer itself are photochemically changed to effect encapsulation. Polymers carrying photo-ionizable groups have been reported to offer photochemical control over properties including surface wettability,[5] viscosity, [6] pH,[7] and binding capacity.[8] A reversible photochemical phase separation of polystyrene carrying azobenzene pendant groups was first reported by Irie et *al.* (Figure 5.2).[9] It was attributed to the azobenzene *trans*-to-*cis* isomerization which altered the balance of polymer-polymer and polymer-solvent interactions in favor of polymer-polymer interactions, likely due to the increased dipole moment of the cis-azobenzene (Figure 5.3).[10,11,12]

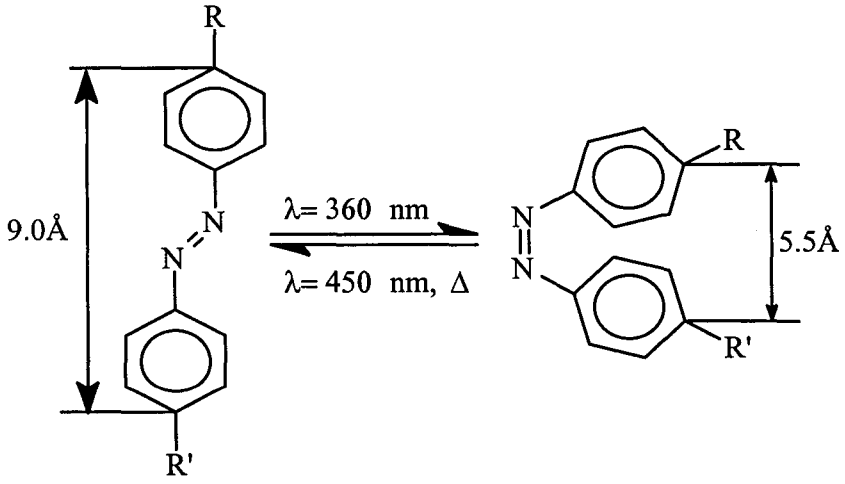

Figure 5.2 – Azobenzene photoisomerization.

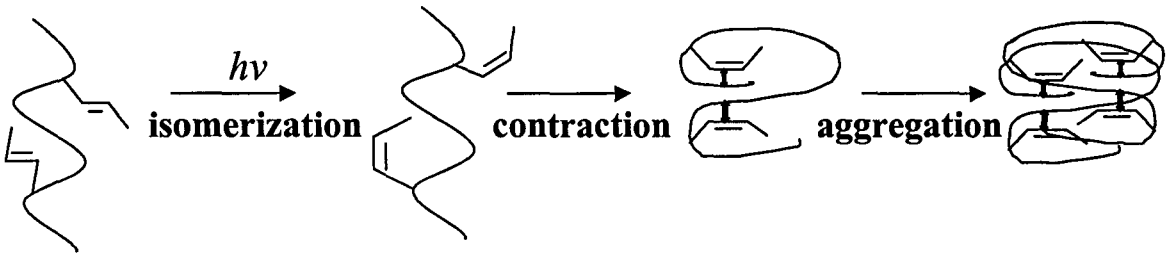

Figure 5.3 – Mechanism of reversible photochemical phase separation of polystyrene carrying azobenzene pendant groups.[9]

We report here the use of this concept in a heterogeneous environment. Specifically, where azobenzene functional polymers that are soluble in their trans-form, are photochemically driven to phase separate from dispersed core oils to form remarkable stable, permanent polymer capsule walls. This new method whereby hollow particles are generated photochemically, and whose macroscopic membrane properties can, in principle, be controlled by irradiation,[13] should provide an important addition to the area of encapsulation.

5.2 Experimental

5.2.1 Polymerization (typical procedure)

Preparation of poly(styrene (50%)-co-(4-phenylazomaleinanil(30%)-phenylmaleimide(20%))) (St50-PAMA30-PMI20) copolymer. The copolymerization of styrene (1g, 9.6 mmol) with 4-phenylazomaleinanil (1.6 g, 5.76 mmol) and phenylmaleimide (0.66 g, 3.84 mmol) was carried out at 70°C in 20 mL 1,4-dioxane in a

100 mL round bottom flask fitted with a nitrogen bubbler, using AIBN as initiator (0.02 g, 0.12 mmol). After 24 h of polymerization the copolymer was isolated by precipitating the cooled reaction mixture into a five-fold excess of cold methanol. The copolymer was filtered, washed with methanol, and dried at 40°C under reduced pressure for 48 hours. The yield of copolymer was 80%, M_W = 15,000, MWD =1.62.

5.2.2 Typical Method for Photochemical Preparation of Microcapsules

The following method describes the preparation of microcapsules from St50-PAMA50 copolymer in methyl isobutyl ketone. 100mL deionized water containing 1g polyvinylalcohol (80% hydrolyzed, 9000 - 10000Da) was placed into a 200mL beaker, stirred at 450 rpm, and the oil phase consisting of 0.25g St50-PAMA50 copolymer dissolved in 10 mL of methyl isobutyl ketone was added dropwise over 60 seconds to form an oil-in-water emulsion. After an additional 20 min of stirring, the emulsion was transferred to an UV-reactor and irradiated for 1 hour. A glass cold finger with circulating cold water was submerged into the emulsion to keep its temperature near room temperature. Following irradiation, the resulting aqueous dispersion of microcapsules was stored at room temperature.

5.2.3 Characterization

A Phillips-2020 Environmental Scanning Electron Microscope (ESEM) was used to obtain electron microscope images. Dilute aqueous dispersions of microcapsules

were deposited on aluminum stubs, dried at room temperature and sputter-coated with a 5nm gold layer.

Optical microscopy was performed using a Olympus BH-2 microscope, equipped with a Kodak DC 120 Digital Camera.

5.3 Results and Discussion

The copolymers used in this study were prepared by free radical solution copolymerization of 4-phenylazomaleinanil (PAMA), phenylmaleimide (PMI) and styrene (St). Styrene and maleimides copolymerize in a strictly alternating fashion,[14] and the use of PMI allowed us to vary the content of photochemically active PAMA while maintaining a stoichiometric styrene/maleimide ratio. The azobenzene content in the final copolymer was estimated by UV/Vis, using the absorption of St50-PAMA50 copolymer, at 353 nm in DMF solution as a standard. The results of the preparation of the azo-aromatic polymers are shown in Table 5.1.

The magnitude of the change in the physical properties of photoresponsive polymers and their solutions depends on the relative stability of the system.[11] For example, when a polymer solution is already close to the point of polymer phase separation, small solubility changes caused by irradiation may cause a large effect, such as polymer precipitation. Thus, the solvent or solvent mixture from which polymer may precipitate out upon irradiation should be a *theta* solvent for the polymer, in which

polymer-solvent interactions are just balanced by polymer-polymer and solvent-solvent interactions.[15] The solvent should also have a low dielectric constant to enhance the mutual attraction between the dipolar *cis*-azo groups.[6] Finally, in order to be used in heterogeneous systems such as encapsulations, the organic solvent should be water immiscible, and have a relatively high boiling point.

Table 5.1 - Azobenzene group content and molecular weights of the copolymers.

Polymer	Relative azo groups content[1]	Mn (GPC)
St50-PAMA40[2]-PMI10[3]	38	16,000
St50-PAMA30-PMI20	29.5	15,000
St50-PAMA20-PMI30	20.6	17,000
St50-PAMA10-PMI40	11.8	15,000

[1] Calculated based on absorption of St50 – PAMA50 copolymer as a standard
[2] PAMA40 = 40 mol % of 4-phenylazomaleinanil in polymerization feed
[3] PMI10 = 10 mol % of phenylmaleimide in polymerization feed

Based on these requirements, methyl isobutyl ketone and toluene were evaluated as core solvents for the photoinduced encapsulation procedure, using a series of poly(styrene-*alt*-maleimide) copolymers containing between 10 and 50% azobenzene groups. Only the St50-PAMA50 copolymer dissolved in these single solvents, while the ternary copolymer, in which some of the PAMA had been replaced with the more polar PMI, required the presence of polar cosolvents such as dichloromethane or aniline in order to dissolve. For example, the St50-PAMA10-PMI40 copolymer dissolved homogeneously in toluene/aniline 1:1 volume ratio to form a yellow solution. Upon irradation at 350nm, the polymer precipitated from this solution, indicating that 10 mol % of azobenzene units in the copolymer chain are sufficient to cause a solubility change of the polymer dissolved in a near-*theta* solvent system. These results are also in a good correlation with literature observations.[11] Similar photochemical copolymer precipitation was observed for all copolymers, from their appropriate solvents.

In principle, one should be able to compensate for the higher polarity of the PMI comonomer by replacing an appropriate amount of styrene with the more lipophilic 4-*t*-butylstyrene, and thus maintain single solvent solubility throughout a range of PAMA content. For this report, we focused our attempts to use photoresponsive copolymers for capsule formation on St50-PAMA50 copolymer.

Homogeneous solutions of St50-PAMA50 copolymer in methyl isobutyl ketone (1g/100 mL) showed phase separation upon irradiation at 350 nm for 60 minutes. The yellow solutions of the azobenzene functional polymer became almost clear following the irradiation, with the polymer precipitating as an orange solid.

For the photo-induced encapsulations, a solution of 5% w/v of poly(styrene-*alt*-PAMA) in methyl isobutyl ketone was dispersed in an aqueous phase containing poly(vinyl alcohol) as colloidal stabilizer. The resulting emulsion was irradiated at 350 nm at room temperature for about an hour, after which time the emulsion droplets had turned into liquid-filled polymer microcapsules. Apparently, the polymer phase separated from the MIK during irradiation, and migrated to the o/w interface to form the capsule wall. This encapsulation process is illustrated in Figure 5.4.

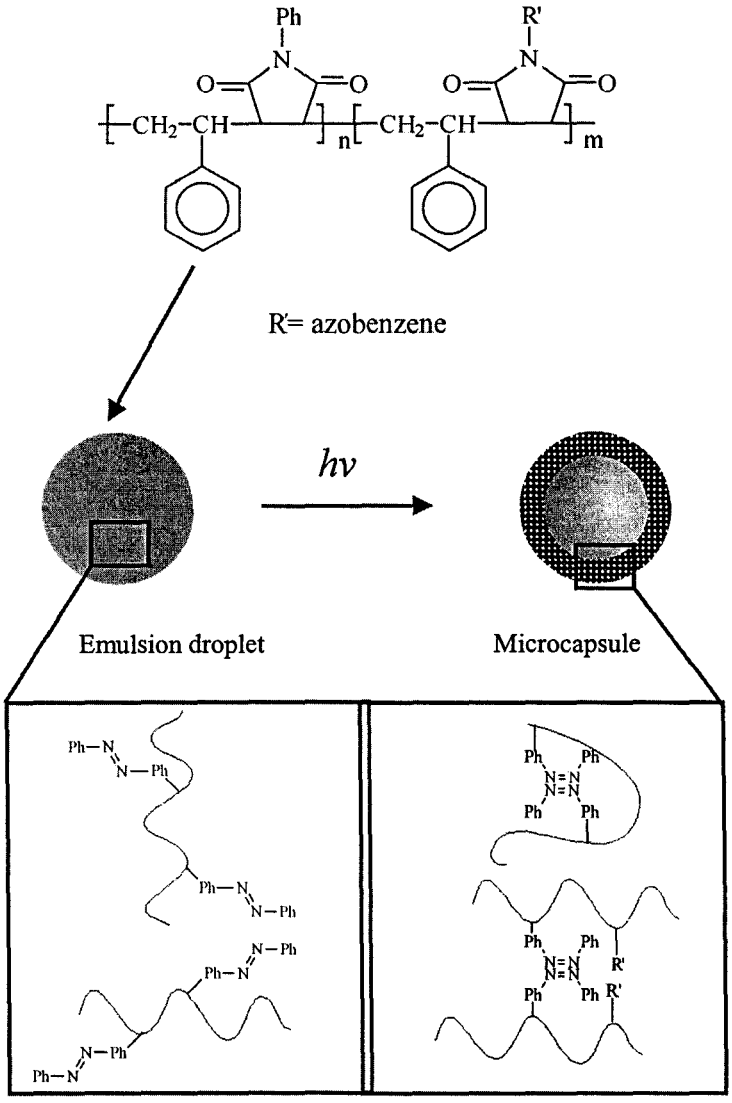

Figure 5.4 - Mechanism of capsule formation by photochemical induced precipitation encapsulation.

Figures 5.5a and 5.5b show environmental scanning electron microscope (ESEM) images of the resulting microcapsules. The polymer capsule walls are thin, on the order of 200 nm. They show indentations on their surface, which are likely due to partial fill release and wall collapse at the shell thin-spots under the high vacuum required for SEM sample preparation.[16] The enlarged area shown in Figure 5.5b illustrates how some of the capsules have burst during ESEM processing.

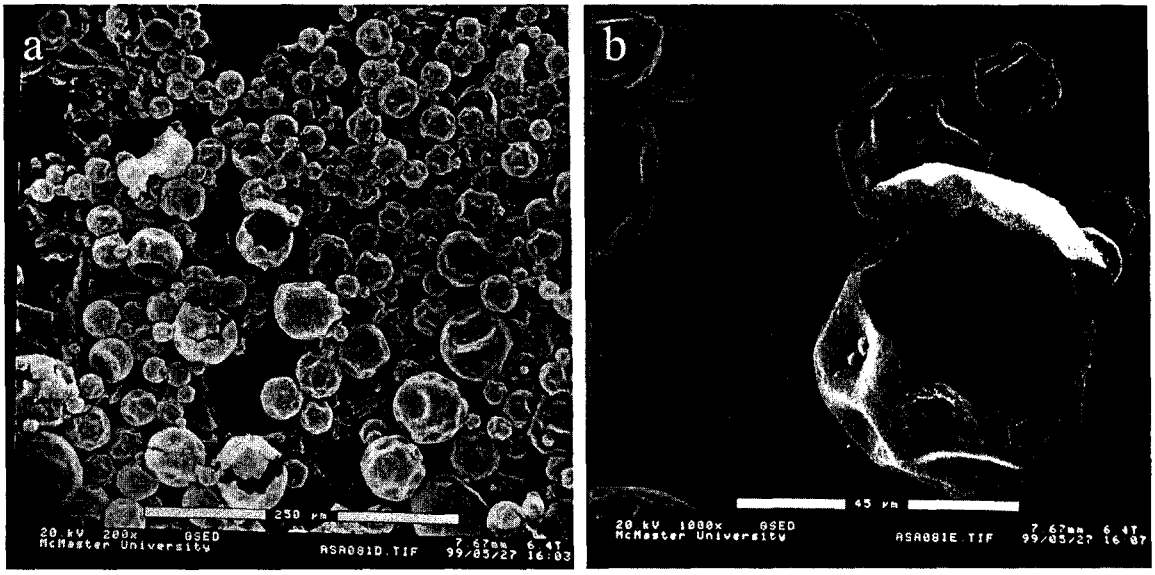

Figure 5.5 - ESEM image of microcapsules produced by irradiation of an emulsion of methyl isobutyl ketone containing 5% St-PAMA50.

Optical microscopy gave further insight into the morphology and the release properties of these microcapsules. Thus, the capsules were clearly spherical and had smooth surfaces while wet (Figure 5.6a). However, after drying on the glass slide for 15 minutes surface indentations were observed indicating the release of the MIK core solvent (Figure 5.6b). This result can be attributed to the high permeability or porosity of the capsule wall.

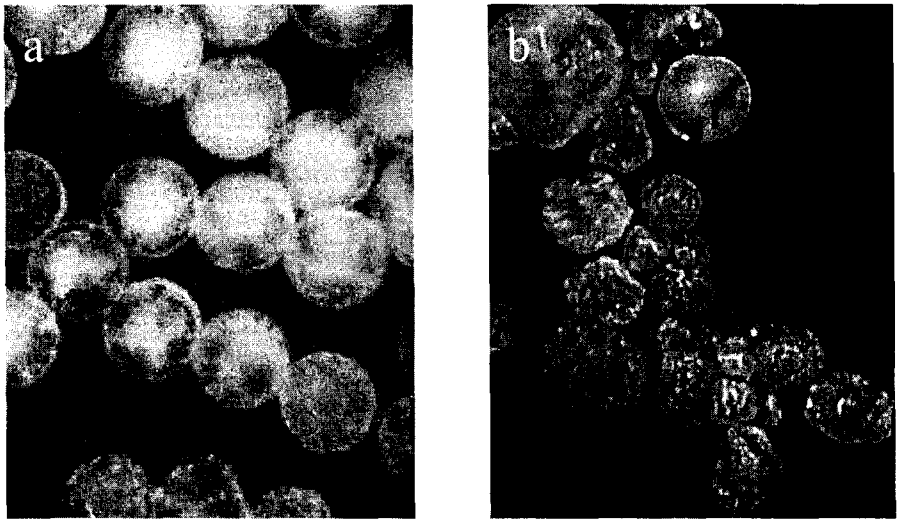

Figure 5.6 - Optical microscope image of microcapsules produced by irradiation of an emulsion of methyl isobutyl ketone containing 5% St-PAMA50; a - wet microcapsules on the glass slide, b - dry microcapsules, 15 min on the glass slide.

The analogous encapsulation, using an emulsion of methyl isobutyl ketone containing 10 weight % of the same copolymer leads to much thicker capsule shells (Figures 5.7a and 5.7b). Figure 4a shows a representative section of the electron micrograph image of the capsules obtained after 90 minutes irradiation. These capsules were stable during ESEM processing and were manually fractured in order to investigate their internal structure (Figure 5.7b). The shell thickness of the microcapsules is related to the concentration of copolymer in the organic phase. Increasing the polymer content in the oil phase should produce proportionally thicker shells. However, the thickness of the capsule walls prepared from 10 weight % polymer solutions is about 1-2 micron for a 10 micron diameter capsule. This wall thickness is more than can be expected from a bulk wall at 10 weight % wallformer loading, and suggests a high porosity of the capsule wall. This result correlates well this the observed relatively fast release from these microcapsules.

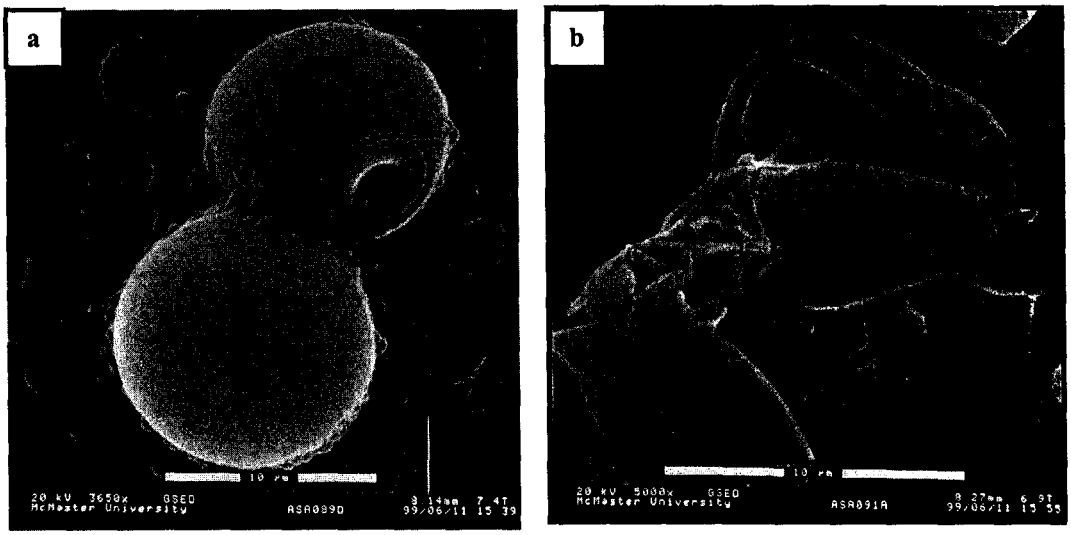

Figure 5.7 - ESEM image of microcapsules produced by irradiation of an emulsion of methyl isobutyl ketone containing 10% St-PAMA50: a – whole capsules; b- capsule wall fragments

Capsules were also prepared from copolymers having less than 50 mol % azobenzene groups. For example, St50-PAMA20-PMI30 capsules prepared from a 5 / 1 toluene / aniline mixture had a very broad size distribution. This may be due to the fact that the density of aniline is higher than that density of the water, making it difficult to disperse the aniline containing oil phase in water (Figure 5.8a). The resulting microcapsules were also very brittle and fell apart upon being transferred to a glass slide.

However, microcapsules prepared with toluene / dichloromethane as a core mixture were smaller in size with narrow size distribution (Figure 5.8b).

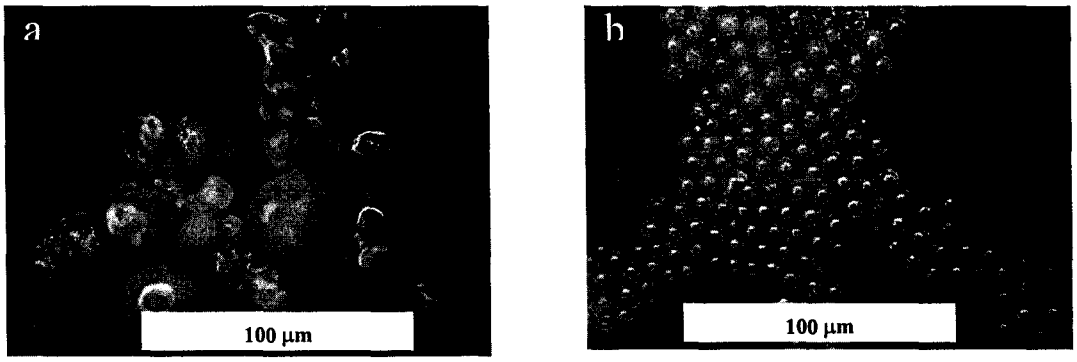

Figure 5.8 - Optical microscope image of microcapsules produced by irradiation of an emulsion of: a - toluene/aniline 5:1 vol. ratio containing 5% St50-PAMA20-PMI30; b - toluene/CH2Cl2 1:1 vol. ratio containing 5% St50-PAMA20-PMI30.

These precipitations of the present polymers are due to the photochemicals trans-cis conversion, and should hence be reversible. Re-dissolution by thermal back isomerization was in fact observed in all homogeneous polymer solutions. However, the capsules formed by irradiation in heterogeneous emulsion systems did not redissolve upon standing in the dark for several weeks. We assume that this permanence may be explained by the fact that the microcapsules prepared by photoinduced phase separation encapsulation contain a small amount of water in the core oil, which prevents the shell polymer from re-dissolving after heating or long period of time in the dark. Water can diffuse into the capsules through the pores of relatively polar shells during the encapsulation process or/and upon storage.

Acknowledgements

We would like to thank NSERC and 3M Canada for funding of this research. A.S. would like to acknowledge the Province of Ontario for an Ontario Graduate Scholarship.

1) Berg, J.; Sundberg D.; Kronberg, *J. Microencapsulation* **1989**, *6*, 327-337.

2) McDonald, C. J.; Bouck, K. J.; Chaput, A. B. *Macromolecules* **2000**, *33*, 1593-1605.

3) Kasai, K.; Hattori, M.; Takeuchi, H.; Sakurai, N. US Patent 4,798,691, 1989.

4) Loxley, A., Vincent, B., *J. Colloid Interface Sci.***1998**, *208*, 49-52.

5) Ishihara, K.; Hamada, D.; Kato, S.; Shinohara, I. *J. Polym. Sci. Polym. Chem. Ed.* **1983**, *21*, 1551-1555.

6) Matejka, L., Dušek, K., *Macromol. Chem.* **1981**, *182*, 3223-3236.

7) Irie, M.; Hirano, K.; Hashimoto, S.; Hayashi, K. *Macromolecules* **1981**, *14*, 262-267.

8) Ferritto, M. S.; Tirrell, D. A. *Macromolecules* **1988**, *21*, 3117-3119.

9) Irie, M., Tanaka, H., *Macromolecules* **1983**, *16*, 210 –214.

10) Kumar, G. S., "Azo Functional Polymers", Technomic Publishing Company, Inc., U.S.A., 1992.

11) Irie, M. *Advances in Polymer Sci* **1990**, *94*, 27-67.

12) Irie, M.; Schnabel, W. *Macromolecules* **1985**, *18*, 394-398.

13) Seki, T.; Kojima, J.; Ichimura, K. *Macromolecules* **2000**, *33*, 2709-2717.

14) Barrales-Rienda, J. M., Gonzalez de la Campa, J. J., Gonzalez Ramos, J., *J. Macromol. Sci., Chem.* **1977**, *A11*, 267-286.

15) Elias, H.-G. Theta solvents; In *Polymer Handbook*; Brandrup, J., Immergut, E. H., Grulke, E. A., Eds. Wiley-Interscience: New York, 1999; p VII/291.

16) Esen, C.; Kaiser, T.; Borchers, M. A.; Schweiger, G. *Colloid Polym. Sci.* **1997**, *275*, 131-137.

Thesis Conclusions

Previous work showed that preformed polymers can be utilized for the preparation of microcapsules based on physiochemical methods such as solvent extraction, electrostatic and hydrophobic interactions. This thesis described the formation and properties of capsule walls formed from the new types of wall-former materials, styrene–maleic anhydride and styrene-maleimide based copolymers.

The first part of the Chapter 2 addressed the novel type of the interfacial encapsulation based on the reaction between hydrophobic styrene-maleic anhydride (SMA) type copolymers and water-soluble polyamine. SMA microcapsules containing only very hydrophilic core–oils can be prepared from styrene-*alt*-maleic anhydride copolymer. Microcapsules containing more hydrophobic core oils were prepared by either increasing the ratio of styrene to maleic anhydride groups in the copolymer, or by incorporating *tert*-butyl styrene instead of styrene into the copolymer. Active ingredients such as dodecyl acetate and dodecanol were successfully encapsulated in SMA microcapsules. The fast rate of release from SMA microcapsules was attributed to the porous nature of the capsule walls. The second part of the Chapter 2 described the hydrolysis reaction of *tert*-butylstyrene-maleic anhydride copolymers to produce non-cross-linked microcapsules. Here only prove of the concept was established and the detail

understanding of the SMA microcapsules formation as well as effect of the pH of the internal morphology of the cross-linked and non-cross-linked microcapsules is the subject for the future work.

Chapter 3 investigated the factors, that effect morphology transitions observed in SMA encapsulation systems and addressed the correlation between wall morphology and rate of the release from the SMA microcapsules. Interfacial reaction between maleic anhydride copolymers and water soluble polyamines was utilized to prepare particles with different morphologies such as hollow particles and matrix structures, by varying several parameters including starting polymer loading and molecular weight of the starting copolymer. The main factors that affect particle morphology were found to be the nature of the core oil solvent, and the rate of amine addition. Solvency strongly influences polymer/ solvent interactions and polyamine partitioning into the organic phase. Thus, under good solvency conditions and high percentage of ethyl acetate as a core-cosolvent, mainly matrix particles were produced, while under poor solvency conditions and high percentage of dodecyl acetate as a core-cosolvent, hollow particles were obtained. However, the rate of polyamine addition strongly affects this relationship between particle morphology and core - solvent. Thus, capsules with thin and dense walls were produced in almost 80 vol. % of ethyl acetate, when polyamine was added slowly.

In Chapter 4 the SMA microencapsulation was investigated on the molecular level. In this work, a comprehensive experimental study was performed of the conversion, time and rates of the interfacial SMA reaction, under the conditions of the SMA microencapsulation. In addition, the competition of amidation versus hydrolysis in interfacial SMA encapsulations has been studied. It was found that the times of the interfacial encapsulation reactions were fast, in order of minutes. The rates of the reactions were found to be dependent on the nature of the core oil. Thus, the rate of the reaction decreased in more hydrophobic core-oils. In addition the encapsulations were performed at constant or close to constant pH. Investigation of encapsulation reaction under these conditions allowed the conclusion that hydrolysis does not play an important role in the interfacial encapsulation reaction between SMA copolymers and amines.

The last chapter of this thesis described a physical, "pure" solvency based approach to capsule wall formation. The work presented in Chapter 5 was designed to test the possibility for the internal photoinduced phase-separation encapsulation. This approach entirely removes the need for selective evaporation of a solvent component, or addition of a cross-linking reagent. It is based on reducing the solubility of azobenzene-containing polymers in near *theta* core solvents by a reversible photochemical reaction of the polymer itself.

Polymer capsules were successfully prepared by photostimulated precipitation of azobenzene-functionalized poly(styrene-*alt*-maleimide) copolymers dissolved in an oil phase and dispersed in a continuous phase. The oil phase was selected to be a near *theta*-solvent for the copolymer, such that the increasing polarity of the polymer due to the photochemical *trans* to *cis* isomerization induces polymer phase separation and migration to the interface. The resulting polymer walls were found to be permanent even during storage in the dark, or irradiation with visible light.